

https://dspace.org/

Regional pillar monitoring at South Deep gold mine, South Africa

Kwangwari, Fungai

2015-05-04
http://hdl.handle.net/10539/17600

Downloaded from a DSpace repository. https://dspace.org/



MSc (Eng) RESEARCH REPORT

Regional Pillar Monitoring at South Deep gold mine, South Africa

Student Name; Fungai Kwangwari

Student number; 715918

Supervised by; Prof J. N. Van Der Merwe

A report submitted to the Faculty of Engineering and the Built Environment, University of the Witwatersrand, Johannesburg, in fulfillment of the requirements for the degree of Master of Science in Engineering.

August 2014

Declaration

I declare that this research report is my own, unaided work and that it has not been submitted at the University of the Witwatersrand, Johannesburg or at any other University before. I have read the University Policy on Plagiarism and hereby confirm that no plagiarism and copyright infringement exists in this report.

Name**:** Fungai Kwangwari

……

Signature

On this ……. day of ……. (year) ……

at …….

Acknowledgements

Firstly, I thank SRK Consulting (Johannesburg) for providing me with the opportunity to develop my career in Rock Engineering, unrestricted access to the state-of-the-art softwares that I used in the research project and unlimited access to the library. To William Joughin and Philani Mpunzi, who dedicated their time to patiently teach me everything worth knowing about the discipline and numerical modelling techniques for underground excavations, I really appreciate and will forever be grateful. William, familiarized me with the concept of seismic data analysis, the method which together with numerical modelling became the tools I used in the monitoring and assessment of regional pillar at South Deep gold mine. Finally I recognize and appreciate the expert supervision and guidance from my supervisor, Professor Nielen Van Der Merwe.

Dedication

To my family and friends, for the love, encouragement and support in pursuing my career in Rock Engineering, thank you for the faith you have always had in me.

Abstract

Regional pillars are designed to manage seismic energy emissions as well as combating rock falls and rock-bursts in deep level tabular stopes where extraction takes place over a large area. These emissions are as a result of high abutment stresses and high closure rates which in turn increase the Energy Release Rate (ERR) that occurs at depth exceeding 2000 m below surface. Generally, regional pillars in narrow tabular stopes are very squat (high width to height ratio) and therefore characteristically stable. However, the regional pillars in massive ore bodies will become more slender during the subsequent extraction and this could eventually increase the possibility of becoming unstable. The complexity and uncertainty of rock as a medium makes pre-determination of rock mass response difficult. The manner in which regional pillars in deep level massive mining react to imposed loads and their failure mechanisms is also still largely unknown.

As such, South Deep gold mine has implemented a monitoring system to assess deformation and associated velocities during ground motion resulting from pillar forming and massive mining. The system monitors and identifies hazardous areas in the mine, and based on seismic history, prediction of rock-bursts, reasonable prediction of the location and magnitude of events is possible in future. Regional pillars, which are of paramount importance during massive mining, are likely to become highly stressed as mining progresses, resulting in an increased number of seismic events in the future.

The case study done for South Deep gold mine showed an observed general increase in the number of high magnitude events per month indicating that the regional pillar may be becoming unstable. These seismic events cannot be accurately modeled using Map 3D due to

the limitations of the software (assumes the rockmass to be isotropic, homogeneous and elastic). There is therefore need to introduce an inelastic modelling software which incorporate geological structures, to represent the actual rock mass performance in order to evaluate instability.

Preliminary inelastic modelling was carried out using Phase 2 to address the shortcomings of elastic Map 3D modelling. Increasing the mining rate increased rock mass deformations and the occurrence of high magnitude seismic events probably due to accelerated slip occurring along geological structures or fracturing of the rock. Additionally, strain meter readings from the mine showed increases in stress changes both tension and in compression. The onset of pillar stability was explained to be associated with the change in the general trends of the seismic and strain data graphs from linear to exponential. The average pillar stress was discovered to be less than 2.5 times the Uni-axial Compressive Strength (UCS) of the footwall but greater than that of the hangingwall material, hence the pillar is likely to punch into the hangingwall.

The analysis of data collected during the course of the project concluded that monitoring needs to be continued, data analysed and numerical models updated regularly especially incorporating geological discontinuities to establish the onset of instability timeously so that an informed decision can be made.

Table of Contents

Abstract ..... **v**

Table of Figures ..... **xi**

List of Tables ..... **xiii**

Abbreviations and Symbols ..... **xiv**

CHAPTER 1 ..... **1**

Introduction **1**

1.1 The Witwatersrand Basin ***3***

1.1.1 Geology at South Deep gold mine 4

1.2 Locality of the mine ***8***

1.3 Mining methods ***10***

1.3.1 Mechanized horizontal de-stress mining 11

1.3.2 Mechanized long-hole stoping 13

1.3.3 Mechanized drift, bench and fill 14

1.4 Support implemented at South Deep gold mine ***16***

1.5 Backfilling ***17***

1.6 Statement of the problem ***18***

1.7 Contents of the Research Report. ***20***

1.8 Project methodology ***20***

1.8.1 Monitoring and Analysis 20

1.8.2 Project Resources 21

CHAPTER 2 ..... **22**

2 Rock mass behaviour and seismicity **22**

2.1 Rock mass behaviour ***22***

2.2 Seismicity ***24***

2.2.1 Causes of mining induced seismicity 28

2.2.2 Seismicity at Witwatersrand gold fields 31

2.2.3 Seismic prediction and control 32

2.2.4 Rock-burst control 33

2.3 Instrumentation ***34***

2.4 Numerical modelling ***34***

2.5 Regional pillar designs in South African deep level mines ***34***

CHAPTER 3 ..... **37**

3 Underground Monitoring **37**

3.1 Objectives of a Monitoring System ***38***

3.1.1 Location of Potential Rock-bursts 38

3.1.2 Prevention 38

3.1.3 Control 38

3.1.4 Warnings 38

3.1.5 Back-analysis 39

3.2 Categories of Instrumentation ***41***

3.2.1 Optical 42

3.2.2 Mechanical 42

3.2.3 Hydraulic and pneumatic 42

3.2.4 Electrical 42

3.3 Different instruments for different parameters 43

3.3.1 Closure Meters 43

3.3.2 Borehole Extensometers 43

3.3.3 Surface Extensometers 44

3.3.4 Discontinuity mapping techniques 44

3.4 Components of a seismic monitoring system 45

3.4.1 Sensors 45

3.4.2 Seismometers 46

3.4.3 Multiplexer 46

3.4.4 Central site 47

3.5 Components of a ground movement monitoring system 47

3.6 Accuracy, Error and Sensitivity of Instruments 49

CHAPTER 4 51

4 Instrumentation at South Deep gold mine 51

4.1 The Ishii strain-meter 54

4.2 Accelerometers 55

4.3 Geophones 56

CHAPTER 5 58

5 Data Gathered 58

5.1 Numerical Modelling 58

5.1.1 Map 3D 58

5.1.2 Phase 2 61

5.2 Strain measurements 63

5.3 Seismic measurements 64

5.4 Mining production data 66

CHAPTER 6 67

6 Analysis of results 67

6.1 Mining 67

6.2 Numerical modelling results 69

6.2.1 Map 3D 70

6.2.2 Phase 2 81

6.3 Measured strain and seismic analysis 88

6.3.1 Principal stresses calculations from measured strain 89

CHAPTER 7 103

7 Conclusions 103

7.1 Numerical modelling 103

7.1.1 Seismic monitoring 104

7.1.2 Pillar strength and stress 106

7.1.3 Energy Release Rate (ERR) and Rockbusrts 106

Recommendations 108

References 111

Table of Figures

Figure 1: 1 Crushed pillar in massive quartzite (after Martin and Maybee, 2000) 2

Figure 1: 2 3D view of the South Deep gold mine, Watson, (2012) 4

Figure 1: 3 Sectional view of the orebody, after Obermeyer, (2009) 6

Figure 1: 4 Location of South Deep mine in the Witwatersrand Basin, after Ryder and Jager (2002) 8

Figure 1: 5 Locality of South Deep gold mine, after Watson (2012) 9

Figure 1: 6 De-stress Mechanism, after Watson (2012) 11

Figure 1: 7 Mining and backfill sequence for mechanized de-stress method (Plan view), South Deep gold mine (2012) 12

Figure 1: 8 Long hole stoping method (South Deep, 2012) 13

Figure 1: 9 Drift and bench mining (South Deep, 2012) 15

Figure 2: 1 Major Principal Stress trajectories around a rounded opening, after Larsson, (2004a) 23

Figure 2: 2 Stress flow lines around stopes separated by typical regional pillars, Hoek and Brown (1982) 24

Figure 3: 1 General features of a seismic system, Joughin (2010) 45

Figure 3: 2 0^0-120^0-240^0 strain gauge rosette orientation 48

Figure 4: 1 Location of the Regional (Remnant) pillar 52

Figure 4: 2 Position of instrumentation in relation to the regional pillar (Plan view) ... 52

Figure 4: 3 Location of instrumentation looking west from below 53

Figure 4: 4 Proposed final pillar layout and size 53

Figure 4: 5 Ishii 3-component strain-meter (Ogasawara, 2011) 54

Figure 4: 6 Triaxial mine piezoelectric accelerometer (photograph courtesy of South Deep gold mine) 56

Figure 4: 7 4.5Hz Borehole geophone (photograph courtesy of South Deep gold mine) 57

List of Tables

Table 1: 1 Stratigraphic layout of the Basin, Bester et al, (2011) 7

Table 6: 1 Material parameters and pre-mining stress state 70

Table 6: 2 Fault names 71

Table 6: 3 Field stresses 82

Table 6: 4 Elastic properties 82

Table 6: 5 Inelastic properties 84

Table 6: 6 Joint properties 84

Table 6: 7 Magnitude probability table 102

Abbreviations and Symbols

θ_1	angle of inclination of strain-meter 1 from the vertical
θ_2	angle of inclination of strain-meter 2 from the vertical
θ_3	angle of inclination of strain-meter 3 from the vertical
APS	average pillar stress
CCT	classified cyclone tailings
CSIR	center for scientific and industrial research
°	degrees
d	distance
ERR	energy release rate
EGS	enhanced geothermal systems
ESS	excess shear stress
FLAC 3D	Fast Lagrangian Analysis of Continua in 3 Dimensions
FPT	full plant tailings
Hz	hertz
ε_x	horizontal strain
σ_x	horizontal stress
JDi	Java Debug interface
k Hz	kilo-hertz
kN	kilo-newtons
Koz	kilo-ounces
LHD	load, haul and dump
ML	local magnitude

σ_1	major principal stress
ε_{1i}	major in-plane strain
τ_{max}	maximum shear stress
m	metres
MJ	megajoules
MPa	megapascals
mm	millimetres
ε_{3i}	minor in-plane strain
σ_3	minor principal stress
ν	poisson's ratio
RIS	reservoir induced seismicity
RTS	run time system
Mo	seismic moment
m^2	square metres
γ_{xy}	shear strain
τ_{xy}	shear stress
ε	strain
S1	strain 1
S2	strain 2
S3	strain 3
$\varepsilon_{\theta 1}$	strain reading in strain-guage 1
$\varepsilon_{\theta 2}$	strain reading in strain-guage 2

$\varepsilon_{\theta 3}$	strain reading in strain-guage 3
σ	stress
SR	support resistance
3D	three-dimensional
UCS	uni-axial compressive strength
ε_{y}	vertical strain
σ_y	vertical stress
E	young's modulus

CHAPTER 1

Introduction

Rock is a complex engineering material whose characteristic behaviour is determined by numerous factors. Pillars are defined as the in situ rock between two or more underground openings and are normally left to stabilize excavations. Most underground mining methods depend on pillars for safe extraction of the ore. Some pillars are left because the rock is situated in non-profitable areas on a temporary or on a permanent basis.

The most common type of pillar failure is continuous slabbing and spalling which in the long run forms an hour-glass shape whereby, according to Maybee (2000), high stresses are normally the cause of progressive pillar failure as indicated in Figure 1: 1. Research has proven that there are inconsistencies between prediction and performance in geotechnical engineering work. The structure of the rockmass in which the pillar is constructed determines its performance. However the rock mass response is difficult to pre-determine due to its uncertainty and complexity.

According to Ryder and Jager (2002), the models used in narrow tabular stopes to predict numerous characteristics of the response of the rock mass to different mining scenarios are based on idealizations, simplifications and assumptions. The manner in which pillars react to imposed loads and their failure mechanisms at deep levels are still largely vague. This is because of the absence of information that describes the pillar before, during and after mining which can be used in design. As a result of the above reasons, underground pillar monitoring research became mandatory in order to provide the rock engineer with data for pillar design

purposes and to ensure that during the extraction process, ground stability is maintained Joughin *et al*., (2007). This project was carried out on a South African gold mine which is located in the Witwatersrand basin. More details of the mine are summarised in Figure 1: 2 showing the mine boundary and are also explained in detail in the following sections.

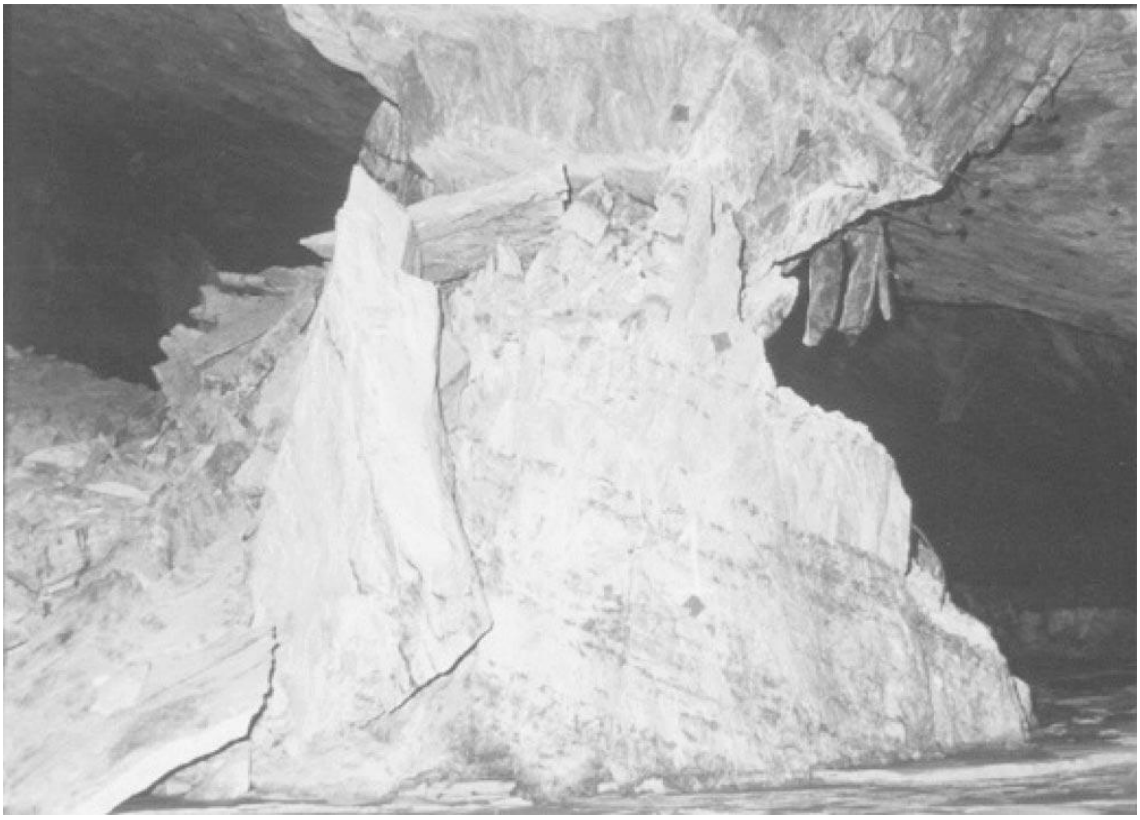


Figure 1: 1 Crushed pillar in massive quartzite (after Martin and Maybee, 2000)

1.1 The Witwatersrand Basin

The Witwatersrand basin is a 6 m-thick geological sequence with thin sedimentary layers which stretches from east of Johannesburg, to the southern Free State south westerly and the shape resembles a shallow elliptical dish ,Witsgold report, (2003). According to Ryder and Jager (2002), with an aerial spread of approximately 350 km long and 200 km wide, the Witwatersrand basin was the first found geological formation near Johannesburg in 1886. Up to now, the Witwatersrand basin is known to be the world's largest known gold producer in South Africa.

Ryder and Jager (2002) further went on to elaborate that conglomerates and quartzites are mainly located in the upper Witwatersrand, while argillaceous clays, tillite, shales and intercalated lava are in the lower Witwatersrand. It is believed that the Witwatersrand basin was a large inland sea draining terrain of basement granites and greenstone belts, containing auriferous bodies. The area was subjected to tectonic upheavals causing advances and retreats of the shoreline and hiatuses and unconformities in the depositional sequence, (Robb & Meyer, 1995). Robb & Meyer (1995), added that shallow water and meandering fluvial systems were accompanying many of these unconformities where sedimentary sorting processes concentrated gold and other heavy minerals together with gravels and pebbles to form remarkably continuous, thin beds of conglomerate.

The delicate sedimentary structures such as ripple marks and cross bedding are still visible and are used to determine flow patterns and gold distribution in the reef horizons, (Jager and Ryder 1999). Thin layers of argillaceous clay material separate beds of strong, brittle quartzites in the vicinity of most of the reefs. These persistent layers mark weaknesses parallel to the stoping horizon and contribute significantly to strata control problems during mining Cook (1998).

The South Deep gold mine orebody is overlain by the Ventersdorp Lavas and it lies within the Central Rand Group of the Supergroup. Figure 1: 2 illustrates the 3D view of the ore body layout at the mine.

1.1.1 Geology at South Deep gold mine

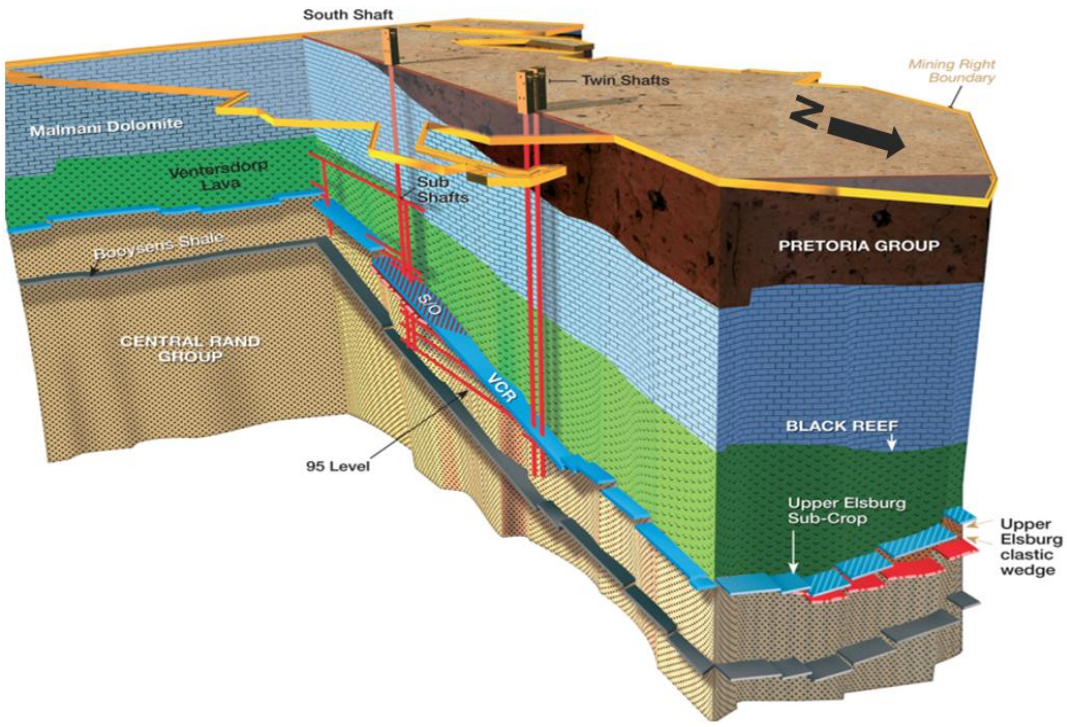


Figure 1: 2 3D view of the South Deep gold mine, Watson, (2012)

South Deep technical report (2011), summarized reef horizons currently being exploited at the mine as comprising of the Upper Elsburgs of the Mondeor Formation and the Ventersdorp Contact Reef (VCR). The Ventersdorp Contact Reef (VCR) and Upper Elsburg reefs are cost-effectively significant with the later sub-cropping against the base of the former causing a major stratigraphic unconformity.

Westerly, the VCR occurs as a single reef horizon that superimposes the lithologies of the Turffontein sub-group. The Upper Elsburgs, which sub-crop with the VCR in a north-north-easterly trend, contains piled reef horizons that form part of a divergent clastic wedge on the eastern side. This 'wedge'has a thickness of up to 120 m to 130 m close to the eastern boundary of the mining right area. About 99% of the South Deep mineral reserves ounces come from the Upper Elsburg Reefs while VCR constitutes the remainder, (South Deep technical report, 2011).

The Upper Elsburg Reefs consist of the Upper Elsburg Individuals (Waterpan Member) and the Upper Elsburg Massives known as the Modderfontein Member. The Upper Elsburg Individuals comprises of four distinct conglomeratic units, separated perpendicularly from each other by poorly developed conglomeratic zones and immature quartz wackes. West of the subcrop, only the VCR, a narrow tabular reef up to 2.5 m thick is developed. The economic viability of the VCR reduces east of the subcrop, Joughin et al., (2011). The Upper Elsburg Massive reefs on the other hand, consist of four conglomeratic packages known as the Modderfontein A Conglomerate (MAC), the Modderfontein Intermediate Bottom Band (MIB), the Modderfontein Intermediate Top Band (MIT) and the Modderfontein B Bottom Band (MBB).

Figure 1: 3 summarizes cross sectional sequence of the mine's geological setting along the east west direction as explained above and shows that the orebody diverges easterly and thickens up to 120 m at the extremity of the mine boundary, with increasing dilution of quartzite middlings occurring. The dip and strike of the orebody fluctuates across the mine, but it generally dips to the South at between 10° and 14°. The lithostatic section showing the rock types constituting the Wits Basin and their strength is further explained in Table 1: 1.

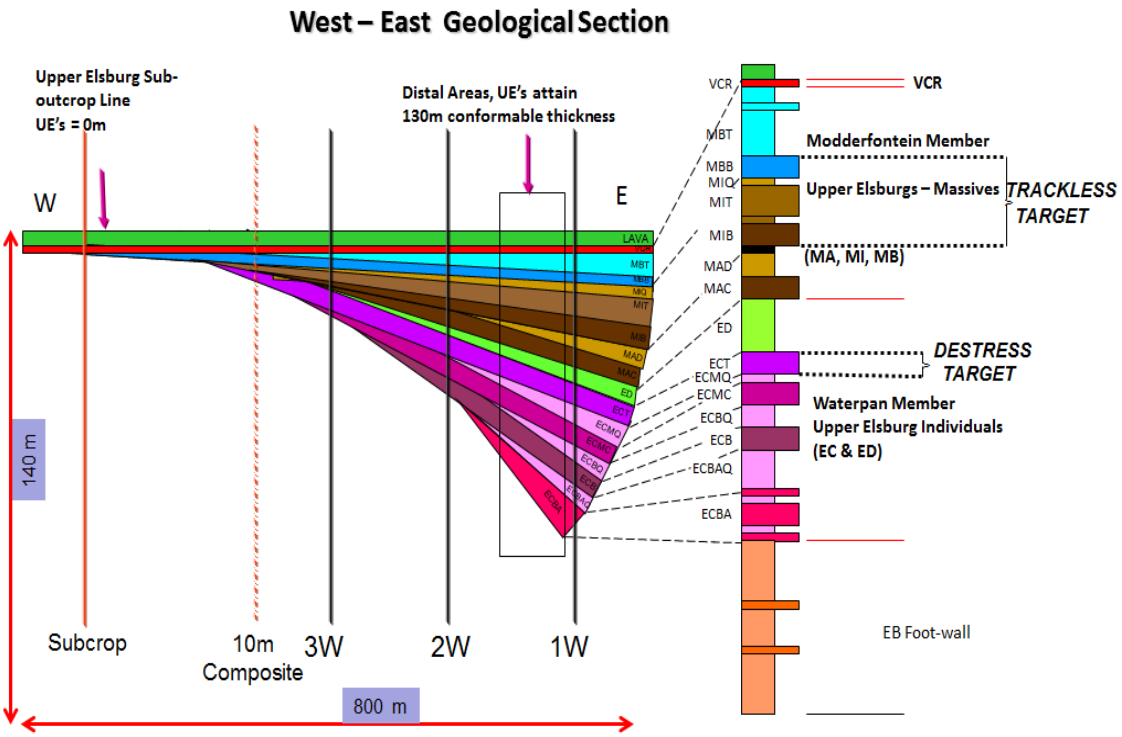


Figure 1: 3 Sectional view of the orebody, after Obermeyer, (2009)

Table 1: 1 Stratigraphic layout of the Basin, Bester et al, (2011)

General stratigraphic units	Detailed stratigraphic units	Description from Paul. Obermeyer (Section Geologist at South Deep)	
Lava-W2b	Lava-W2b	Jointed lava, forming part of the Westonaria formation.	Jointed lava 100 MPa
VCR	VCR	Unit 3 Tuffaceous quartzite, 1.0m thick continuous bed.	VCR (Tuffaceus quartzite) 100 MPa
MB	MBT	Quartzite and conglomerate 50/50 - generally siliceous, phyllonite on bedding planes (2mm), 1.0m bedding on average 30cm to 3.0m, Phase 2 up to 80/20 quartzite conglomerate.	Strong, brittle, massive conglomerates and quartzites >200 MPa
	MBB	Quartzite and conglomerate 50/50, generally siliceous, phyllonite on bedding planes (2mm), 1.0m bedding on average 30cm to 3.0m, Phase 2 up to 80/20 quartzite conglomerate.	
	MBQ	Quartzite and conglomerate 20/80 - generally current mine to top Phase2 siliceous, phyllonite on bedding planes (2mm), 1.0m bedding on average 30cm to 3.0m, 50/50 bottom half of phase 2.	
MI	MIT	Bedding 2.0m average, 90% conglomerate generally siliceous.	
	MIB	Combination of MBT and MIT, varies, main tm3 target.	
MA	MAD	Slightly argillaceous quartzite, quartzite and conglomerate 50/50, phyllonite on bedding planes (2mm), 1.0m bedding on average 30cm to 3.0m.	
	MAC	Opens up to 12m thick (corridor 2 and 3), robust conglomerate, bedding 2 - 3m thick, bottom phase 2 (thins) 50/50 quartzite conglomerate, remains siliceous, rough surfaces.	Argillaceous quartzite 170 MPa
ED	ED	Argillaceous quartzite, phyllonite abundant on bedding planes (0.5cm to 5cm), 30cm to 60cm	
EC	ECT	2 cycles average thickness 2.0m, top cycle sub argillacious, bottom cycle siliceous, rough surfaces, cycle may be split by phyllonites	Variable – strong brittle, massive conglomerate > 200 MPa to weak 100 MPa, layered quartzite
	ECMQ	Argillaceous quartzite, phyllonite abundant on bedding planes - 0.5cm to 5cm, 30cm to 60cm	
	ECMC	Bedding 2.0m average, 90% conglomerate generally siliceous, 3 bedding planes, rough tight no infill.	
	ECBD	Quartzite / conglomerate/ quartzite, bedding 60cm - 30cm to 120cm	
	ECB	Bedding 2.0m average, 90% conglomerate generally siliceous, 3 bedding planes, rough tight no infill.	
	EC9Q	Argillaceous quartzite, phyllonite abundant on bedding planes - 0.5cm to 5cm, 30cm to 60cm	Footwall sequences of quartzites and conglomerates Alternating strong >200MPa and weak 100 MPa sequences
	EC9C	60/40 conglomerate, multiple cycles (up to 5, thickness) 1 - 3m, conglomerate separated by capping of argillaceous quartzite and/or phyllonites	

1.2 Locality of the mine

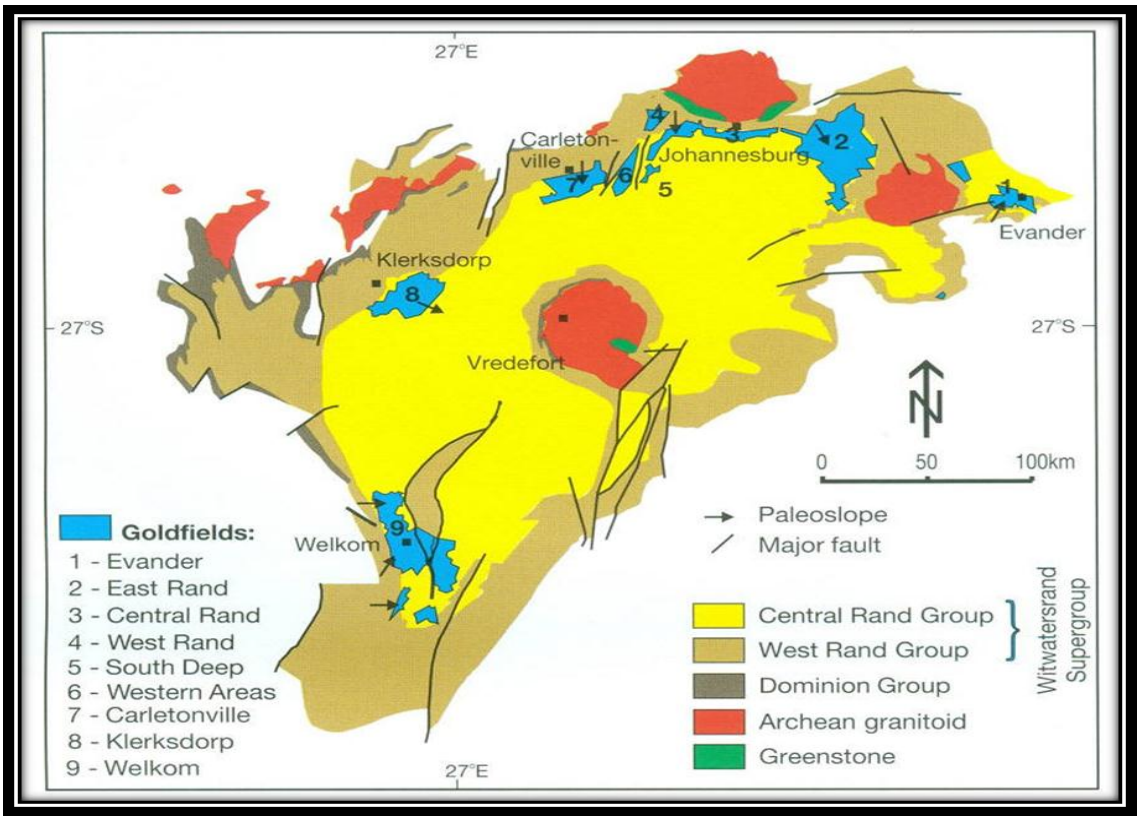


Figure 1: 4 Location of South Deep mine in the Witwatersrand Basin, after Ryder and Jager (2002)

South Deep is located in the superior localities of Westonaria, 45 kilometers southwest of Johannesburg and 20 kilometers south of Randfontein in the West Witwatersrand mining region of the Witwatersrand Basin (Figure 1: 4). The entire mining lease covers 3 563 hectares and extends for 9.5 kilometers north-south and 4.5 kilometers east-west at its widest points. The mine is considered as the flagship for growth of the South African gold mining industry with an estimated life expectancy of approximately 70 years. With a production rate of 330,000 tonnes per month, the mine will produce approximately 700 Koz per year from the current 270 Koz and is currently estimated to maintain this production rate until 2057. Current production at the mine is at a depth of more than 2000 m below surface. The production commenced in

1961, and according to the South Deep technical report (2011), the mine has a plant recovery factor of 97, 3 % and a head grade of 5, 5 g/t. Figure 1: 5 shows the location of South Deep gold mine in proximity to other gold mines as well as the city of Johannesburg.

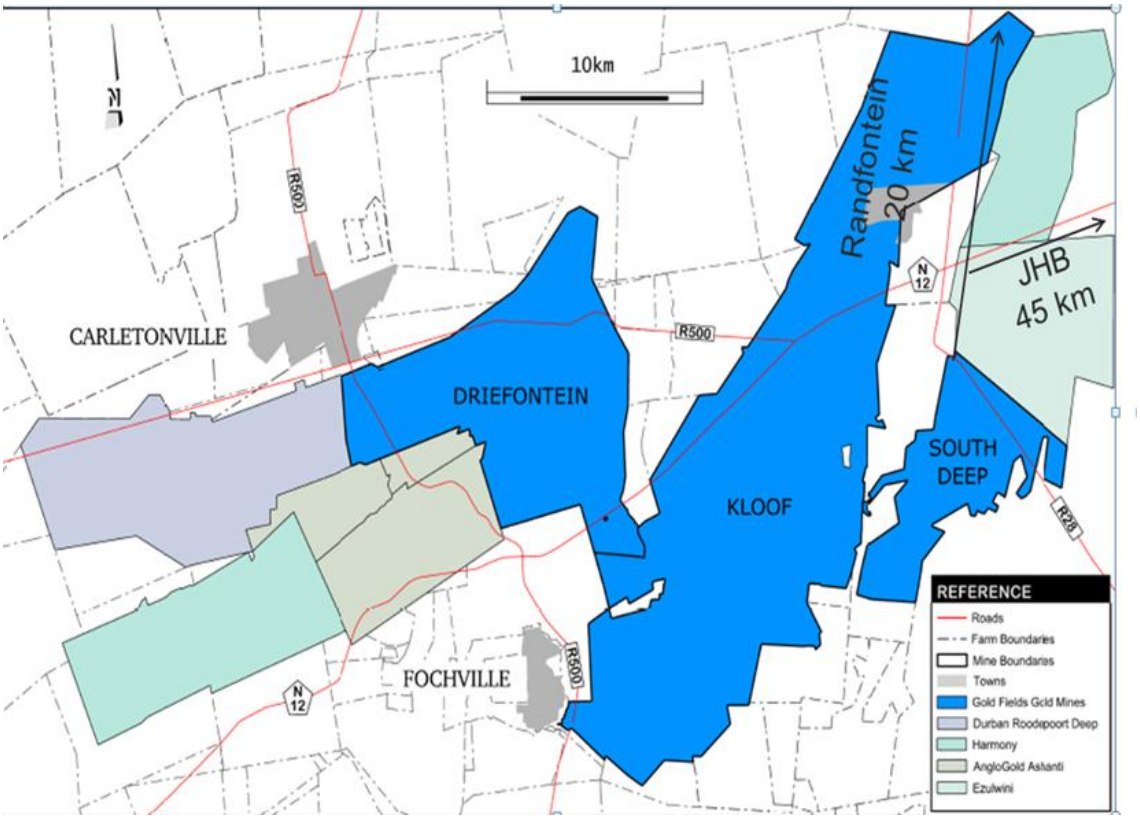


Figure 1: 5 Locality of South Deep gold mine, after Watson (2012)

1.3 Mining methods

South Deep gold mine is a fully mechanized operation for both stoping and development. A complement of different mining methods mainly mechanized de-stress, long hole stoping, drift and fill and drift and benching are currently being implemented at South Deep gold mine in order to optimize the extraction of ore resource. The mine strives to ensure that these are the safe, efficient and cost effective mining methods available depending on the thickness of the profitable orebody. The mining methods used on and around the remnant pillar include de-stress and long hole stoping and there is only one de-stress cut in the remnant area. Initially a conventional mining method with a mining height of between 1.8 m to 2 m was used for remnant pillar mining, however, it was stopped in 2008 when massive mining was introduced.

Due to the depth of the ore body, mining of de-stress horizons has to be planned such that abundant mineral reserves are available for massive extraction at a relatively low stress environment at a depth of more than 2000 m below surface. The de-stress mining method used at South Deep gold mine lowers the vertical stresses by cutting out a horizontal 2 m slice of ground and then backfilling. According to Watson (2012), the modelled rock stresses are reduced from 70 MPa to about 40 MPa enabling extraction of the ore resource at depths more than 2500 m below surface. This becomes equivalent to a shallow mine and therefore ore bodies having thickness greater than 20 m can be mined with reduced seismic risk. Stress shadows are formed in the massive ore body underneath and above the de-stress cut as shown in Figure 1: 6, Watson (2012). Nonetheless, high stresses are channeled to the edges of the cuts and sometimes fracturing occurs internally presenting rock-burst problems. These de-stressed areas are then made available for massive mining and are mined using drift and fill (if the thickness of the ore body is 6 m or less), drift and benching (6 m to 15 m thickness) and long hole stoping (if thickness is greater than 15 m) .

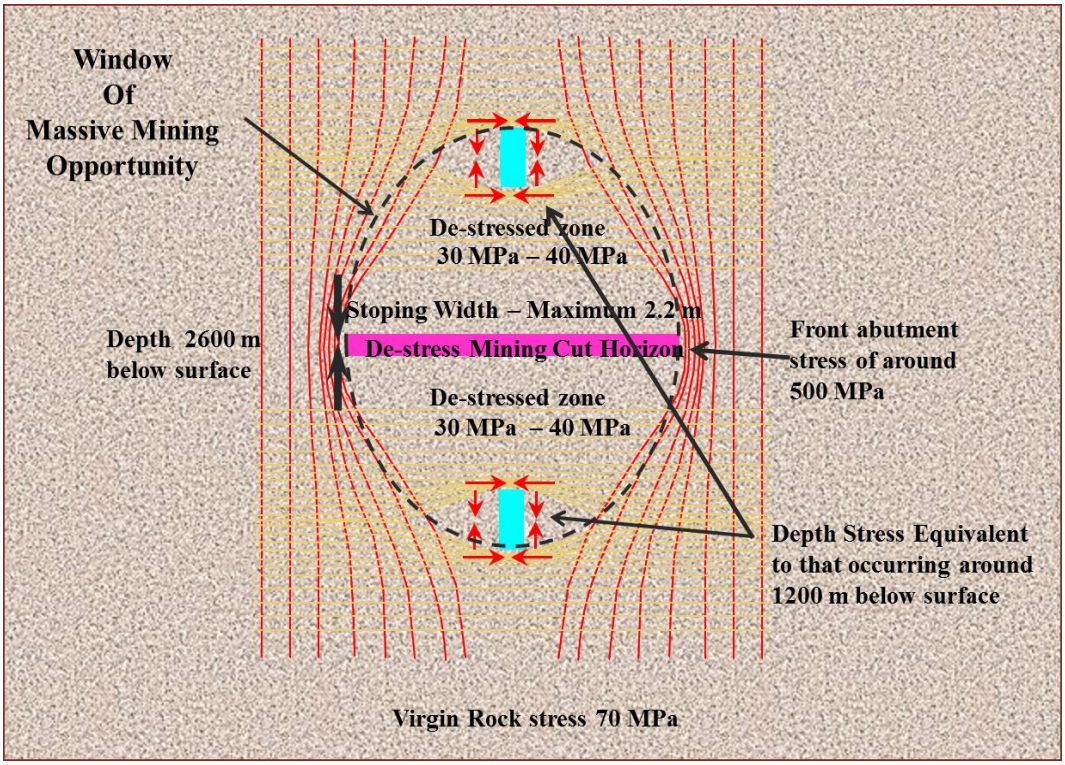


Figure 1: 6 De-stress Mechanism, after Watson (2012)

1.3.1 Mechanized horizontal de-stress mining

To enable the extraction of the massive ore body safely, the prevailing high stress environment in deep level mines has to be effectively de-stressed. The de-stress method involves mining layered horizontal de-stress cuts. Access to these cuts is accessed through a spiral decline, which is positioned beneath a previously mined area that is always de-stressed. The horizontal de-stress cuts are excavated from the footwall, cutting across different reef horizons targeting the massive pay regions that will be extracted eventually.

Access drives will be developed horizontally from the spiral decline to each horizontal de-stress horizon. Maximum mining height for any de-stress cut is 2.2 m while Main Access Drives (M A D's), Stope Access Drives (S A D's) and Stope Drives (S D's) maximum excavation width is 5.0 m. The MADs are mined in one direction (along dip) while the SADs are mined along strike of the orebody, spaced at 10.0 m apart (Figure 1: 7).

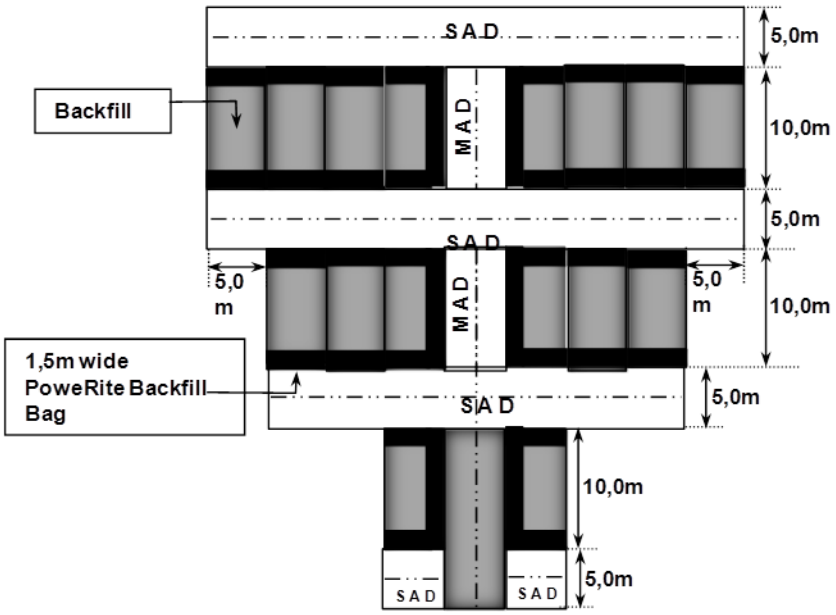


Figure 1: 7 Mining and backfill sequence for mechanized de-stress method (Plan view), South Deep gold mine (2012)

The mining and backfill sequence always ensures that the leads and lags are kept to a maximum of 10.0 m which ideally should be limited to a more acceptable distance of 5.0 m. As all the drives advance, the footwall must be ripped to ensure that the excavation height of 5.0 m is attained at a safe distance from the faces. The primary objective for ripping the drives is to create access for large equipment for massive mining such as the Load, Haul and Dump machines (L H D's) and drill rigs for long hole drilling. These drives also allow for the required ventilation as well as services to be carried close to the working face. 4.5 m mechanical anchors (roof bolts) are installed for support.

The main advantages of horizontal mechanized de-stress method include higher grade de-stressing, adjustments to the layout to avoid geological structures and multiple long-hole stopes can be stacked on top of each other to form one large stope.

1.3.2 Mechanized long-hole stoping

Long-hole stoping is the currently preferred method because it is more efficient. Main ramps are developed on the upper and lower levels and can be up to 30 m apart, (stage 1 of Figure 1: 8). Top and bottom drives are developed from the top and bottom access ramps with dimensions of 5.5 m × 5.5 m. Stage 2 indicate a slot raise being developed from the access drives, and later the slot is completed using overhand or underhand drilling (stage 3). The slot acts as a free face for the long-hole drilling and blasting of the stope as shown in stage 4 of Figure 1: 8. The stope will be 15 m wide and 60 m long. Stope height depends on geological complexities and grade considerations and it is expected to go as high as 35 m in the future. Primary stopes are mined initially and then filled. Once the backfill has cured, the adjacent secondary stopes can be extracted. PoweRite bags are being used to provide a more robust bulkhead and enable faster fill rates.

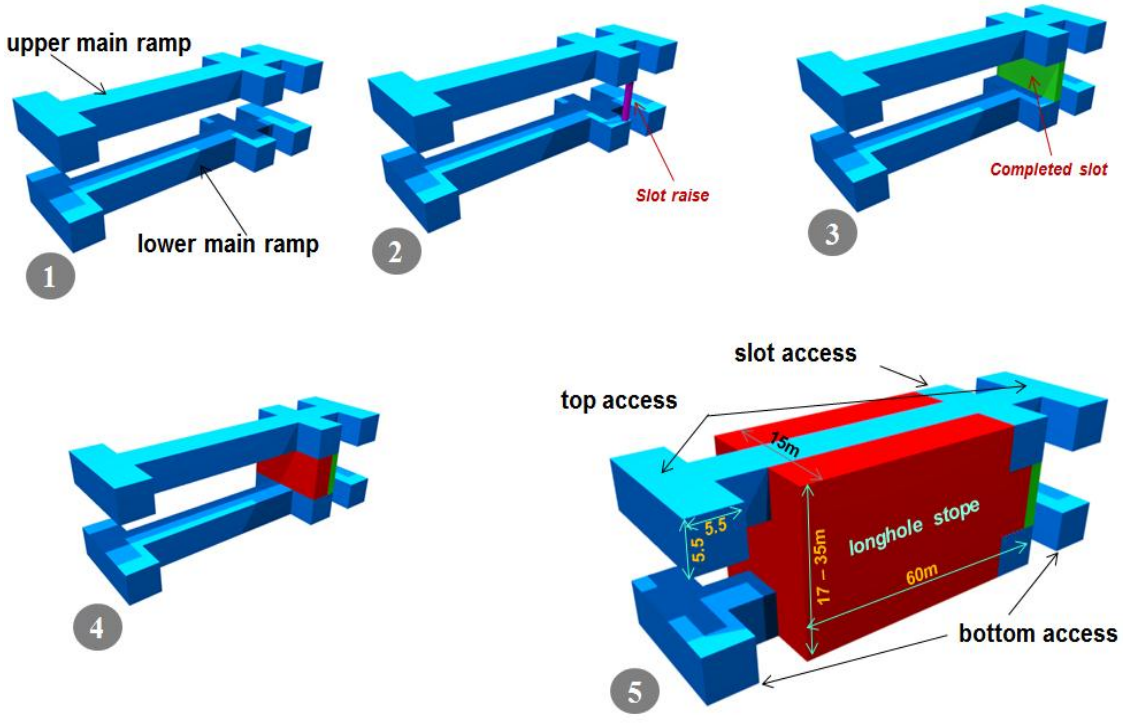


Figure 1: 8 Long hole stoping method (South Deep, 2012)

1.3.3 Mechanized drift, bench and fill

This method is commonly used at South Deep, although in future it will be used only where selective mining is required (Figure 1: 9). According to Joughin *et al*., (2011), benches are drilled with a long-hole drill rig, and usually blasted in a single round. These benches are normally 6 m deep although up to 15 m deep benches have been blasted.

Firstly, drifts are accessed by means of the drift accesses which advance at approximately 3.7m for each blast (stage 1 of Figure 1: 9). Later the benches are mined from the opposite direction (stage 2) at a lower elevation using vertical holes (stage 3). The lower main ramp is used for mucking the broken ore from the bench and the mucking is carried out remotely to prevent exposure of people to the unsupported bench walls and backfill from adjacent benches. Once the bench is mined and backfilled the neighbouring drifts and benches are mined. Alternate drifts are developed, benched and filled. Split sets are used as primary support and the secondary drifts are mined in a sequence retreating back towards the point of access. Backfill bulk heads are constructed at the entrance to the bench from the lower main ramp.

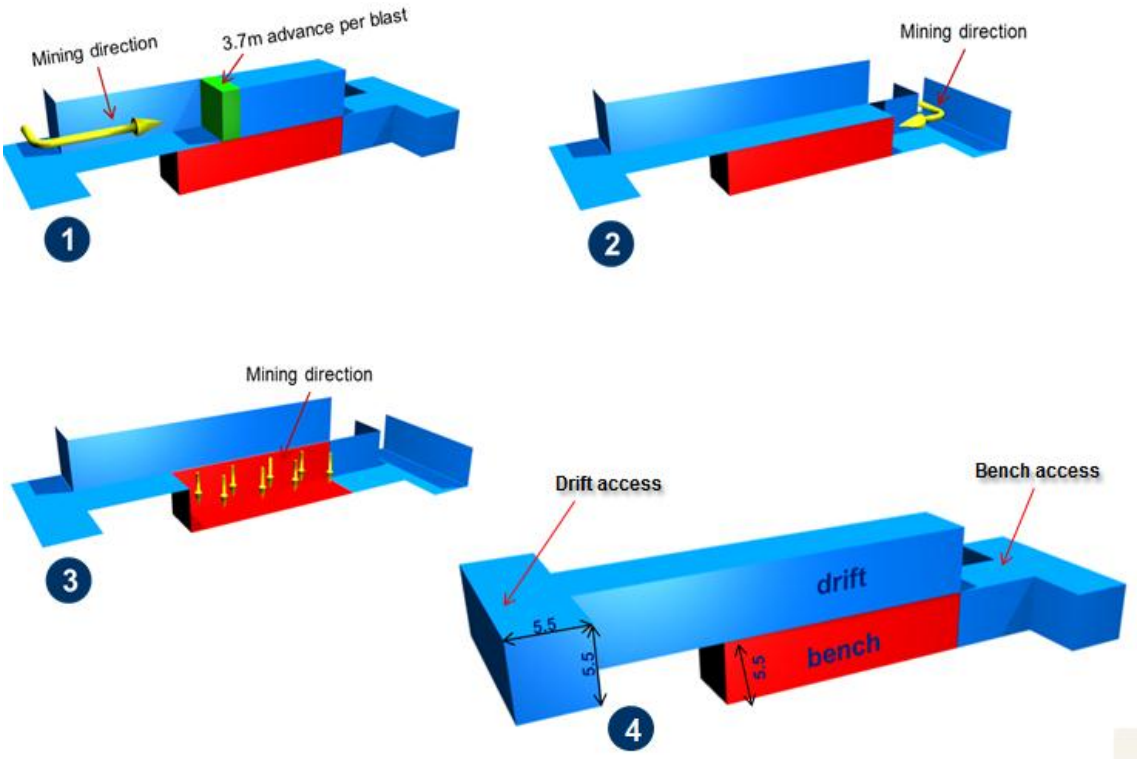


Figure 1: 9 Drift and bench mining (South Deep, 2012)

1.4 Support implemented at South Deep gold mine

When an underground mine reaches maturity the mining activities move from development towards the mining of stopes of noteworthy sizes and the retrieval of pillars, increasing the support design problems encountered.

According to the South Deep support standard (2012), mechanical props with load spreaders are the temporary support units on the mine de-stress cut. Additional temporary support is installed at any geological feature exposed within 0.5 m from the contact and not exceeding 1.0 m along the length of the geological feature on either side. When supporting an excavation alongside the development of that excavation, based on the 'tributary area theory', a static Support Resistance (SR) of 39.4 kN/m² is required for the mechanized de-stressing mining method, (South Deep support standard, 2012). The hanging wall is supported by means of tendons not shorter than 1.8m, installed on a maximum of 1.0 mx 1.2 m rectangular pattern. Support holes in the hanging wall are almost vertical, drilled not less than 70º to the horizontal. The first ring of tendons must not be further than 0.5 m from the face of the drive.

Drilling of blast holes in the drives is done after the installation of the permanent tendon support and weld mesh as areal support in the hanging wall. Additional tendon support is installed at all fault and dyke intersections as per standard and any damaged support due to blast damage or rock fall-out, must be re-installed as soon as practically possible.

For ventilation drives and escape routes, the already installed permanent tendon support and weld mesh as aerial support installed in the hanging wall of the stope drive will remain. Additionally, reinforced 1.5 m wide re-inforced backfill bags are constructed on either side of these escape routes in the identified stope drives, leaving an access-way of 2.0 m in width.

1.5 Backfilling

Cemented Cyclone Tailings (CCT) backfill was introduced at South Deep Mine in 1996 as an alternative to the former tailings-and- aggregate fill. The type of backfilling is used for both the narrow tabular stopes (de-stress level) as well as larger stopes. The primary purpose of backfill is to provide regional support for mined-out areas (stopes) underground, maximize ore extraction above the de-stressed level, and improve underground ventilation. The coarse texture of the custom made CCT backfill also allows for good drainage underground.

Backfill scheduling at South Deep is also incorporated in the extraction sequence, both for the de-stress and the massive horizons. Plans are underway to introduce Full Plant Tailings (FPT). The backfill used was recommended by Murray and Roberts taking into consideration their properties which include resistance to closure, free standing height criterion and limiting of seismic events. The use of backfill reduces rock-burst damage due to its superior stiffness, areal support and energy absorption capacity. The presence of backfill on a seismically active rockmass lowers the damaging frequencies of stope vibrations as compared to conventionally supported stopes. The massive mining, which forms the greater portion of production, can then take place safely and efficiently within a de-stressed environment, Joughin *et al.*, (2011). Cemented backfill is necessary when the walls of backfilled stopes are exposed to people or equipment during the recovery of an immediately adjacent panel. Floors may also require to be cemented for improved vehicle performance and easier muck recovery, 'O' Hearne (2009). In addition backfill allows the conduction of stresses from hanging to footwall and furthermore efficiently controls the bedding plane in the hanging wall strata separation resulting in high stresses being redirected from working face to an inactive area. Note that although backfill allows transfer of stress from the hangingwall to the footwall, virgin stress levels are not

reached and therefore, the backfill permits the stress reduction effect of the de-stress cut within the de-stress shadow.

Recently, South Deep gold mine has implemented massive mining method (complementing the drift and fill method) from the previously practiced conventional methods due to the varying thickness of the orebody from just a few meters to 120 m. This mining method was found to be sustainable through the use of remnant pillars together with backfill as a form of regional support during massive ore extraction. This resulted in the need for design of pillars which can withstand high stresses exerted by mining at depths exceeding 2000 m below surface, as well as the increasing seismic activity that the mine is currently experiencing.

1.6 Statement of the problem

The safe, efficient and economically viable deep level hard rock mine is one with shaft systems, ore passes, stoping areas and other underground excavations which are designed to endure and accommodate the rock stress conditions that will be generated by mining operations. The configuration of regional pillars must be designed to reduce the risk of seismic activity whilst maintaining maximum possible extraction and accommodating the requirements of subsequent mechanized massive mining. Pillar failure is eventually inevitable, despite all efforts to reduce strain energy acting on these pillars during mining operations at great depth, Joughin *et al*.,(2011). In massive mining regional pillars eventually become slender and hence stress concentration at the edges of the pillars will result in spalling and slabbing during the subsequent extraction of the massive orebody and this may lead to instability, Petho and Joughin (2007). If one pillar fails, the weight on the adjacent pillars increases and the result is a chain of pillar failures which can be extremely difficult to stop, Petho and Joughin (2007).

In order to reduce the load on the regional pillars, backfill is used as regional support, thereby carrying portions of the load acting on these pillars.

Regional pillars are designed to reduce seismic energy emissions as well as combating rock falls and rock-bursts in deep level tabular stopes where extraction takes place over a large area. These emissions are as a result of high abutment stresses and high closure rates which in turn increases the Energy Release Rate (ERR). South Deep gold mine uses a system of these regional stabilizing pillars together with the cemented cyclone classified tailings (CCT) to minimize seismic energy emission. The complexity and uncertainty of regional pillar behaviour is greater in deep level massive mining since hard-rock pillar design in these circumstances has not been thoroughly explored or investigated as much as in narrow-reef or coal pillar design. This is because the regional pillars have never been implemented in deep level massive mining in South African gold mines.

The aim of this project is to understand the behaviour of regional pillars during both de-stress and subsequent massive mining. This will better enlighten the reader on the unfamiliar problem surrounding regional pillar design in massive hard rock mining at great depths.

This will be done through analysis of data captured by the monitoring systems installed at South Deep gold mine in order to assess deformation on the regional pillar and associated velocities during ground motion. The valuation will assist in both localizing and estimating seismic events magnitude and monitoring the rock mass behaviour during mining. This project is vital to the mine since the extraction of their ore reserves is entirely dependent on the sustainability of these regional pillars. The information obtained from instrumentation

will eventually be used for forward planning to ensure maximum extraction without compromising the safety of workers and avoiding damage to machinery.

1.7 Contents of the Research Report.

The next chapter encompasses researched information on the rock mass response to mining, history of regional pillar design as stope support for deep levels in South African mines as well as the influence of mining and seismicity in deep level hard rock mines. General types of instrumentation available in the mining industry are thereafter summarised, focusing on the objectives of monitoring and when to implement instrumentation. In the fourth chapter there is summary of all the data collected during the course of this project. This is followed by an in-depth analysis of that data, observing trends and evaluating any correlations between measured and modelled data. Finally, conclusions and recommendations are drawn from the data analysis.

1.8 Project methodology

This research will involve gathering information on the past projects done on the design of regional pillars, any previous work done.

1.8.1 Monitoring and Analysis

The monitoring programme will be carried out at Goldfields' South Deep Mine by means of mine visits, collecting data from monitoring systems installed underground and these instruments include;

- High resolution seismic monitoring (accelerometers and high-frequency geophones).
- Stress-change monitoring (Ishii strain-meters).

Later assessment of the seismic risk associated with mining is highlighted by;

- Data processing, presentation and interpretation of data,
- Highlighting factors that may influence measured data and
- To carry out numerical modelling.

1.8.2 Project Resources

Information and resources required for the smooth progression of this project was made available from the following;

- South Deep gold mine provided the data they captured from the instrumentation installed at the mine and the geological background of the mine, mining methods employed and extent of mining done on the pillar.
- SRK reports details previous work done on pillar design and the risks perceived to be associated with these designs. The SRK library has wide variety of text books that assisted in further research.
- Wits University library, for access to research papers and text books.

CHAPTER 2

2 Rock mass behaviour and seismicity

Chapter 1 provided an overview of South Deep gold mine and the research objectives. The following chapter looks at the characteristic behaviour of the country rock mass mainly focusing on the rock mass response to mining. Definitions and general causes of seismicity are also explained with particular attention to mining induced seismicity. Finally, a summary of the history of regional pillars as a strategy of support in South African deep level mines is briefly described.

2.1 Rock mass behaviour

The stability of an excavation made underground is entirely dependent on the strength of the rock mass in which it is constructed as well as the presence of any existing discontinuities. Depending on the mining geometry, sequence and depth, movement occurs along geological discontinuities if the rock shear strength is less than the resultant shear stress due to re-distributed stresses causing disturbances, Larsson (2004a).

If the rock is assumed to be elastic and under any type of loading, there would be stresses re-distribution forming paths around the opening and these paths could be represented in principal stress trajectories. An example for a rounded excavation is shown in Figure 2: 1, Larsson (2004a). Shorter distance between the flow lines resembles an increase in stress and a wider spacing indicates stress relaxation compared to the virgin state of stress. The stresses are expected to return to virgin state as the distance from the excavation(s) boundary increases, i.e, excavation(s) only disturbs the stress field in close proximity.

A rounded shape gives a smoother flow of stresses around the excavation, compared to a square or rectangular shape as stresses become concentrated at the corners. If a non-circular cross-sectional opening is much longer in one direction with sharp corners, zones with decreased stresses may form in the middle of the roof (Figure 2: 2), while increased stress zones are in the sidewalls. There is stress re-distribution over the whole area if stopes are close to the existing one because the stress distribution around an opening will have an effect on the state of stress around the others. Numerical methods are normally used when the cross-sections become more complicated in order to study how the openings will influence each other and what the resultant stresses would be.

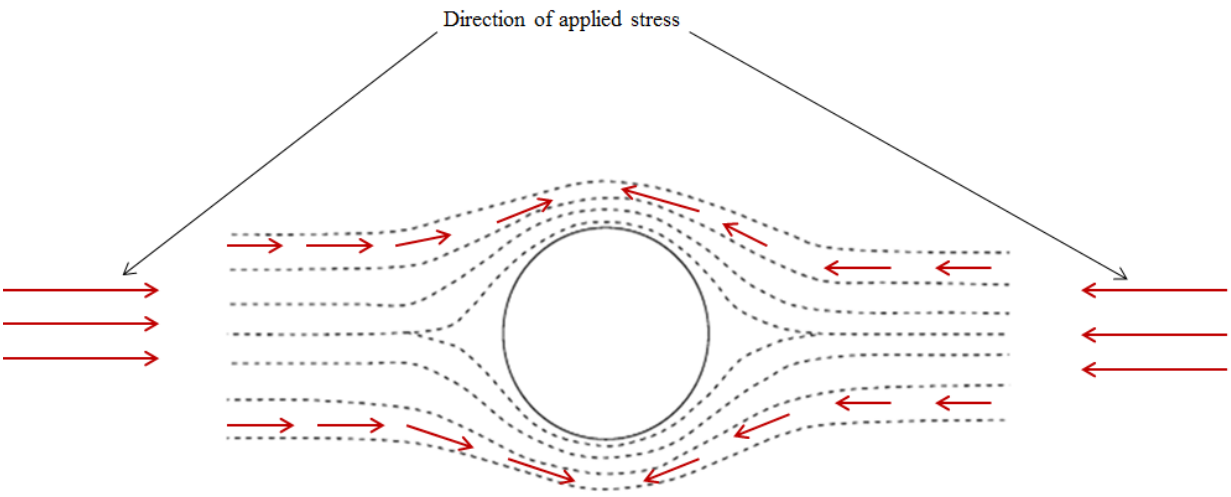


Figure 2: 1 **Major Principal Stress trajectories around a rounded opening, after Larsson, (2004a)**

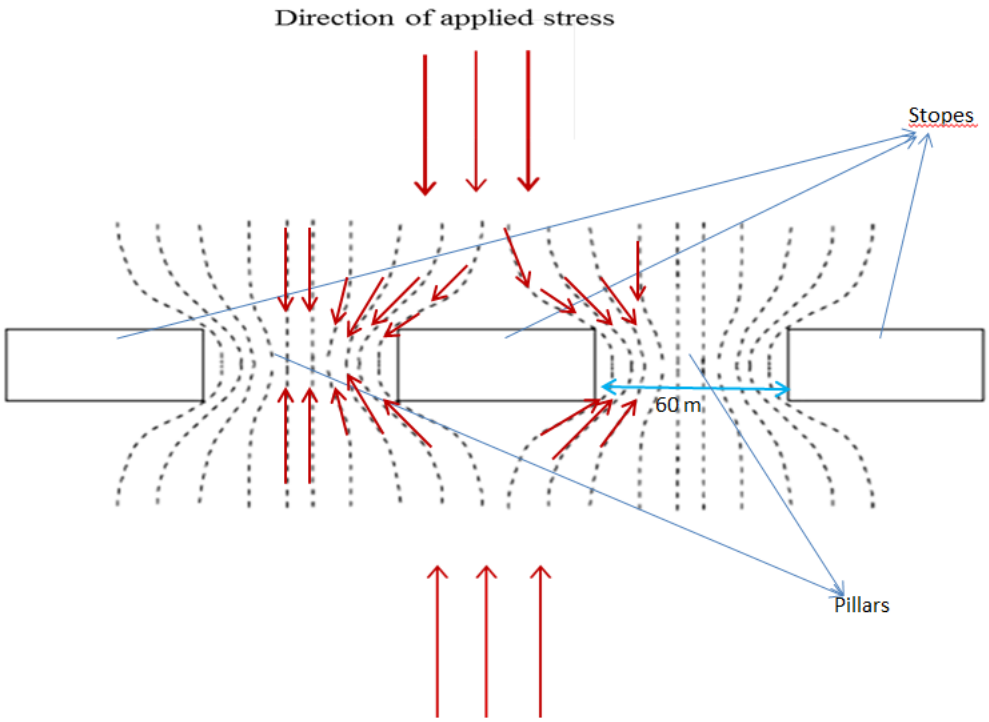


Figure 2: 2 **Stress flow lines around stopes separated by typical regional pillars, Hoek and Brown (1982)**

2.2 Seismicity

Seismicity is defined by Cook (1976), as the violent response of the rock mass to stresses in the form of deformation and failure. A seismic event is a sudden inelastic deformation which causes the release of stored energy in the rock mass. This energy is released when a frictional strength of pre-existing geological structures is exceeded by induced stresses acting on the contact planes causing slip along those geological planes, resulting in instability. The released energy is then emitted in the form of seismic waves. This however, rarely manifests in the form of rock-bursts, which is defined as a mining-induced, sudden, explosion-like seismic event that causes damage underground, posing a hazard to the safety and causing damage to mine structures. Salamon, *et al*. (1984) and Ortlepp and Stacey (2004) said the definitions of rock-

burst and seismicity used by Cook (1976) are vague since they do not elaborate on how large the damage is expected to be.

Development of excavations during mining disturbs the virgin stress state of the rock mass, resulting in increases or decreases in stresses in close proximity to these excavations. The most important factors prompting the occurrence and severity of seismicity are virgin stress state, rock properties which incorporate geological structures present in the rockmass and the influence of the mining methods implemented.

As mining continues to greater depths, the impact of rock-bursts and seismic events may have substantial economic and safety implications and therefore an understanding of the rock mechanics is critical for the design of effective and efficient mining operations. This is due to the uncontrolled disruption of the rock equilibrium and the release of the strain energy stored in the rock body, Cook (1976). Mine sequencing, geology and mining activities, significantly contribute in triggering seismicity. Presence of geological structures in the rock mass weakens the rock promoting rock-burst occurrences. Induced stress generation is unavoidable during mining, therefore this generated stress has to be controlled by designing optimum sequencing plans to limit their adverse effects. Slip along geological discontinuities leads to re-distribution of rock mass stresses and this manifests mine seismicity.

The South Deep cut-and-fill mines are comparable to the Canadian mines studied, Larsson (2004a), regarding state of stresses, mining method and rock properties, therefore the similar seismicity problems are to be expected as mining depth increases. At present the damage caused by seismicity is restricted and can be controlled with the use of stiff reinforcement in the

form of backfill. However, the reinforcement must be supplemented with more yielding and energy absorbing mechanisms for large magnitude events. According to Larsson (2004a), the rock mass in Canadian mines is mainly high strength brittle rock types hence seismic and rock-burst risks increase with increasing mining depth as a result of increasing stress levels, the same situation with what is currently being experienced at South Deep gold mine.

According to Ebrahim-Trollope and Jooste (2005), the seismic monitoring system was developed in the late 1980's and they have assisted in the real time quantification of seismic parameters regularly. These parameters are quantified in terms of time location and magnitude. Inelastic deformation at the source is also measured in terms of seismic moment (Mo) and radiated energy (E). The energy index (EI) concept introduce during the 1990's has seen engineers and management optimistic about predicting almost accurately, the exact time, location and magnitude of existing events. A seismic monitoring system enables a quantitative description of seismicity, thereby managing these seismic hazards and rock-bursts based on an informed decision. The effect of rock-bursts on mining operations can be enormous hence monitoring is vital for proper assessment and alleviation of seismic hazard and risk, consequently minimizing the exposure of equipment and personnel.

Seismic data is used to calibrate and update numerical models and identify key seismically active geological structures to allow strategic placement of enhanced support. Therefore, model factors are adjusted until a good correlation is attained between observed seismicity and expected fracture patterns from modelling results. Potential locations of future rock-bursts are estimated using these adjusted models. Mining operations and sequencing can then be modified in response to modeled predictions, Trifu (2000). Currently technology only identifies high

potential rock-burst areas using numerical models and experience but cannot predict when rock-bursts will occur.

Micro-seismic monitoring systems have gained wide acceptance in most deep hard rock mines in a bid to characterize mining induced seismicity and evaluation by giving mining engineers information concerning the local stress state and rock mass conditions. Seismic data is regularly assessed for mine development activities through optimized mine sequencing, de-stressing and ground support. Micro-seismicity gives an indication of the rock-mass degradation as a result of elevated stresses. The occurrence of seismicity defines whether a geological structure is active. Both the individual characteristics and quantification of geological discontinuities are critical for a reliable evaluation of the seismic hazard in mining operations.

By receiving real-time, up-to-date information on the location of seismic events, engineers and operators can determine where these events are occurring relative to active mine workplaces and assess how the rock mass conditions are changing with time. A micro-seismic monitoring system is expected to be installed at the beginning of a mine's life and it will become a valuable instrument for mine sequence optimization. Through use of seismic monitoring, knowledge of the rock mass response is gained more quickly and a better idea of how ground conditions are changing in response to mining. Research has concluded that there is a variety of ways in which induced seismicity has been seen to occur. However, this report is mainly focusing on the seismicity resulting from mining.

2.2.1 Causes of mining induced seismicity

This can be described as the failure of rock mass as a result of mining-induced changes in stress levels. Seismic events vary in size from barely noticeable ground waves to very large tremors. The main types of mining-induced seismicity as described by the Anglo Gold Ashanti Safety and Health Report (2004), mainly include failure along already existing geological weaknesses such as faults, dykes and joints which typically result in medium to large events far away from workings. Additionally, shear failure of the in-situ rock mass along fractures that results in larger events close to workings and localised bursting or brittle rock failure also known as strain or face bursting are other causes of mining-induced seismicity.

Mining generally leaves voids which result in stress re-distribution in the rock and these openings may collapse producing seismic waves. Higher stresses in mines can result in both strain bursts around rock mass excavation boundaries and structurally-induced seismic activity along the structures. The latter can occur when resultant stresses are higher than the cohesive strength of these structures causing them to separate along their planes of weakness commonly known as fault slip or fracture propagation. Damage of the intact rock mass can occur in major unconnected or stepped continuous geological structures. Ground support systems are continuously improved based on analysis of the ground response and changes in stress levels, confirmed by seismic monitoring.

The seismic response of the rock mass to mining is monitored by seismic systems. The information recorded by the seismic monitoring system is expressed as seismic waves. Numerical and seismic back-analysis of large instabilities is extremely important even though there is not much damage. The rock-mass behaviour connected to pillars, backfill, different

mining layouts and rates of excavation are also important to investigate in order to achieve safer, economic and more productive mining operations.

2.2.1.1 Seismic events associated with stopes

From the research done by Larsson (2004a), the location of the damage and the location of the energy release when seismic events have occurred are one and the same. Several types of failures belong to this category but only three most common will be described here; strain burst, pillar burst and face burst. Ortlepp (1997), confirmed that the following types of events cannot occur if there is no opening.

2.2.1.1.1 Strain burst

A strain burst is probably among the most common forms of rock-burst in mines and also in civil engineering structures. The term describes a violent event where pieces of rock are ejected from the boundary of an excavation. This failure causes spalling or slabbing of surface rock hence pre-existing geological structures are not necessary for fallouts to occur. In an already jointed rock-mass at the excavation boundary, the failure tends to end at the discontinuities or cause buckling of thin laminates of near-surface rock. A strain burst normally causes comparably limited damage and the amount of energy that is released is fairly small.

2.2.1.1.2 Pillar burst

Violent pillar collapses due to local stress re-distribution and the damage severity depends on the location of the failed pillar and the condition of other nearby pillars and rock-mass strength. More energy is released from a pillar burst when compared to a strain burst hence the radiated seismic wave is likely to cause shake-down of already loose rock. Failure of one pillar causes

stresses to be re-distributed to nearby pillars, which may consequently fail violently depending on how close they are to failure.

2.2.1.1.3 Face burst

This is a different form of strain burst whereby there is accumulation of strain energy in the rock mass ahead of the face. Face bursts are characterized by violent ejection of material from the face into the excavated area.

2.2.1.2 Seismic events associated with geological discontinuities

Larsson (2004a), further explained that as a mine grows, a larger area around it is affected by the stress re-distribution and this can lead to re-activation of faults in the area and violent formation of new fractures through intact rock. Shear rupture occurrence has so far only been positively proven in South Africa, Ortlepp (1997) but the most common large-scale seismic event so far is fault slip. The severe damage can result from these events and they can affect a large area and sometimes can be felt on the surface. These events are called mining induced seismic events and may also cause damage on the surface. The events are as follows;

2.2.1.2.1 Fault slip

Fault slip describes slip on a geological structure. Mining activities can influence by reducing the clamping force across the fault, resulting in reduced shear resistance across the fault and increases the shear force along the fault prompting slip to occur. The damage to excavations is as a result of the energy that is released when the slip occurs. The released energy is radiated as a seismic wave, and when the wave hits an opening in the rock it causes;

- ejection of blocks defined by existing joints and fractures, tensile failure close to the boundary of the opening,

- large compressional stresses which causes ejection of the failed rock and
- shake-down of loose rock.

2.2.2 Seismicity at Witwatersrand gold fields

Durrheim (2010), explained that the 1915 Rock-Burst Committee concluded that the shocks originate from specific locations in the mining operations. However, even though there was speculation of high magnitude events in the future in Johannesburg, their severity was not expected to be sufficiently great to rationalize the apprehension of any disastrous effects, Annon (1915). The 1924 Witwatersrand Rock Burst Committee was thereafter appointed to investigate the occurrence and control of rock bursts in South African mines as well as the safety measures to be implemented to preclude accidents and loss of life resulting from these rock-bursts, Annon (1924). Mining induced seismicity and its hazardous manifestation (rock-bursts), were first encountered in the early 1900s when widespread stopes, supported only by small reef pillars, extended to depths of several hundred meters.

Rock-bursting is still one of the most serious and least understood problems facing deep mining operations, claiming the lives, Durrheim (2010). The largest mining-related seismic event recorded in South Africa was in the Klerksdorp district on 9 March 2005 with a local magnitude (ML) of 5.3 whose main shock and aftershocks trembled the nearby town of Stilfontein, damaging several buildings and minor injuries to 58 people. Basic scientific research was then conducted to examine the properties and behaviour of the rock mass and the engineering materials that are used to stabilize and support the mine, Durrheim (2010).

A handbook by Lee (2002), suggests that the study of mine induced and triggered earthquakes started early in the 20th century. Current gold production is at the depths between 2000 m and 4000 m in an extensional setting and is achieved by excavating sub horizontal tabular stopes, with widths ranging from just more than a metre and extending laterally from 100 m to several kilometers. The high level of seismicity characteristically within several hundred meters of the active mine faces, is associated with substantial stress changes in the brittle layers adjoining the stopes. Magnitudes occasionally exceed 5 on the Ritcher scale and higher levels of ground velocities as much several meters per second have been recorded and can be highly damaging (Cook, *et al*, 1996). The rate of seismic deformation has been correlated quantitatively to the rate of ore production, McGarr (1976). The stress changes high enough to cause seismicity often involves increases in the shear stress as well as decreases in the normal stresses clamping the fault plane. The volumes of stope collapse associated with mining induced seismicity can be used to calculate the energy radiated seismically, Lee (2002).

2.2.3 Seismic prediction and control

Techniques were developed to investigate seismograms and seismicity patterns after realizing that early work only concentrated on the quantitative description of the seismic source and seismicity, Mendecki, *et al.* (1996). This time attention was given to the rock-burst damage mechanism, Durrheim, *et al.* (1998). Failed attempts were made to predict seismic events on a routine basis, De Beer (2000). The focus then turned to the management of seismic risk through the continuous assessment of the seismic hazard, optimizing mine layouts, improving support systems, and integrating seismic observations with numerical modelling to have a better simulation of rock mass behaviour, Mendecki, *et al.* (2001). There was a significant change in layout viewpoint in deep gold mines in the early 1990s in which the orientation of regional

pillars changed from strike to dip, since the pre-development of tunnels enables identification of hazardous structures and bracket pillars to be implemented prior to stoping, Vieira *et al.*, (2001).

2.2.4 Rock-burst control

Preconditioning was introduced in South Africa as a way of improving rock-burst conditions in deep mines. This was motivated by the realization that face bursts often occur on deep level mines that practice long-wall mining. Preconditioning is the method used to de-stress the rock ahead of the face being mined by setting of a blast resulting in fractures ahead of a mining face. These fractures control and limit the amount of damage resulting from face bursts as defined by Toper, *et al*. (2000).

Two techniques for preconditioning the faces have been developed which are the face parallel and the face perpendicular methods. These two methods are described by Toper *et al*, (2000), where he noted that to reduce the potential for violent failure, either the stiffness of the rock mass should be decreased or shearing on existing fracture surfaces should be promoted.

Toper, *et al* (2000), went on to suggest that preconditioning does not form any new fractures ahead of the face but promotes slip on pre-existing fractures as a result of high pressure from the explosive gases. The fractured rock mass from the preconditioning blast forms a "shielding cushion" (rock mass with lower modulus) ahead of the face. Seismic events will occur away from the preconditioned face forming a dynamic tensile wave from that event would not cause as much damage as for a normal face. The effect of a preconditioning blast is localized in space so as to avoid face bursting on a specific area. The mechanism of preconditioning is to transfer high loads from the fractured rock further ahead into the face and allow the fractured rock to deform more and stably.

2.3 *Instrumentation*

The main task of instrumentation is to check and verify the rock mass response during mining and for safety. Henceforward, alterations to the designs or counteractive actions are taken to avoid potential damage caused by unsafe mining conditions. This is of outmost importance in the rock engineering and planning aspects. The accuracy of predictions made in project design calculations must be critically verified and there should be a feedback loop to allow changes in the design and its optimization as time progresses and more data become available. The instrumentation implemented at South Deep gold mine include a strain-meter, geophones and accelerometers and these are explained in detail in Chapter 4.

2.4 *Numerical modelling*

Two numerical modelling methods were carried out for pillar stability analysis during this project namely Map 3D and Phase 2. Map3D is a three dimensional, boundary element method of stress analysis which relies on the assumption that the host rock is elastic, isotropic and homogeneous. Phase 2 looks at the two-dimensional cross sectional view of the pillar, highlighting the nature and extent of the surrounding for assessment of possible pillar punching. The objective of the numerical modelling was to assess the potential risk associated with mining in the proximity of the regional pillar as well as subsequent de-stress mining.

2.5 *Regional pillar designs in South African deep level mines*

The greatest challenge in any deep level mining operation is the ability to extract as much ore as possible (Spearing, 1995). Stope support is of paramount importance in deep level mines as it enables the safe and economic extraction of the bulk of the ore resources. Lack of better understanding of the rock mechanics makes effective design of stope support a nightmare.

Gold mines in the Witwatersrand Basin exploit the conglomerate reefs that are thin layers over a wide spread area. The mining excavations left after these reefs have been mined out are tabular due to their small height compared to the lateral extent, Maccelari and Cichowicz (1999). The shape of the resultant excavations will give rise to high stress concentrations at the faces of the stopes causing serious fracturing and resulting in rock- burst occurrences. In an effort to overcome this problem, strips of unmined rock have been left along strike as strike stabilizing pillars. This has so far provided regional support in the stope back-areas and reduces stress concentrations ahead of the face.

To this day, stabilizing pillars are now part of the mine layout in a number of deep level South African gold mines. The motivation of stabilizing pillars was based on the principle of the Energy Release Rate (ERR) concept, which evaluates the spatial rate at which energy is released during mining (Cook *et. al,* 1966). Research done by Maccelari and Cichowicz (1999), showed that the presence of these stabilizing pillars limits convergence in the stopes (reduces stope closures) hence reducing the ERR thereby, limiting rock-bursts and seismicity levels at the stope faces. Factors influencing the regional pillar design are low pillar strength of the material, weak layers within the pillar, and weak layers or partings in the immediate hangingwall and footwall. Due to the uncertainties concerning pillar strength, pillar stress, and loading stiffness, monitoring in experimental mining sections (even in established mining areas) is an essential tool to assess the stability of pillar layouts in different ground control districts.

Seismicity induced by mining in deep level has been analyzed as well as their associated hazard. It was discovered that large seismic events associated with these pillars are prone to

cause extensive damage to active areas. Improving the design of stabilizing pillars is desirable in order to reduce the associated seismic hazard. The computation of average pillar stress values is an important design criterion for the analysis of the regional pillar stability for tabular mining layouts. Numerical modelling can be used exclusively to provide a concrete basis for pillar stability prediction. According to Maccelari and Cichowicz (1999), realism has revealed that the majority of these stabilizing pillars, irrespective of their dimensions and close proximity to adjacent stopes, will inevitably give rise to seismic events with magnitude, $M \geq 2$.

The seismic investigation carried out by Lenhardt and Hagan (1990), at Western Deep Levels Limited indicated that high magnitude events occur below the pillar some distance behind the advancing face. They went on to explain that as mining progresses and stope closure continues in the back area, the pillars stresses also re-adjust. If these pillars become highly stressed, slip along shear planes or punching (if there is more than one shear plane) is likely to follow. This will result in damage to the footwall and reef drives close to the pillars leading to loss of production since some areas won't be accessible. Lenhardt and Hagan (1990), emphasized the need for additional stabilization forms like backfill so that the stresses re-distribute evenly reducing the hazard of foundation failure in pillars.

Maccelari and Cichowicz (1999), emphasized that the rock mass in close vicinity to the mined out areas behave in an in-elastic manner contrary to currently employed design methodologies which assume elastic behaviour of the rockmass, making accurate design of stabilizing pillars a predicament especially in massive deep level mining. It was due to these challenges the writer felt the need to investigate the regional pillar behaviour during massive mining at South Deep gold mine.

CHAPTER 3

3 Underground Monitoring

The previous chapters covered the general causes of seismic events from a mining point of view. This chapter details the purpose and objectives of the instrumentation in general, the different types of instrumentation available in the mining industry. Later, the research is narrowed down to explain in detail the seismic and strain systems currently implemented at South Deep gold for measurement of the ground response to mining.

Before implementing any monitoring programme, there should always be a distinct problem statement to describe and validate the purpose. As mentioned in Ryder and Jager (2002), Dunnilciff and Green (1988) made the following statement in this regard;

"Every instrument on a project should be selected and placed to assist in answering a specific question: if there is no question, there should be no instrumentation."

South African underground mines are experiencing increasing stress levels with increase in the mine depth and this has resulted in increased risk of instability around excavations. Due to the brittle nature of most rocks in underground gold mines, those increases in stresses can be expected to lead to violent failures. Another problem posed by the rockmass quality is the growing cases of activation of faults which consequently lead to release of large energy amounts thereby damaging underground constructions. There is high exposure of workers in close proximity during face or hangingwall bursting. Determining the risk is difficult, hence the need for implementation of instrumentation to monitor the extent of these failures and assess the extent of damage done to the host rock during mining.

3.1 Objectives of a Monitoring System

According to a handbook by Jager and Ryder (1999), a quantifiable description of seismic events and seismicity is considered necessary but not adequate, in accomplishing the following objectives of monitoring the seismic response of the rockmass to mining:

3.1.1 Location of Potential Rock-bursts

To alert management by specifying the whereabouts of potential rock-bursts linked to intermediate or large seismic events and to assist in possible rescue procedures.

3.1.2 Prevention

It is important to check the critical assumptions of numerical modelling such as the sensitivity of parameters to stability thereby assisting in controlling these parameters leading to correction of the designed layout, mining sequence and the support strategy given rate of mining.

3.1.3 Control

To detect changes in seismic factors such as an increase in the number of intermediate and larger magnitude events and their distribution with time. The rate of acceleration in seismic deformation or changes in seismically induced stress can also be identified through the use of a monitoring system. This would enable timeous implementation of control measures such as limit workers exposure to seismic areas at different times.

3.1.4 Warnings

Warnings are required to perceive unanticipated strong changes in the three-dimensional and/or chronological behaviour of seismic parameters and certain characteristic patterns that could result in dynamic instabilities affecting working places. This would assist in warnings to manage the exposure to potential rock-bursts.

3.1.5 Back-analysis

Back analysis of seismic rockmass behaviour connected with pillars, backfill, different mining layouts, rates and ways of excavating is an important technique in ensuring safe and more productive mining. It is necessary to maintain a comprehensive database of seismicity (times, locations, magnitudes, seismic moments, radiated energies, sizes and stress drops) for all seismic events recorded. The availability of the seismic event waveforms recorded prior to large events and rock-bursts located within a short distance from that event would assist in back analysis and research. The use of simple monitoring instruments make it possible to get valuable deductions about rock mass response to mining.

A seismic monitoring system is a commendable endeavor for mines experiencing seismicity, not only for localization and estimation of seismic event magnitudes, but to monitor the rock mass response during mining as well. This can provide valuable input for production planning and sequencing. The amplitude and frequency of seismic waves depend on the strength and state of stress of the rock, the size of the seismic source, the magnitude, and the deformation rate of the rock during fracturing, Mendecki *et al.*, (1999). When a number of seismic events within a given volume and over a certain time have been recorded and processed, the changes in the strain and stress regime in that volume can be quantified. This gives the opportunity to validate results obtained from numerical modelling, where elastic parameters Young's modulus and poisson's ratio (E and ν respectively) are assumed to be constant within a given volume, making stress a function of strain ($\sigma = E * \varepsilon$). The strain and stress changes caused by seismicity, however, are independent, Mendecki *et al.*, (1999), thus, for ground displacement measurements, South Deep installed a strain meter in close proximity to the regional pillar to

record strains induced as a result of the mining and thereafter calculations for the associated stress build up are made.

Induced microseismicity recordings from geophones and accelerometers allow for the remote monitoring of active fractures. Seismic monitoring identifies variations in principal stress orientations during sequential stages of mining, providing insight into the failure mechanism, including possible fracture and stress orientations and characteristics of the source (source strength, the extent of slip, energy and stress release). As such, microseismic events which are defined as events with magnitudes less than zero and comprise the largest percentage of seismic observations at a mine site, can now be used to provide information on the mechanics of strain energy accumulation due to mining and the changing rock mass conditions leading to the generation of rock-bursts. As a result, a better understanding of seismic source inhomogeneity, Mc Garr *et al.*, (1991) and source scaling behaviour as related to mining can be achieved.

Seismology has become an available technique for remote on-going description of rock mass conditions as a result of mining influence. In underground mines, geological structures of different sizes can be activated by the presence of active excavation areas and their interaction with the local regional stress fields. The location of these fractures is provided by the spatial distribution of seismic events. By postulating that the dominant mode of failure is shear, it is possible to use seismic waveform information but the effectiveness of using this approach as a mapping tool can be studied in the context of known geological structures, Trifu (2000). This has resulted in a better understanding of the interaction between excavations, the regional stress field and local structural geology being achieved in mines.

The dilemma faced by mine managers is to find ways to effectively and efficiently extract ore without jeopardizing safety. Recent improvements in seismic monitoring permit the estimation of the deformation and relative stress state of the rock mass in the presence of excavations, as well as the potential for evaluating the hazard associated with ground motion. An extensive array of high-frequency accelerometers are designed to provide real-time location and display of microseismic events with local (Richter) magnitudes as low as approximately -5.

The parameters that may be monitored in underground operations can be divided into those that can be measured directly and those that are derived indirectly. The following is a list of parameters that can be monitored directly in underground conditions;

- Movement across a fracture, joint or fault,
- Convergence of points on the boundary of an excavation,
- Displacements in the rock mass away from the excavation boundary,
- Stresses generated in backfill and

Absolute stress or changes in stress at a point in the rock mass, seismic emissions (ground velocity or acceleration) and wave propagation velocities can be monitored indirectly in underground environments. Although it may seem as though a wide range of parameters are monitored, in the bulk of geotechnical instrumentation only displacement (deformation) and stress are the basic physical responses measured using the available technology and time is always recorded as a fundamental variable.

3.2 Categories of Instrumentation

Four wide-ranging groups of instrumentation are recognizable, and are therefore listed in order of decreasing simplicity and reliability, after Dunnilciff and Green (1988);

3.2.1 Optical

Often referred to as the simplest method that can provide a quick assessment of prevailing conditions, mostly at relatively low cost. These systems include borehole cameras, petroscopes and conventional photogrammetric surveying methods for establishing excavation profiles, boundary movements and for recording natural and mining-induced fractures.

3.2.2 Mechanical

They are used for displacement measurements and involve the use of rods, wires, cables, and tapes to achieve this. However, remote reading or continuous recording is impossible as these types of instrumentation have been overlooked in favour of less dependable electrical systems.

3.2.3 Hydraulic and pneumatic

Hydraulic and pneumatic devices are diaphragm based transducers whereby fluid pressure acts on the side of a flexible diaphragm made of metal, rubber or plastic which are used for measuring support loads and normal components of stress. Read-out is typically done through a standard pressure gauge, but for remote or continuous reading an electrical pressure transducer can be used.

3.2.4 Electrical

These devices afford themselves to be remotely and continuously read, and this is always an advantageous factor in their selection in comparison with others. However, research and experience has proven that electrical instruments are prone to failure especially in the harsh underground environment. The setting up of a suitable power supply underground is also sometimes an issue, however, in some cases the use of battery power can alleviate this problem.

3.3 Different instruments for different parameters

Rock deformation is the main factor in the stability of underground excavations and inevitably it is the most regularly monitored parameter. A diverse range of instruments have been technologically advanced to measure the amount of deformation affecting underground excavations and the rock mass surrounding them. Ryder and Jager (2002), evaluated some other related practises used in hard rock mines.

3.3.1 Closure Meters

These are also known as convergence meters and are probably the most universally installed rock mechanics monitoring devices especially in most South African hard rock mines. This is mainly because of the importance of convergence in the mining excavations situation and the comparative simplicity of the instrumentation. Closure meters are used to define the convergence of the underground excavation boundaries and this is generally attained by determining the amount and rate at which two opposite faces of an excavation move towards each other.

3.3.2 Borehole Extensometers

These devices measure the amount of movement inside the rock mass around an excavation, mainly inelastic enlargement, which contributes to the closure of the excavation. They can also identify the depth extent of discontinuities into the rock mass. According to Ryder and Jager (2002), the change in distance of a reference point at the collar of the borehole from a number of reference points fixed at known distances along the length of the hole are recorded. In this way the axial deformation of the borehole can be determined, and the regions of surrounding rock contributing to the closure of the excavation can be identified.

3.3.3 Surface Extensometers

There is a wide variety of instruments available for monitoring lateral or shear displacement on a rock surface, specifically the dilation and contraction of individual fractures or discontinuities. By recording the initial readings at the beginning of the experiment, measured deformation can be converted to strains. The instruments vary in accuracy and complexity from the simple method of paint lines and tape measure to the highly accurate strain gauge range.

3.3.3.1 Stress measurements

These are instruments used to determine changes in stress and measure the load in support units.

3.3.3.2 Strain meters

Normally strain (or stress) monitoring in mines is carried out using strain cells such as a doorstopper or the CSIR cell, Amadei and Stephansson (1997). Most techniques can accommodate strain changes larger than 10^{-3} but resolutions are no better than 10^{-6}. Stress is calculated using the back-analysis method from the strain readings involving a series of transformation equations (from Hooke's law) with an assumed but mostly measured, modulus of elasticity (E) of the rock mass and the Poisson's ratio.

3.3.3.3 Load cells

These are used for determining the in-situ load and/or stress generated by support items. The support items monitored vary from elongate supports through roof-bolts to backfill.

3.3.4 Discontinuity mapping techniques

These techniques are utilized in mapping exposed fractures or other discontinuities by optical means. Recently more advanced electromagnetic or seismic means are also available or in the process of being developed for mapping out structures deep in the rock mass.

3.4 Components of a seismic monitoring system

Joughin (2010), states that the instrumentation systems used to monitor a given parameter will generally comprise of the sensors, seismometers, multiplexers and the central site. Figure 3: 1 is an illustration of a typical seismic system and these components are explained in detail in the following sub-sections.

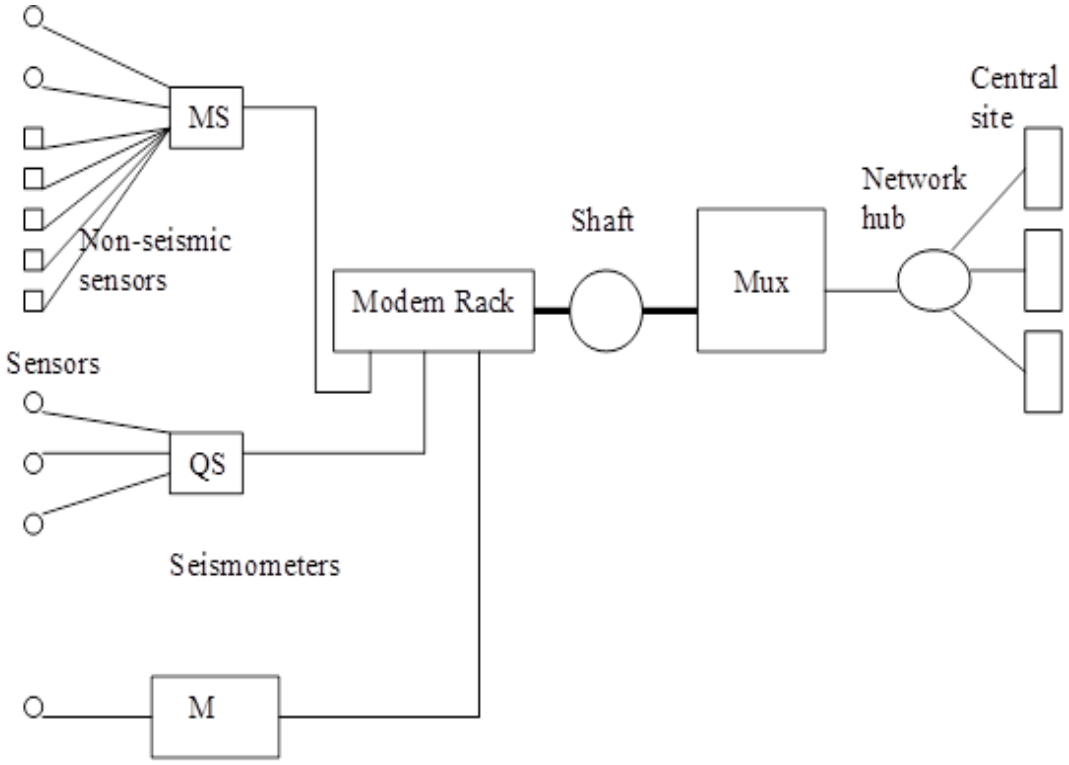


Figure 3: 1 General features of a seismic system, Joughin (2010)

3.4.1 Sensors

The sensors used in mine seismic systems are generally geophones and accelerometers. Each geophone or accelerometer unit measures ground motion uniaxially, so for tri-axial measurements three sensors are mounted together, orthogonal to one another. Triaxial sensors are essential for inversion or calculation of seismic source parameters. Sensors should be installed in a drilled hole at a depth beyond the fractured zone surrounding the excavation.

Generally sensors are installed in a vertical hole, which can be up into the hangingwall or down into the footwall. The competency of the rock should be considered when deciding whether to use up holes or down holes. Down holes are easier for installation, though water is often trapped in the hole, which may cause resonance. The sensors should be well grouted in the hole, so that a solid contact is formed between the sensor and the rock. The sensor cable should not be installed near any form of electrical interference, such as a power cable, electric sub-stations and fans. Noise can also be caused by mechanical vibrations from fans, pumps, ore passes, shafts and locomotive transport (Joughin, 2010).

3.4.2 Seismometers

In the Integrated Seismic Systems International (ISSI) seismic system, seismometers record the signals received from the sensors. The analogue signals are converted to digital signals, using an analogue to digital converter. Digital signals represent the data as discrete values and are not susceptible to interference and distortion. Transmission of data between seismometers and the multiplexor and central site is digital. Seismometers can only transmit one waveform at a time and time is kept through a clock and an extremely accurate time counter. The settings of the clock and time counter are updated on a regular basis.

3.4.3 Multiplexer

Multiplexers provide a means for condensing the data from a number of stations in the network onto one single communication link, especially when the number of communication lines is limited. There is a modem rack and modems communication with the stations with the former normally separated from the multiplexer and placed underground. A fibre optic link is then used for transmission of data between the multiplexer and modem rack, (Joughin, 2010). Originally a serial port joined the multiplexers to the central site but recently, the current systems have the multiplexers linked to a network. The system has the ability to install more

than one multiplexer on the network and this is ideal when the underground network is separated between shafts.

3.4.4 Central site

The seismic system is controlled at the central site. The central site continually communicates with the seismometers, through the multiplexer. The Run Time System (RTS) comprises of numerous co-operating software components that result in many logical communication links. This is controlled and managed at the central site (Joughin, 2010). Seismograms which are received from the seismometers are grouped into seismic events and stored in a database. The seismic events are automatically processed at the central site. Manual processing can be carried out at the central site or on computers linked to the central site.

3.5 Components of a ground movement monitoring system

Strain-meters were initially developed as small multi-component borehole strain-meters for earthquake prediction study, Ogasawara, *et al.* (2005). The strain-meter fundamentally measures diameter change of cylindrical vessel in a rosette layout format as shown in Figure 3: 2. A strain gauge rosette is defined as an arrangement of two or more closely situated gauge grids, separately oriented to measure the normal strains along different directions in the underlying surface of the rock mass for back calculation of stress. Research has proven that for the common case of the simple biaxial stress state, three independent strain measurements (in different directions) are essential for determination of the magnitudes and directions of principal strains and stresses.

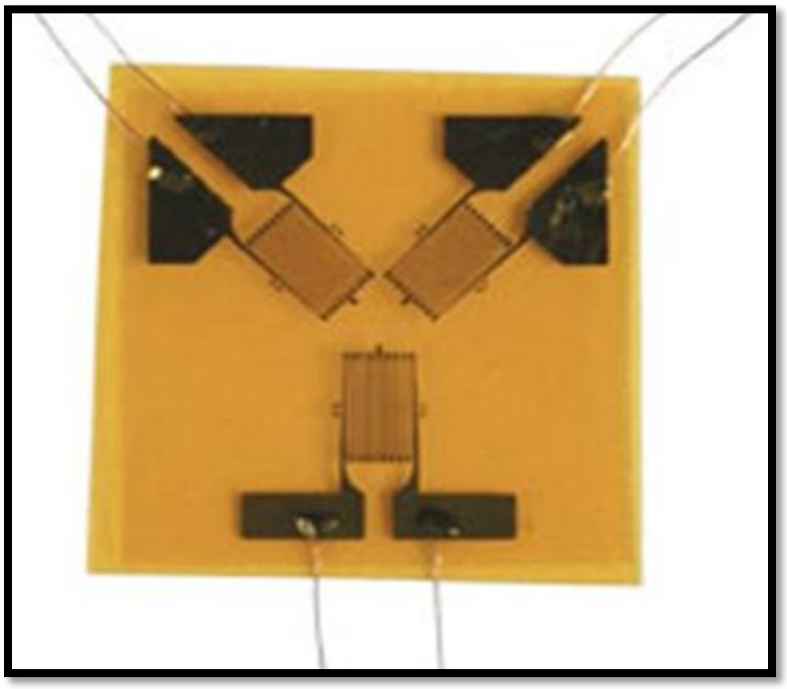


Figure 3: 2 0^0-120^0-240^0 strain gauge rosette orientation

Ishii *et al* (2002), later designed a mechanical enlargement system enabling them to increase resolution and sensitivity. The principle of a lever is engaged and the system is able to magnify about forty times diameter change of the instrument due to applied stress. The displacement sensor is magnetic, which can transfer change of instrument diameter into output voltage change. The strain-meter equipped with mechanical amplification system has sensitivity more than 10^{-9} strain.

3.6 Accuracy, Error and Sensitivity of Instruments

Careful selection of the instrumentation has to be made especially on the design aspects so that they meet the critical requirements of reliability, simplicity and robustness. This factor is of importance due to the harsh conditions (temperature, moisture, abrasive dust and grit, rough handling) related to the underground environment. Dunnilciff and Green (1988) linked reliability with maximum simplicity, and narrowed down the selection requirement by saying: "When selecting instruments, the overriding desirable feature is reliability". For the monitoring system to fulfill its intended functions economically and reliably in the underground mining environment, they must be simple to monitor and process, reliable, easy to install under hostile conditions, adequately sensitive, accurate, robust, easy and immediate access to the data and minimum interference with mining operations.

When selecting the instruments for a monitoring programme they have to be compatible with other instruments used in the program and not only monitoring the given task at hand. According to Jager and Ryder (2002), higher accuracy instruments result in an accurate monitoring system. Instruments vary in precision, sensitivity, reliability and durability and their importance varies with purpose of the program such as collecting design data or monitoring mining. Measuring inevitably involves errors and uncertainties and it is important to be aware of these errors (which include computational errors, duplicate readings, improper calibration, instrument design limitations, etc.), their effect they have and how to minimize them. Final processed data is expected to be clearly and understandably represented. Temperature changes, vibration and corrosion, humidity control in enclosed boxes, noise, friction and environmental effects are some of the factors which can contribute to errors in the monitoring system.

Disparities in measurements are mainly caused by external factors such as electrical interference, and noise vibrations. After installation of the instrument, they should be verified

and checked periodically during monitoring and upon project conclusion for precision. Reliability is the ability to operate under hostile situations even beyond the desired range, high pressures, mining activities, dirty environment, water, erratic power supply, inaccessibility for maintenance. Serviceable life determines how long an instrument can be expected to perform its required function and this can vary from a few weeks to up to several years. The life is influenced by the design of the instrument to endure the adverse conditions.

Although there is evidently a wide variety of instrumentation available for underground operations, but for this project, South Deep gold mine's reliance was placed on the tried and tested monitoring equipment which have proven to be reliable in the harsh underground environment.

CHAPTER 4

4 Instrumentation at South Deep gold mine

The following chapter details the instrumentation installed at South Deep gold mine and their location in relation to the regional pillar that is being monitored. The advantages and shortcomings of these instruments that supported the management's choice are henceforth enlightened.

By assessing the stress build up, displacements and seismic activities that occur during mining adjacent to pillars, this project will ultimately help to safely and economically design regional pillars for massive mining based on an informed decision.

As such instrumentation has been installed in close proximity to the regional pillar in 90 3W to assess the effects of pillar forming and concurrent massive mining. Two 3G 4.5Hz triaxial geophones, four 2.3kHz piezoelectric accelerometers and an Ishii 3-component (42mm diameter) strain meter have been installed around the pillar. Figure 4: 1 shows the regional pillar position relative to the whole mine layout whereas Figure 4: 2 is a plan view showing the location of the instrumentation in proximity to the pillar. Figure 4: 3 is a view looking west from below the reef position.

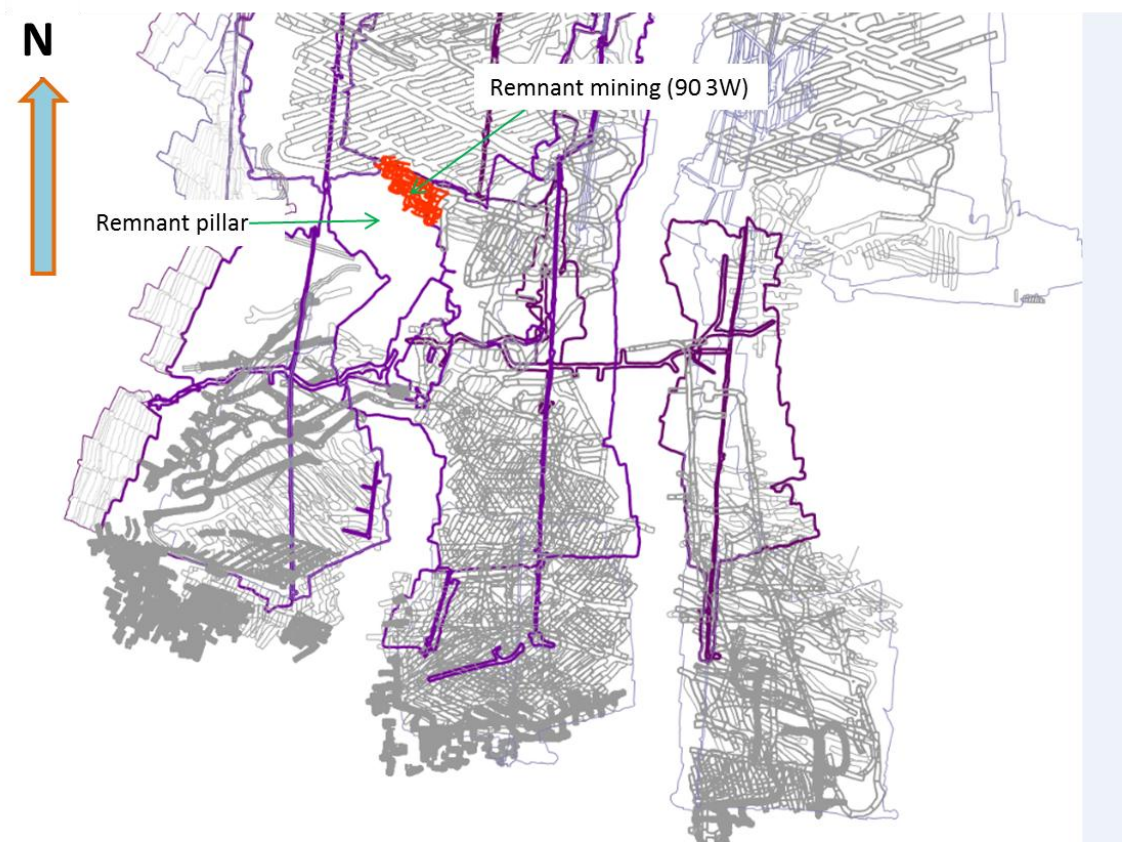


Figure 4: 1 Location of the Regional (Remnant) pillar

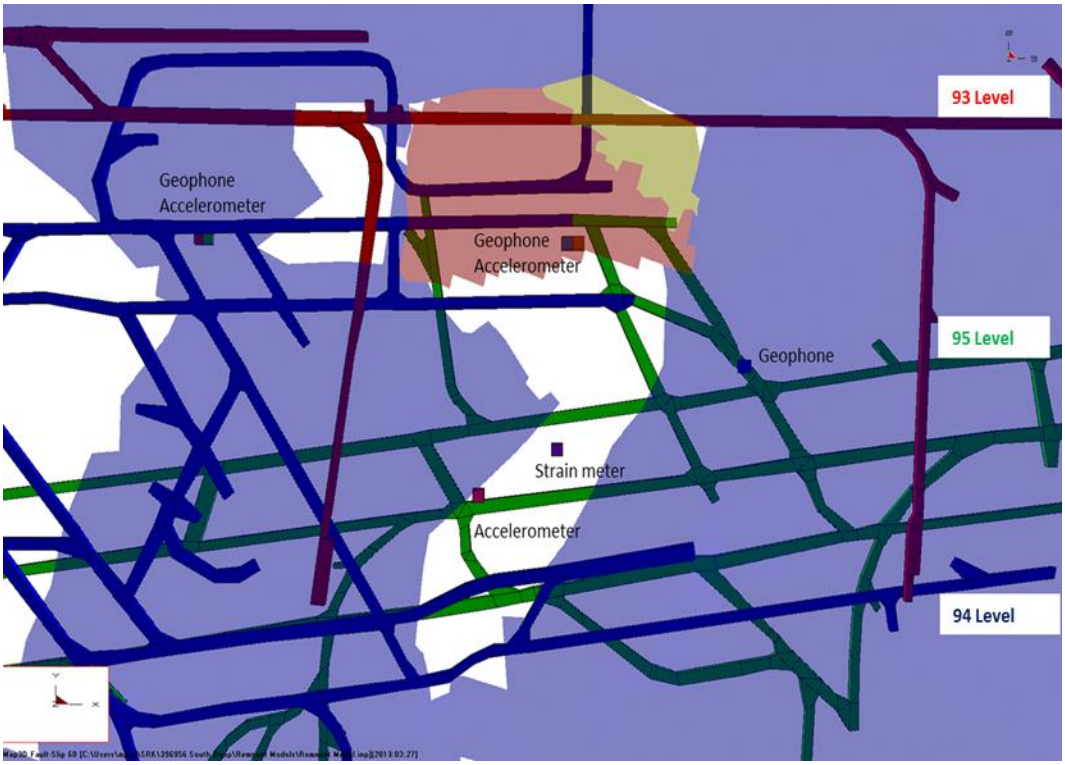


Figure 4: 2 Position of instrumentation in relation to the regional pillar (Plan view)

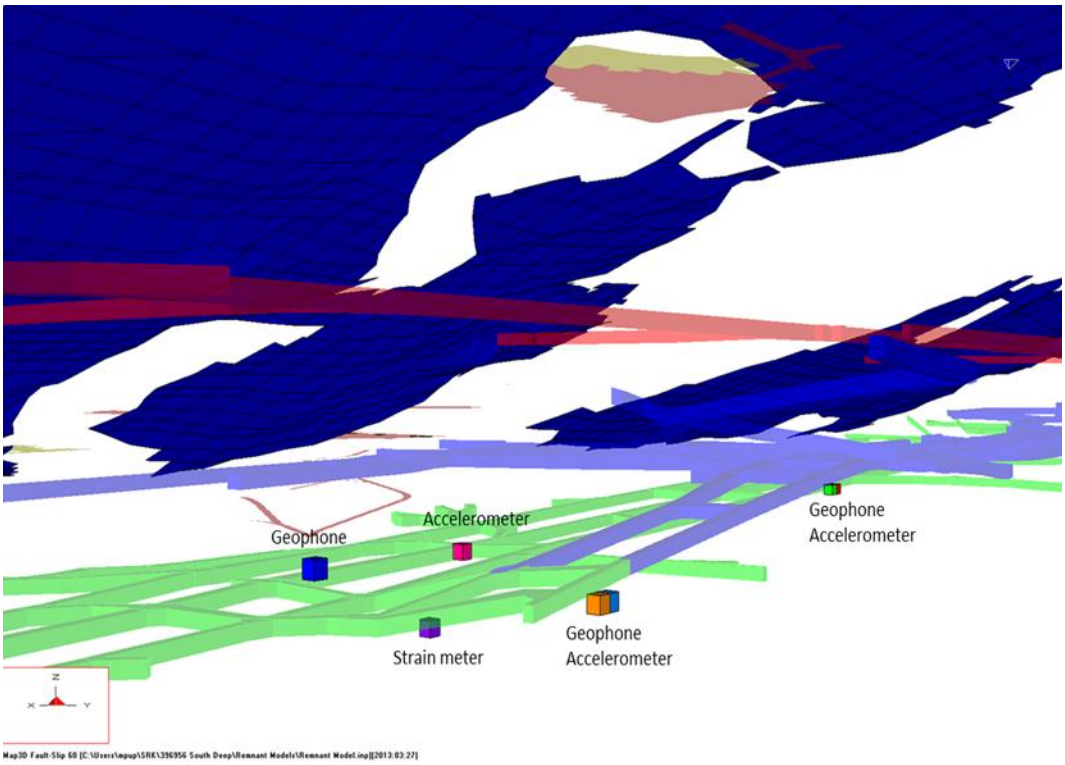


Figure 4: 3 Location of instrumentation looking west from below

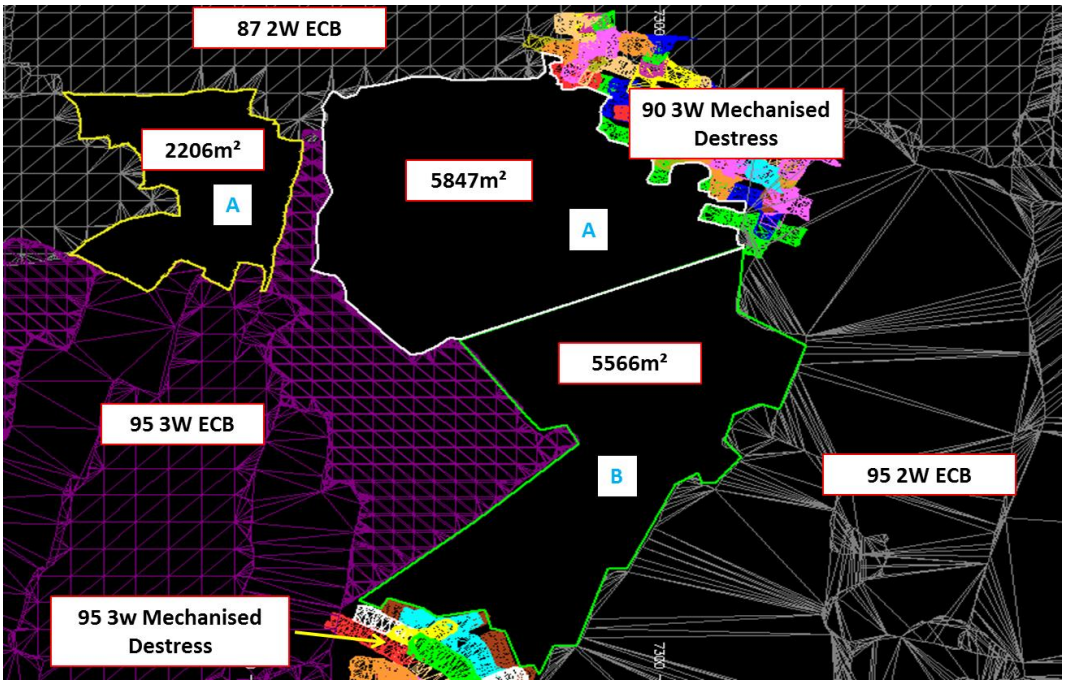


Figure 4: 4 Proposed final pillar layout and size

Figure 4: 4 shows the size (area) of the remnant pillar as at the 4th of April 2013 and the expected final layout of the pillar. Sections labelled A (Total area of 8053 m^2) are to be mined from level 90 3W and section B (green colour outline) is the proposed final pillar size (area of 5566m^2).

4.1 The Ishii strain-meter

These strain-meters can be installed into boreholes at depths from 150 m to 800 m in seismically active areas. Ogasawara (2013), confirmed during an interview held at SRK Consulting in May 2013 that a number of the 3- component strain-meters have been installed in gold mines of South Africa about 3 km deep and strain data is currently being stored in a database.



Figure 4: 5 Ishii 3-component strain-meter (Ogasawara, 2011)

The instrument has a diameter of 0.04 m to 0.1 m, is about 0.5 m long and has a service life longer than ten years. Figure 4: 5 shows strain-meter installed at South Deep gold mine. It is 42 mm in diameter and 1 m long. This strain-meter records 3 components of strain. According to Ishii, *et al*. (2002), the Ishii strain-meter is a borehole strain-meter detecting strain changes in diametric and borehole-axis directions. The strain-meter is much smaller in diameter as compared to the Sacks and Evertson dilatometer, enabling easier drilling and installation.

The drilled core is carefully checked to determine the least-fractured installation location. The strain-meter is then installed at a depth which sufficiently away from fractured zones or stress concentration areas around the cross-cut tunnel. Strain-meters are fixed to rocks by expansive cement grout and the remainder of the hole is filled with ordinary cement nearly to the collar, Ishii, *et al*. (2002). Channel 1 is set vertically to detect strain in the direction of maximum principal stress at the site.

4.2 Accelerometers

During an interview, Watson (2012), confirmed borehole tri-axial accelerometers (see Figure 4: 6) are used at South Deep due to their applicability in mine seismology and ground vibration monitoring. These accelerometers are preferred because of their high frequency and high acceleration (ground motion) measuring capability.

These units are permanently grouted into position and can be monitored remotely. These instruments are sensitive to higher frequencies (up to 2.3kHz) which has direct influence on the smallest event that can be accurately recorded. However, with the recent advances in 24-bit digitizers and high sensitivity geophones, this advantage is marginal, after Goldswain (2013), from Institute of Mine Seismology (IMS). Additionally, they are less sensitive to low frequencies, meaning that they will not clip when very close to the source of a large event.



Figure 4: 6 Triaxial mine piezoelectric accelerometer (photograph courtesy of South Deep gold mine)

The aluminium body gives them high resistance to water ingress, high pressure application and high precision and excellent reliability. Accelerometers can also be installed at any inclination. Given these advantages, 2.3 kHz piezoelectric accelerometers were decided to be best suited for dense monitoring networks at the mine.

4.3 Geophones

Geophones are commonly implemented in combination with accelerometers. A wide range of frequencies from 4.5 Hz to 14Hz is available but at South Deep, only the 4.5 Hz, triaxial ones are being used at the moment shown in Figure 4: 7. The 4.5 Hz geophone has a usable frequency bandwidth of between 3 Hz and 200 0Hz, however, it must be installed to within 2 degrees of its pre-set orientation with respect to the vertical.

These are passive devices (do not require powering) which are cheaper than accelerometers and generally more reliable. Geophone sensors are frequently the sensor of choice in most mining applications because they have all the advantages of accelerometers but at low cost. Additionally they have long term stability, accuracy and are generally less susceptible to electrical interference or noises since they produce differential signals. Geophones are generally easy to maintain due to passive coil configuration.



Figure 4: 7 4.5Hz Borehole geophone (photograph courtesy of South Deep gold mine)

CHAPTER 5

5 Data Gathered

This chapter reviews the data processed from the information gathered at the mine and seismic services centre. The information collected from the mine includes magnitude of seismic events, strain readings and mining tonnages. Additionally, the geological information showing the structures around the regional pillar which have a significant influence on the stability of the pillar is also incorporated into the numerical model. The mining tonnages were compiled and presented on a monthly basis. The seismic events and strain readings from the mine was collected on an hourly basis and therefore in this report the data is summarised in the form of graphs.

5.1 Numerical Modelling

Two numerical modelling methods were carried out using Map 3D and Phase 2 softwares. This is because Map 3D modelling evaluates the three dimensional distribution of the pillar stresses. On the other hand, Phase 2 looks at the two-dimensional cross sectional view of the pillar, displaying the nature and extent of the hangingwall and footwall rock and provides a qualitative assessment of possible pillar punching.

5.1.1 Map 3D

An elastic model was constructed using the information provided by the mine in Datamine format which was converted to dxf format. A three dimensional numerical model package Map3D was used for the analysis. The overall model is shown Figure 5: 1. It should however be noted that the analysis is elastic and therefore, does not simulate failure and associated

plastic deformations. The model was used to assess the magnitude of the seismic events and stresses in the regional pillar and compare with the measured results. The enlarged regional pillar is shown in Figure 5: 2 where areas labeled “A” represents the part of the pillar scheduled to be mined out to leave the final proposed pillar layout labeled “B”. The actual pillar mining sequence is represented by Figure 5: 3 where the number inside each block represents the time it was mined relative to others and mining is in ascending order (*i.e.* 2 was mined before 3 and so on).

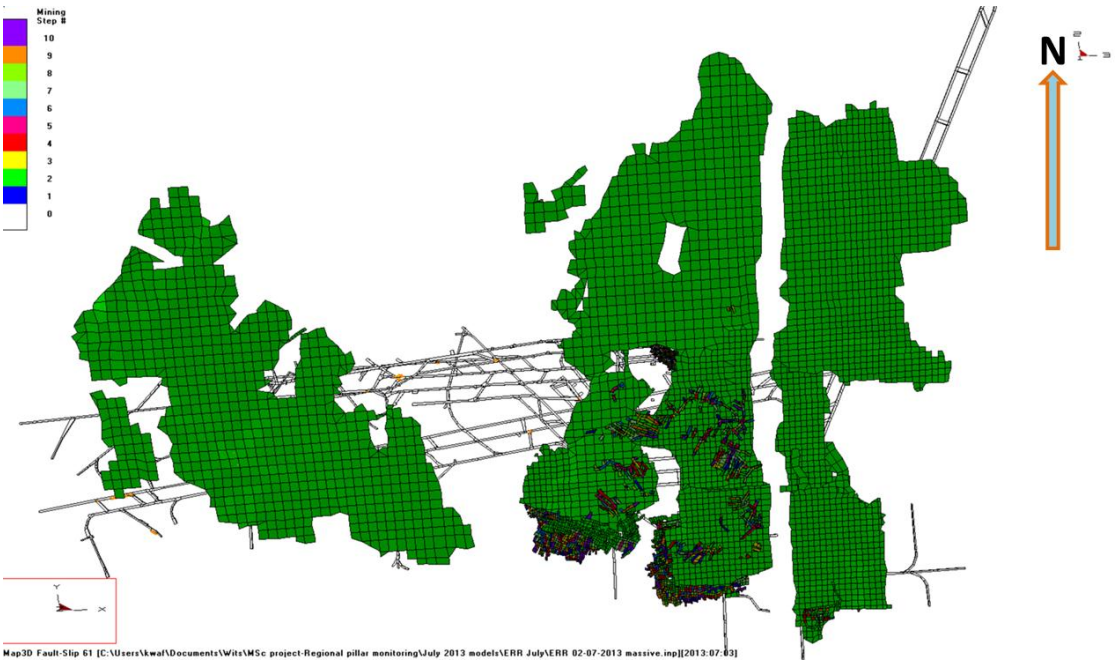


Figure 5: 1 Overall model showing de-stress mining (green) and massive mining (blue, red and yellow) on top

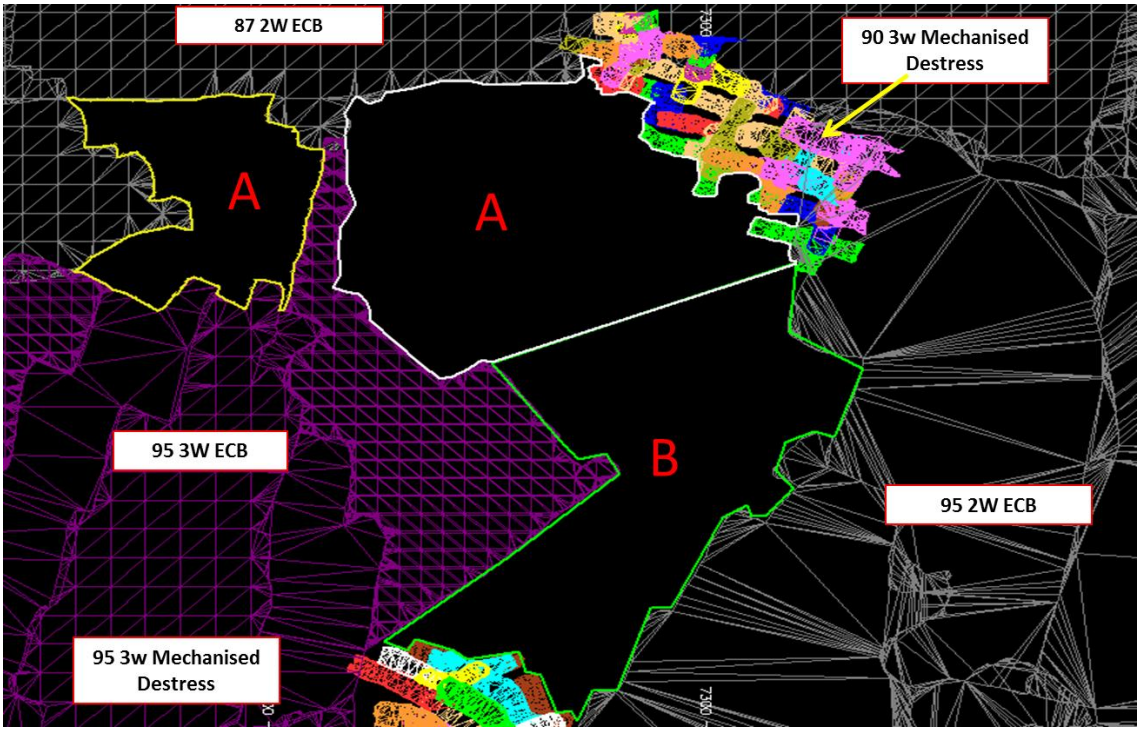


Figure 5: 2 Remnant pillar layout

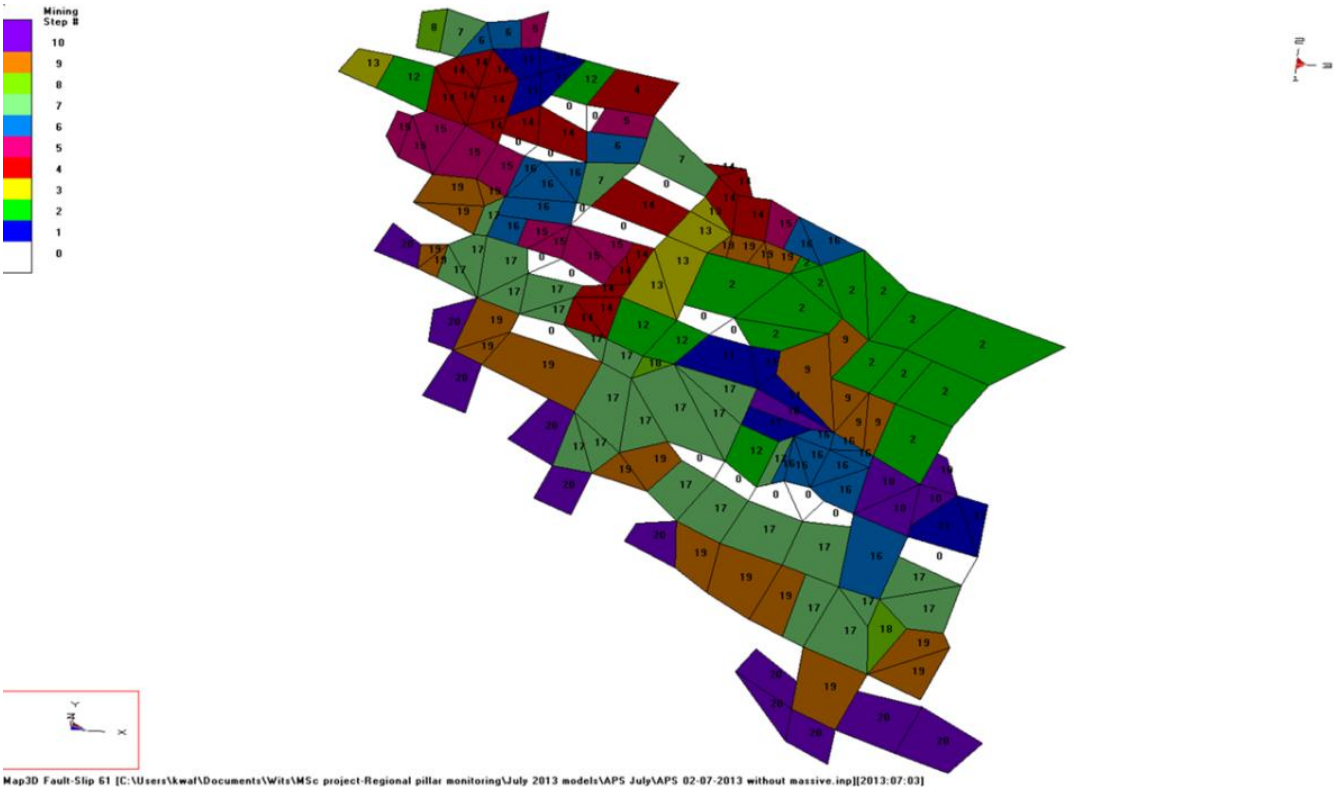


Figure 5: 3 Actual up to date mining sequence done on the remnant pillar on 90 3W

5.1.2 Phase 2

This modelling was carried to improve understanding of the rockmass behaviour. Figure 5: 4 shows how the elastic model which was later was modified (Figure 5: 5) to represent the actual rock inelastic properties and include geological structures cutting across the pillar.

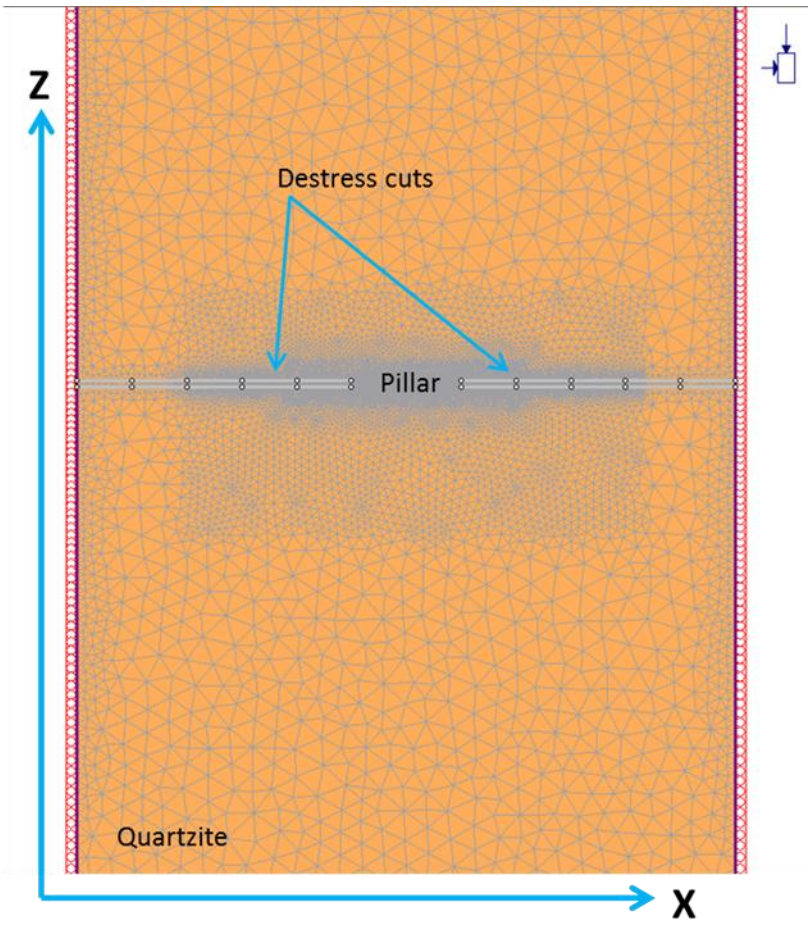


Figure 5: 4 Phase 2 elastic model

The parameters (orientation, cohesive strength and friction angle) of these structures were input into the later model. Analysis was carried out to evaluate the effects of geological structures on the pillar strength. The models show the two dimensional cross sectional view of the pillar cut along the z-x axes as seen on Figure 5: 4 and Figure 5: 5. This was done to clearly assess the

stress re-distribution as a result of de-stress mining around the pillar in order to identify are any signs of instability.

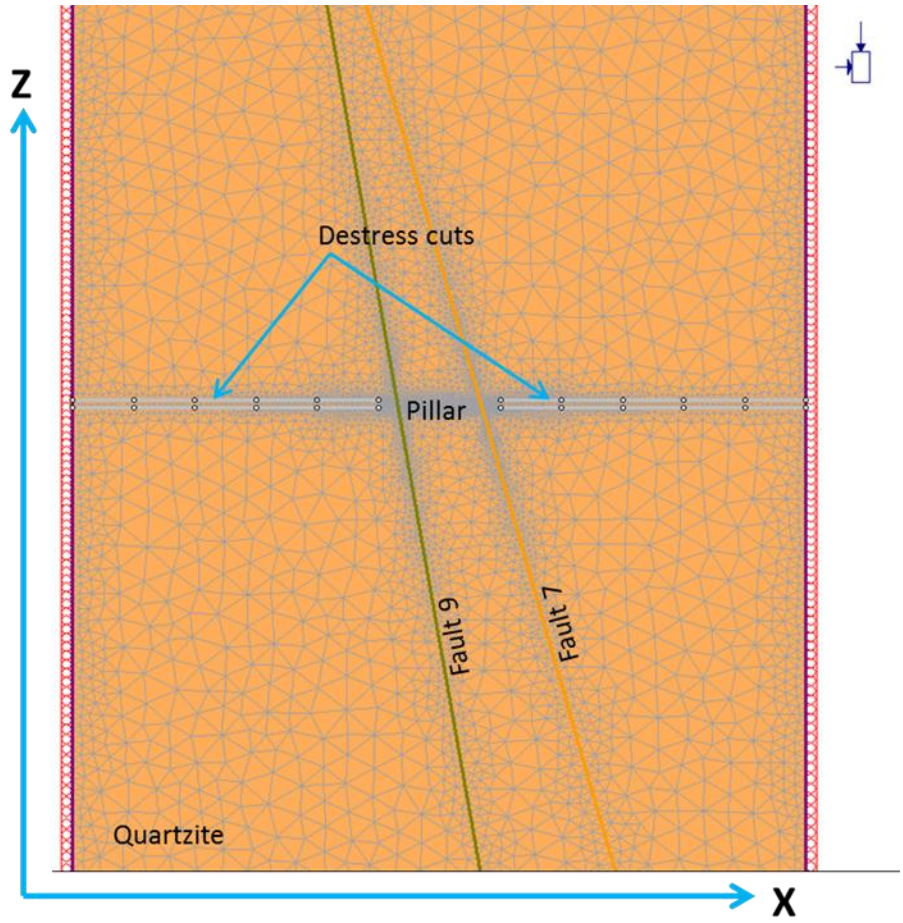


Figure 5: 5: Phase 2 inelastic model displaying the cross sectional view of the regional pillar.

5.2 Strain measurements

The strain data was collected from an Ishii 3-component (42mm diameter) strain meter which has been installed inside the regional pillar (Figure 4: 2and Figure 4: 3 of Chapter 4). The data presented is from August 2012 to May 2013. The induced strains (S1, S2 and S3) are the directional strains inside the borehole. S1 corresponds to the strain gauge oriented to the vertical of the borehole axis, S2 is 120^{o} from S1 and S3 is 240^{o} from S1. To determine the induced strain, the concurrent readings are subtracted from the initial reading. A summary of induced strain against the corresponding date and time is plotted in Figure 5: 6. The orientation of the three strain gauges mounted inside the borehole relative to the pillar position resulted in one strain gauge to be in tension while the other two were in compression.

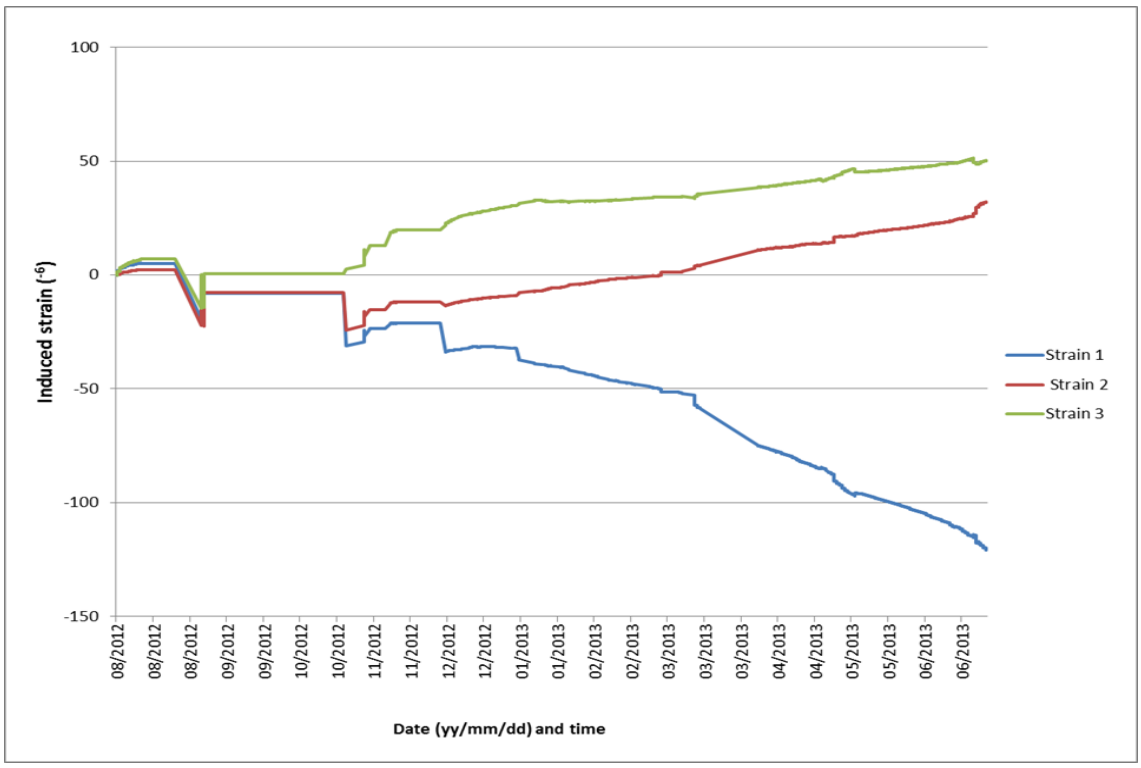


Figure 5: 6 Summary of measured strain data

5.3 Seismic measurements

The data was recorded from the accelerometers and geophones and the signals are sent to the data processing offices where the seismologists use a triangulation method in JDi software. JDi locates the event and further processes the data to get magnitude using a built-in function of the seismic software. The graphs plotted are those of magnitude against date as shown Figure 5: 7. The seismic events considered in the report are those greater or equal to zero since the assumption is that the smaller events as a result of drilling, blasting and tramming operations are also recorded by the instruments.

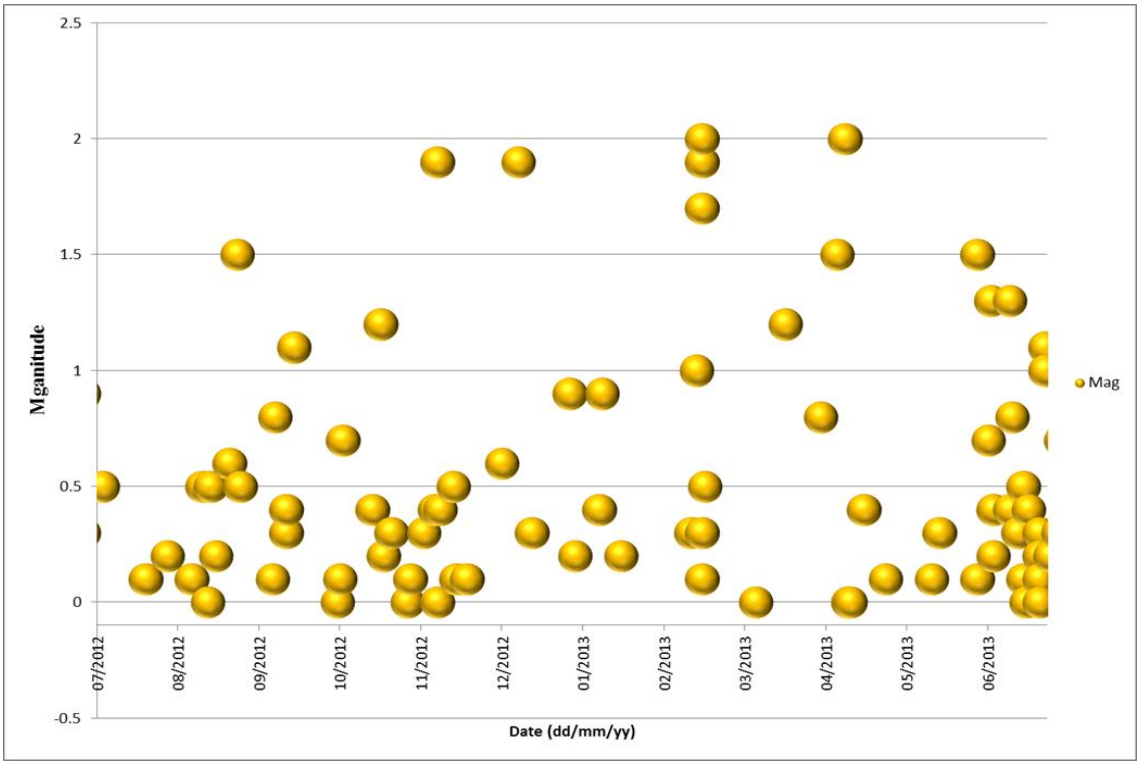


Figure 5: 7 Summary of seismic events (M>=0) from July 2012 to June 2013

Figure 5: 8 shows the location of seismic events recorded inside the regional pillar and in relation to the positions of the geological structures. This illustrates that most of the events recorded were along these geological structures. It should be noted that there are many structures within the regional pillar, nevertheless, only critical ones were selected.

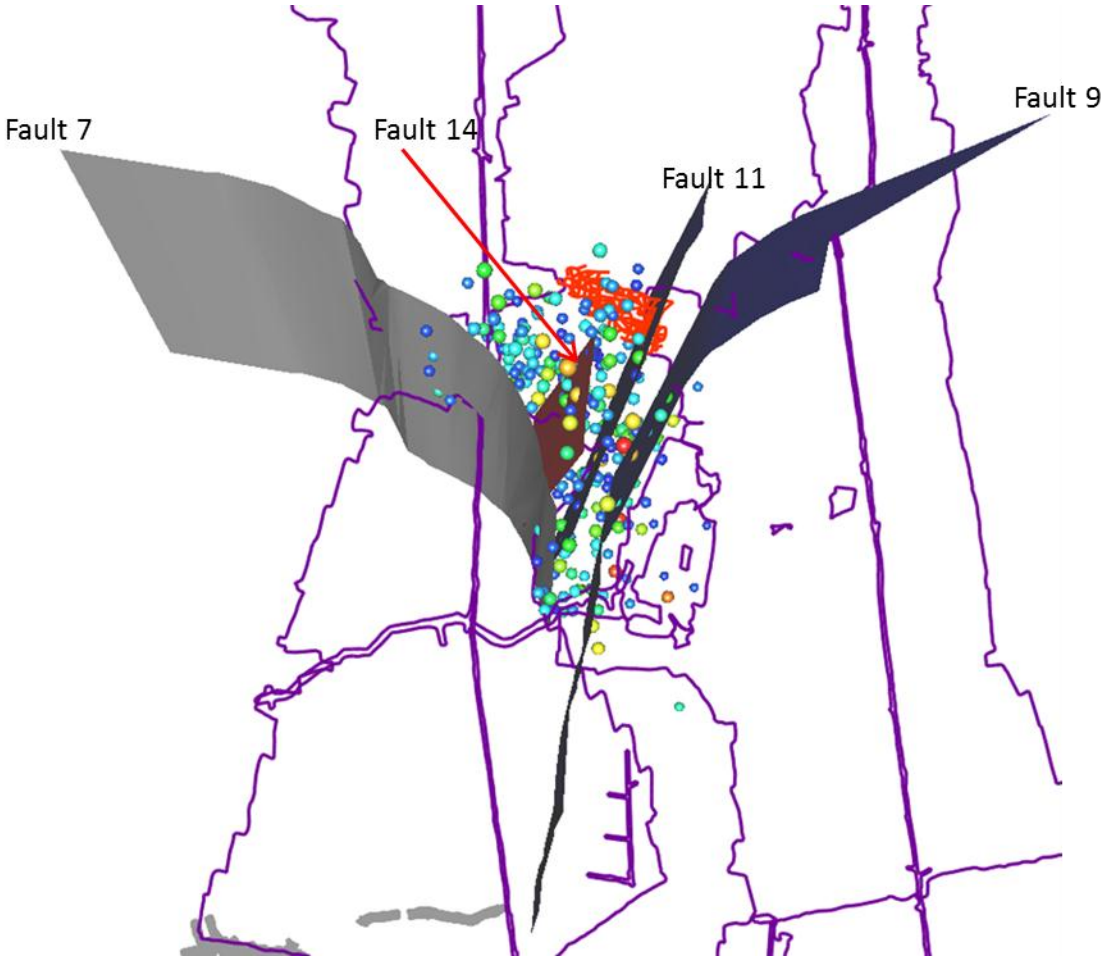


Figure 5: 8 Seismic events inside the pillar and geological structures

5.4 Mining production data

The areas of interest include 87 2W, 90 3W, 95 2W, 95 3W, Corridor 3 and Corridor 4 as shown in Figure 5: 9. These areas surround the regional pillar hence any de-stress or massive mining taking place on those areas is likely to activate geological structures inciting seismicity.

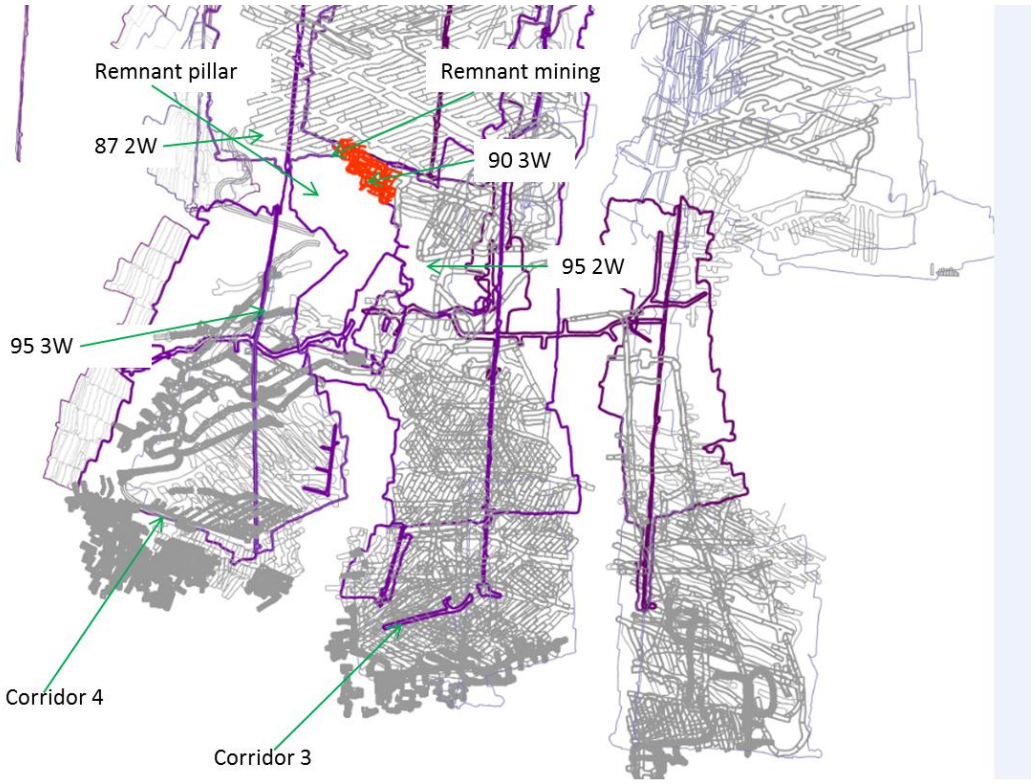


Figure 5: 9 Production areas considered for pillar monitoring

CHAPTER 6

6 Analysis of results

This chapter focuses on the analysis carried out on all the data collected during the project period to assess any trends and correlations between the modelled and measured data for evaluation of the remnant pillar stability. Thereafter, conclusions will be drawn from the results of the analysis and recommendations are made to enable remnant pillar design in future, based on a historic database.

6.1 Mining

The production data was collected on a monthly basis from areas which surround the remnant pillar that are considered to have an effect on the seismic activity and deformations. Tonnage of both ore and waste that was mined in the above mentioned areas is shown in Figure 6: 1: 1. This includes the summation of all the mentioned working places that have a direct influence to the remnant pillar as explained in Figure 5: 9 of Chapter 5.

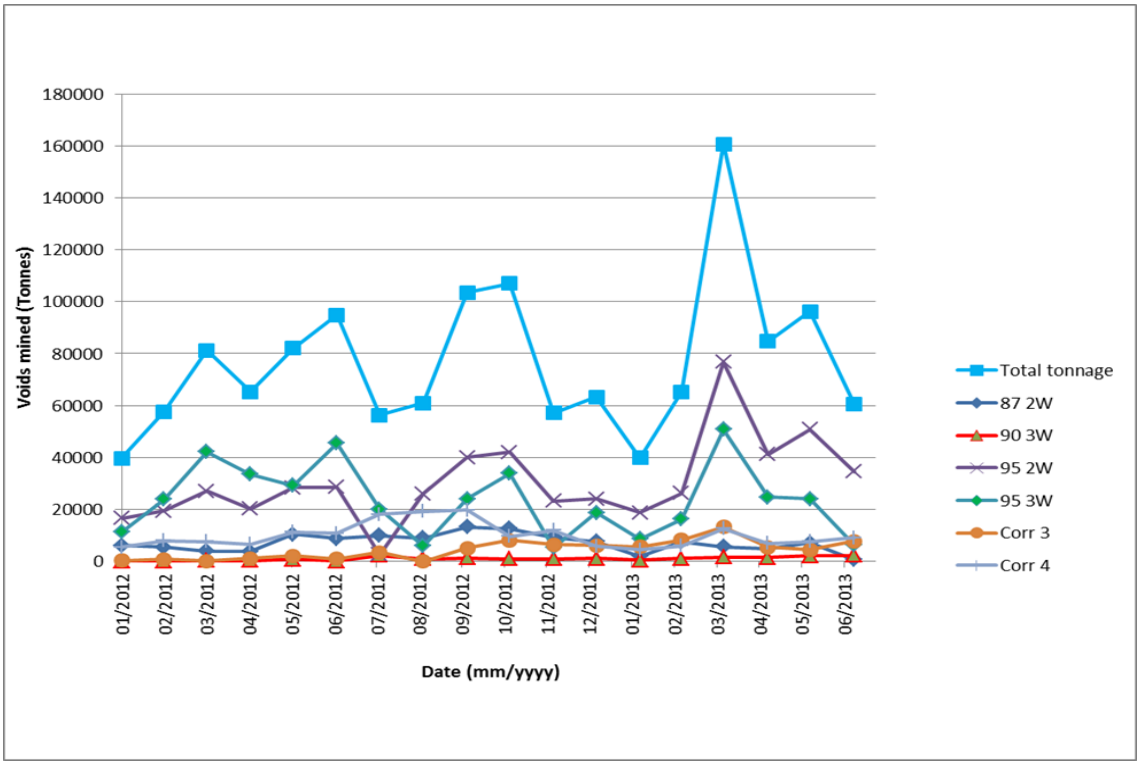


Figure 6: 1: 1 Mined tonnages for areas around the remnant pillar

As the total mined tonnages increased in October 2012 and March 2013 (Figure 6: 1: 1), high seismic events were recorded during same months (Figure 5: 7) subsequently, triggering high strain changes (Figure 5: 6) highlighted in the previous chapter and ERR values in March 2013 (Figure 6: 2: 6).

Figure 6: 1: 2 shows the production data for de-stressing cuts only. A jump in destress mining in December 2012 resulted in high modelled and measured stress changes as indicated in Figure 6: 3: 2. Increase in remnant mining in March 2013 caused an increase in expected magnitude for the same month as indicated earlier by Figure 5: 7 from chapter 5.

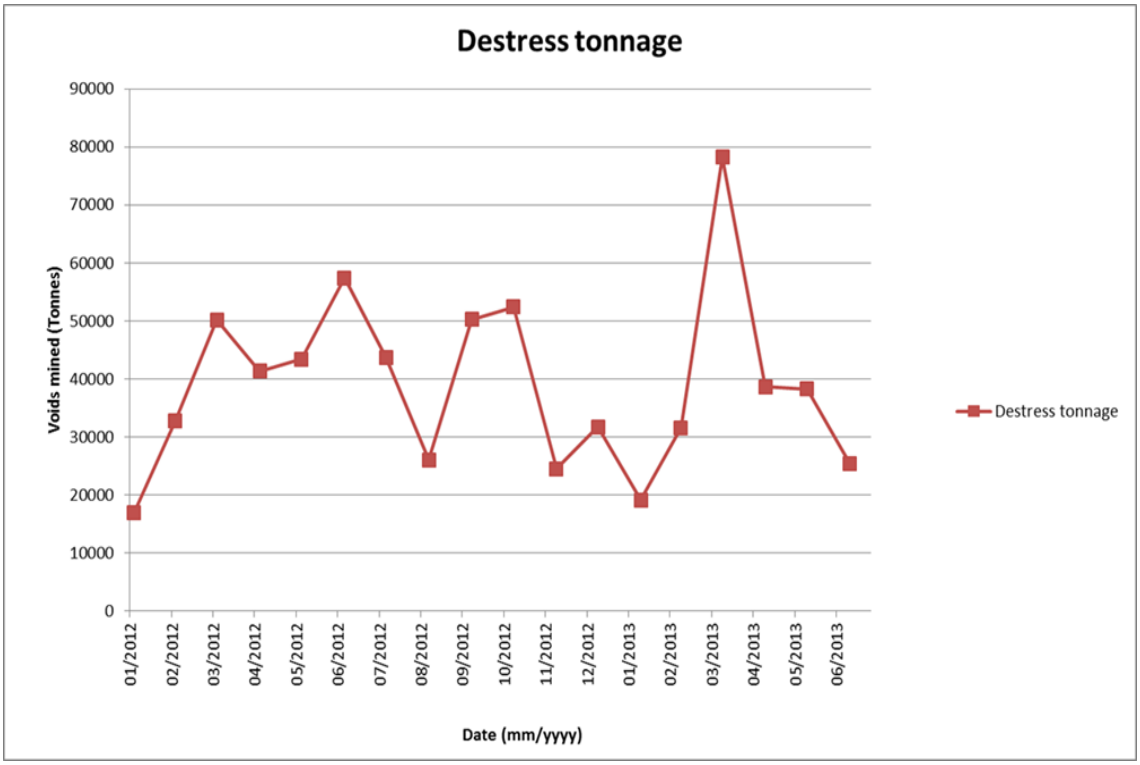


Figure 6: 1: 2 Total de-stressed tonnages

6.2 Numerical modelling results

Generally the identification of areas where seismicity is likely to occur is achieved by using an elastic model of the mine in 3D modelling of the actual and proposed mining sequence. The purpose of the model is to increase the understanding of the rock-mass behaviour and to identify areas of high seismic hazards. The inelastic Phase 2 model was implemented to connect geology with seismic events and address the shortcomings of Map 3D modelling. These models will be regularly updated for future planning purposes. This provides valuable input data for production planning and sequencing, Larsson (2004b).

6.2.1 Map 3D

Numerical methods were used for description and prediction of seismic events using parameters such as excess shear stress (ESS) and these events were calculated without having seismic records. Numerical modelling was carried out using a 3-dimensional linear elastic program Map3D which applies the Boundary Element Method (BEM) of stress analysis. Map3D relies on the assumption that the host rock is elastic, homogeneous and continuous. The rockmass modulus, Poisson's ratio and pre-mining stress state of the horst rock used in the models were obtained from the mine's Rock Engineering department and is presented in Table 6: 1.

Table 6: 1 Material parameters and pre-mining stress state

Young's Modulus (GPa)	Poisson's Ratio	σ_{xx} (MPa/m)	σ_{yy} (MPa/m)	σ_{zz} (MPa/m)
49	0.28	0.0164	0.0244	0.0269

The mining layout and extraction sequence by the South Deep planning department. Map3D model de-stress part was constructed using displacement discontinuity (DD) elements. These DD elements are simplified 2-dimensional surfaces which take into consideration the excavation thickness. DD elements are normally used for the construction of narrow tabular stope outlines where the thickness of the stope is considered to be small compared to the mining span.

Massive mining geometry was modelled using Fictitious Force (FF) elements above the horizontal (DD) elements. The magnitudes of expected incremental seismic events resulting from mining done during that period as well as associated stress changes were then calculated and analysed. Incorporation of geological structures in numerical modelling was done by means of using grids to represent these structures. Table 6: 2 shows the modeled fault numbers and their corresponding actual fault names as they are known from the mine. The overall model

showing these faults and their orientation as well as a plot of major principal stress on them is indicated in Figure 6: 2: 1

Table 6: 2 Fault names

Modelling Fault Number	*Actual geological name (South Deep gold mine)*
7	D008
9	F046
11	F054
14	F113
17	Fltb001

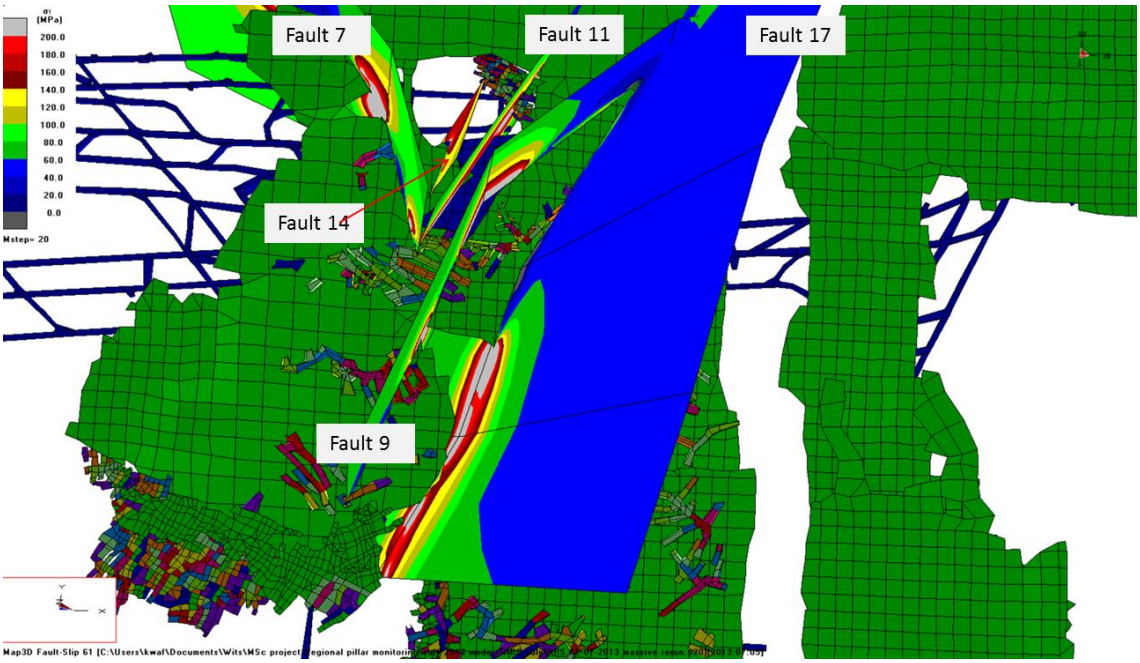


Figure 6: 2: 1 Location of faults and sigma 1 plot

6.2.1.1 Excess Shear Stress and seismic event magnitude

Studies carried out indicated that majority seismic events accompanied by rock bursts recorded are a result of mining in close proximity to geological structures (Jager and Ryder, 1999). Most high magnitude events cause shearing along these structures when the cohesive strength of these faults, dykes or joint sets are exceeded by the induced stresses from mining. Figure 6: 2: 2

illustrates the areas of high shear stress zone where slip is likely to occur if the plane of weakness is located inside them.

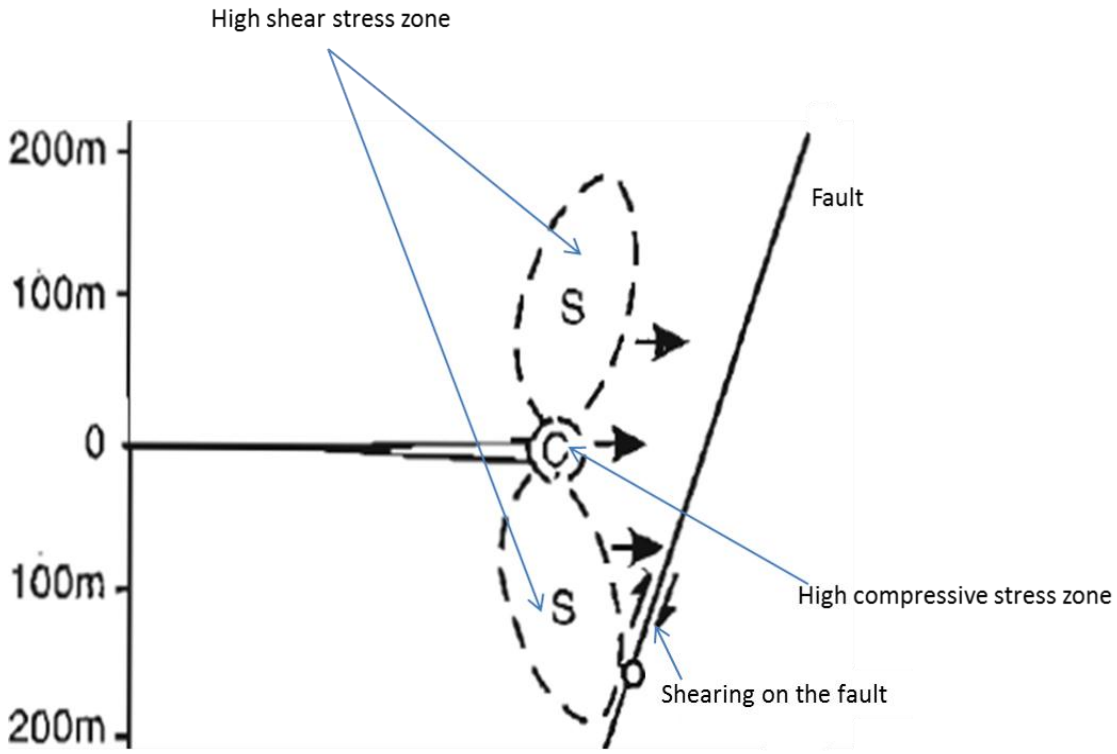


Figure 6: 2: 2 ESS lobes in front in excavation face, (after Jager and Ryder, 1999)

The Ryder equation for rounded geometries was simply used in all cases. The equation is as follows;

ESS = τ_e = $|\tau|-\mu\sigma_n$ where;

τ shear stress before slip,

μ tangent of the frictional angle (θ) and

σ_n normal confining stress.

The geological structures used in the model were provided by the South Deep Geology department. The Excess Shear Stress (ESS) was calculated on each fault grid. A method for

estimating seismic moment from ESS proposed by Ryder (2002), was used to determine event magnitude. This method adds up areas of positive ESS which is then used to obtain an equivalent radius represented by this sum of area. However, only positive ESS along the faults is applied in the practical situation and the strength of the fault and hence the method overestimates the event magnitude. In order to overcome overestimation of the ESS_{max} an attempt was made to investigate the influence of ESS.

The following methods were also used:

- Shear stress ESS_{max} was obtained by averaging the top ten values and is denoted by ESS Top10 average.
- Shear stress ESS_{max} was capped at a maximum of 15MPa as suggested by Ryder (1988) and is denoted by ESS 15MPa max.

ESS_{max} for each case is subsequently obtained and incremental seismic moment was estimated for each mining step (mining period). This represents the potential maximum seismic moment in that step. The Hanks Kanamori moment magnitude formula (Grandin, et al., 2011) used for magnitude calculations is;

$$M = \frac{2}{3}\log M_o - 6.03$$

Where;

M Ritcher magnitude and

M_o seismic moment.

The mining sequence on the remnant pillar from October 2011 to June 2013 was shown in Figure 5: 3 of Chapter 5. Figure 6: 2: 3 summarizes the results of the five most influential faults selected. The figure shows that the expected event magnitudes from the numerical modelling

are generally higher than the measured included in the same figure. This could be due to the fact the moment calculated using only the maximum ESS as previously mentioned, hence the high magnitudes.

The maximum expected magnitude during the mining is generally above 3.5. The trend shows a general increase in magnitude towards the end of the mining sequence, which indicates potentially increased seismic risk towards the end of the mining life. Fault 11 recorded the highest magnitude of 4.8 in July 2012. This is mainly due to the fact that the fault is across the remnant area (Figure 6: 2: 1) and also increased mining during the previous month (June 2012) activated the fault (Figure 6: 1: 2).

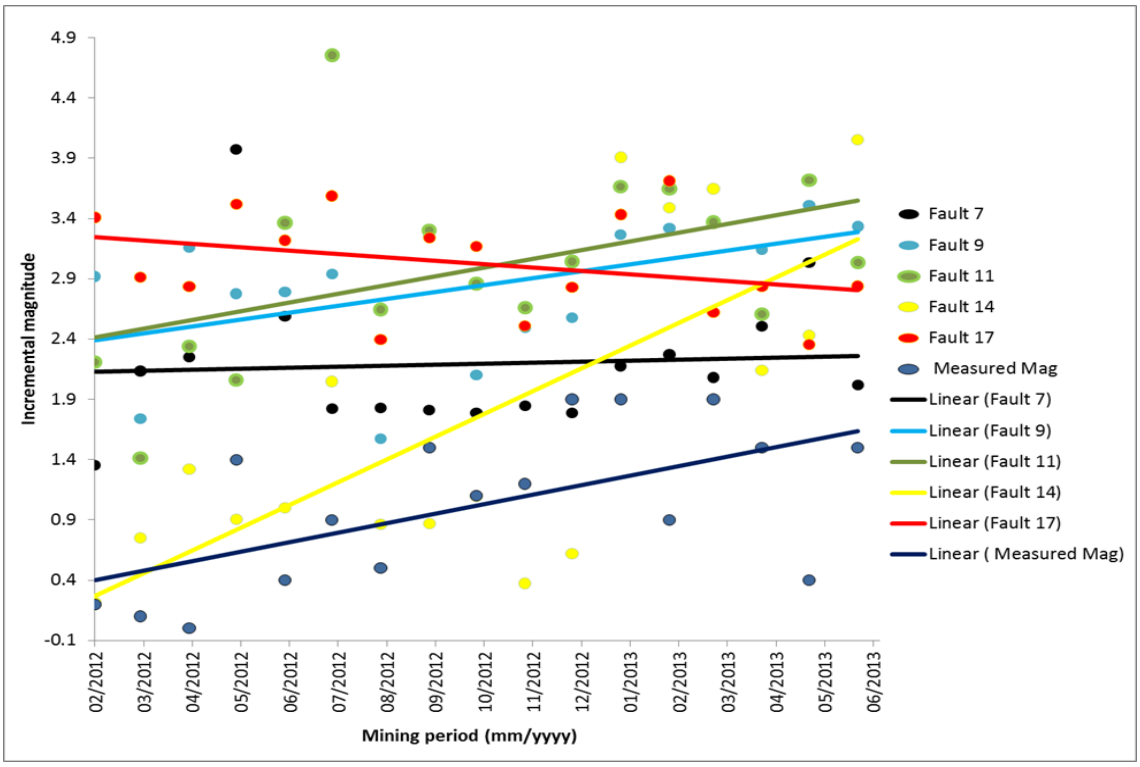


Figure 6: 2: 3 Expected event incremental magnitude for actual mining sequence from maximum ESS values

As a result of exceptionally high modelled magnitude values, the method had to be reviewed. Averaging the highest ten positive ESS resulted in a better comparison between measured and modelled results especially Fault 14. The results are presented in Figure 6: 2: 3 and as can be seen, the expected magnitude is slightly lower compared to the maximum ESS method of analysis with the maximum now around 3.5. This seismic analysis method is a better representation of reality than Figure 6: 2: 3

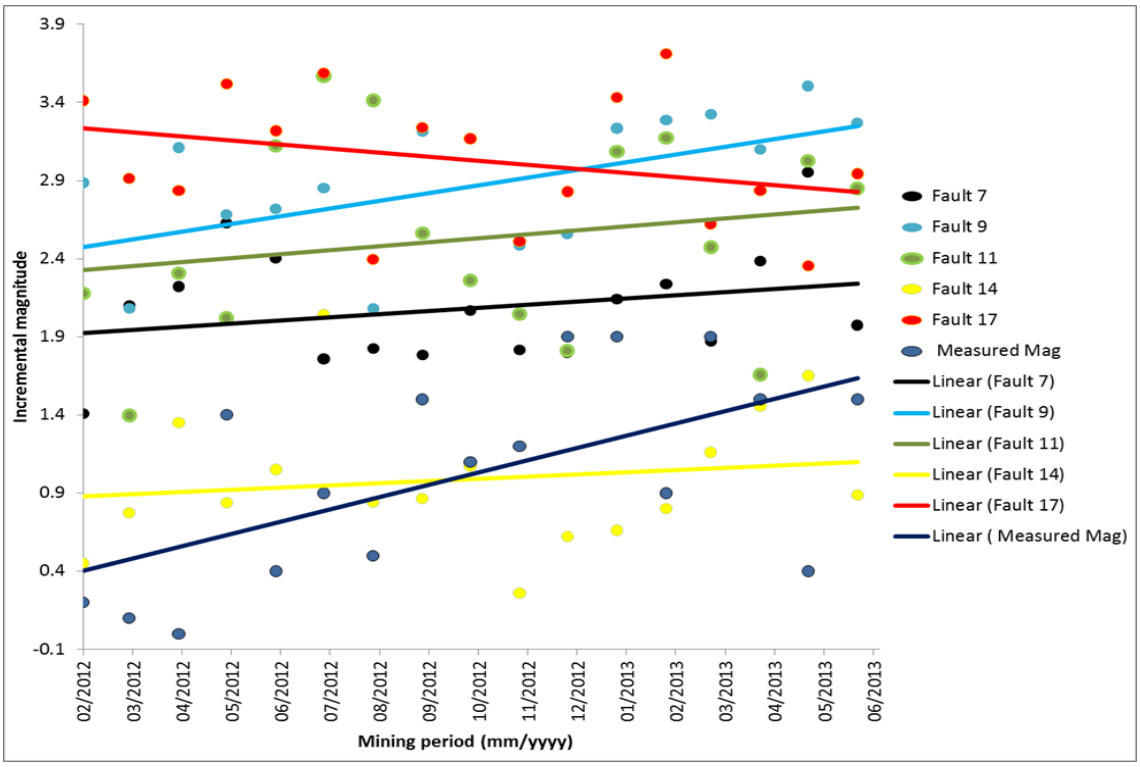


Figure 6: 2: 4 Expected event incremental magnitudes for actual mining sequence averaging 10 maximum ESS values

Jager and Ryder (1999) suggested that if positive ESS is greater than 15 MPa for a fault or 30 MPa for intact rockmass, a prior event would have occurred in the previous mining stages. Using their theory the third magnitude analysis method, the maximum ESS values for each fault during each mining period were capped at 15 MPa and the magnitude values dropped further to about 2.5. This third approach has resulted in modelled seismic values being closely

related to those measured underground. However, Fault 14 recorded the highest magnitude during the month March 2013 as highlighted in Figure 6: 2: 5 below. This was due to high mined out tonnages (Figure 6: 1: 1) which probably might have resulted in slip along the fault. Fault 7 in this scenario shows a trend line that compares well with that of the measured data displaying an increase in high magnitudes events with time.

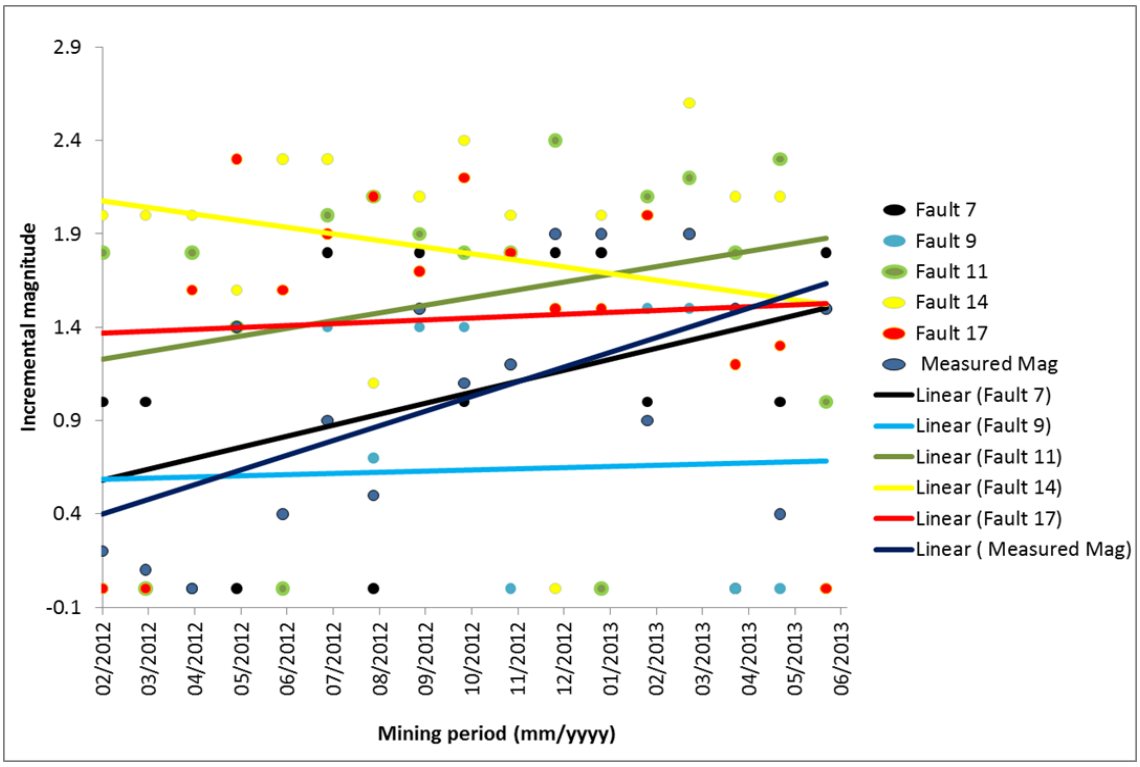


Figure 6: 2: 5 Expected event incremental magnitudes for actual mining sequence capping maximum ESS value at 15 MPa

6.2.1.2 Average pillar stress (APS)

An average pillar stress criterion is used for evaluating the stability of the regional pillars. The design of hard-rock pillars in massive mining has not received the same research attention as was the case in tabular conventional methods. This is because fewer mines are practising massive mining at depths.

Regional pillars are squat rib pillars with a (width: height ratio >10). However, as mining depth increases the potential for the failure of hard-rock pillars also increases. These pillars do not fail by crushing, nevertheless, foundation failure occurs when APS>2.5σ_c, where σ_c is the UCS of the foundation material.

Average Pillar Stress (APS) on the regional pillar was obtained from Displacement Discontinuity, (DD) elements placed across the pillar size and allocated the last mining step in the mining sequence. The accumulated stresses on that pillar during each mining period (month) were divided by the pillar area to obtain the APS. The elastic modelling results show extremely high stresses on the edges of the pillar as shown in Figure 6: 2: 6 below.



Figure 6: 2: 6 Normal stresses in the remnant pillar at mining step 18 of 90 3W

Figure 6: 2: 7 illustrates the average pillar stress from February 2012 to June 2013. Following Ryder and Jager (2002), the stability of the regional pillars is assessed for foundation failure

and the criterion states that foundation failure occurs if the average pillar stress (APS) is more than 2.5 times the UCS of the rock-mass making up the footwall and the hangingwall.

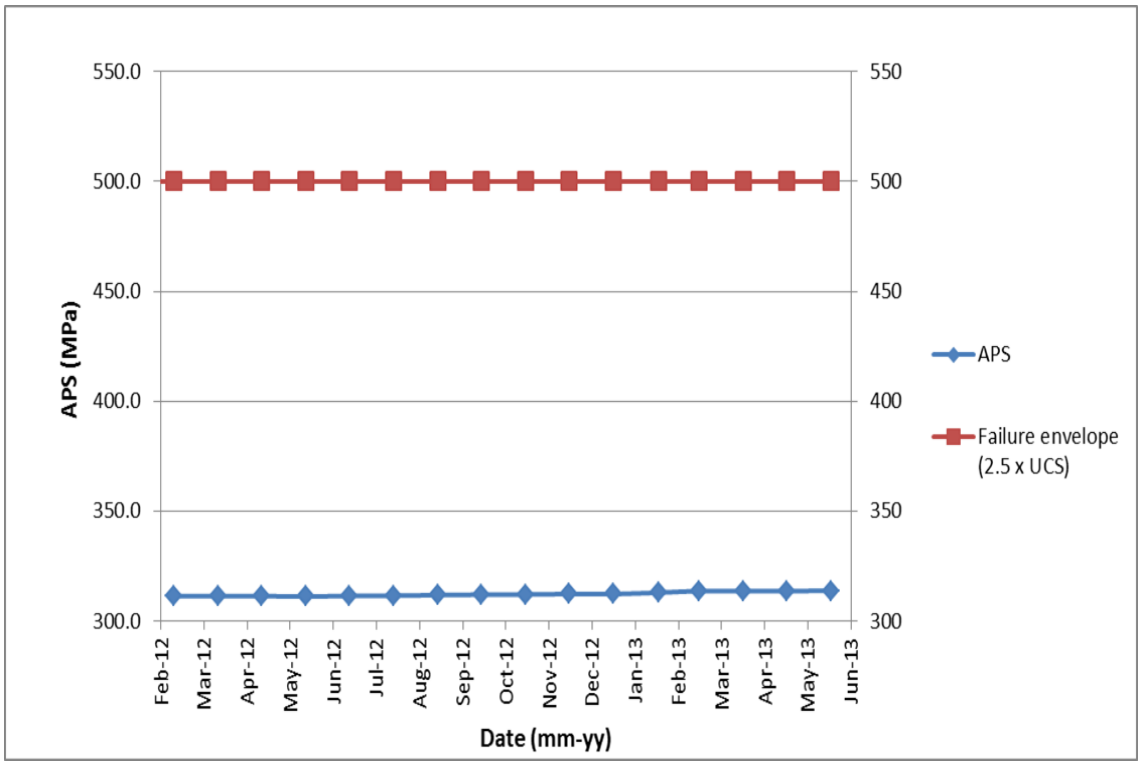


Figure 6: 2: 7 Average pillar stresses of the remnant during mining on 90 3W

From the graph it can be observed that there is no significant increase in the average pillar stress, for a period of almost one and half years (from 311 MPa in February 2012 to around 314 MPa in June 2013) indicating that the pillar is being loaded gradually . The strength of the rock making up the pillar is approximately 200 MPa while the footwall is from 60 MPa to 160 MPa and the hangingwall ranges from 60 MPa to 90 MPa. Following Ryder and Jager (2002), the results show that at present, punching is most likely expected into the hangingwall.

6.2.1.3 Energy release rate (ERR)

Regional stability pillars are implemented in deep level mines to control or limit the energy release rate (ERR). The ERR is the measure of stress concentrations and the resultant underground conditions at any given face or pillar during mining, Ryder and Jager (2002). It takes into account the stresses acting on the stope abutment and also the volumetric closure taking place in the back area of a stope.

The un-accounted for energy can be converted by fracturing or frictional sliding into heat and often the small part of it is radiated away as kinetic energy in the form of seismic waves. It does not however represent seismic energy released during mining. The energy release rate (ERR) calculation quantifies the release of the gravitational potential energy of the rock mass into the environment as mining progresses.

The ERR calculated in the deep hard rock mines of South Africa was found to have a significant correlation (Sear, 2009) with the risk or potential of damaging rock bursts. The energy release rate (ERR) for regional pillars is recommended to be less or equal to the threshold of 40 MJ/m2, (Jager and Ryder, 2002) to avoid rock-bursts occurrences. However, the ERR is insensitive to local geological conditions, such as discontinuities which usually lead to major local increases in seismicity levels along with footwall and hangingwall instability.

The ERR, after Jager and Ryder (1999), is defined as follows:

$$\text{ERR} = {}^{1}/_{2}\ \sigma_a \delta_b \text{ MJ / m}^2$$

Where:

σ_a existing normal stress and

δ_b is the deformation behind the new face.

Energy release rate was calculated using the ERR tool built in Map3D. Stress and closure at each mining step is calculated on the Displacement Discontinuity (DD) elements. Energy release is calculated from stress and closure and finally ERR is then obtained by dividing energy release by the mining area.

Increasing the mined out tonnages while maintaining the backfill rate, means a lag in the backfill and inevitably a large unsupported span. The large unsupported span will result in increase in deformation and consequently high ERR values (Figure 6: 2: 8), hence the direct correlation with mined out tonnages. High magnitude events experienced in October 2012 and March 2013 in Figure 5: 7 (Chapter 5) caused by high mined out tonnages (Figure 6: 2: 8) resulted in more energy being released contributing to high ERR values.

The ERR values in the figure below are valid for the faces adjacent to where mining is taking place. However, influence of mining in areas away from the regional pillar inevitably increases the pillar stresses hence the energy released (from the ERR formula in the previous section), indicated by the correlation between ERR and mined out tonnages in Figure 6: 2: 8.

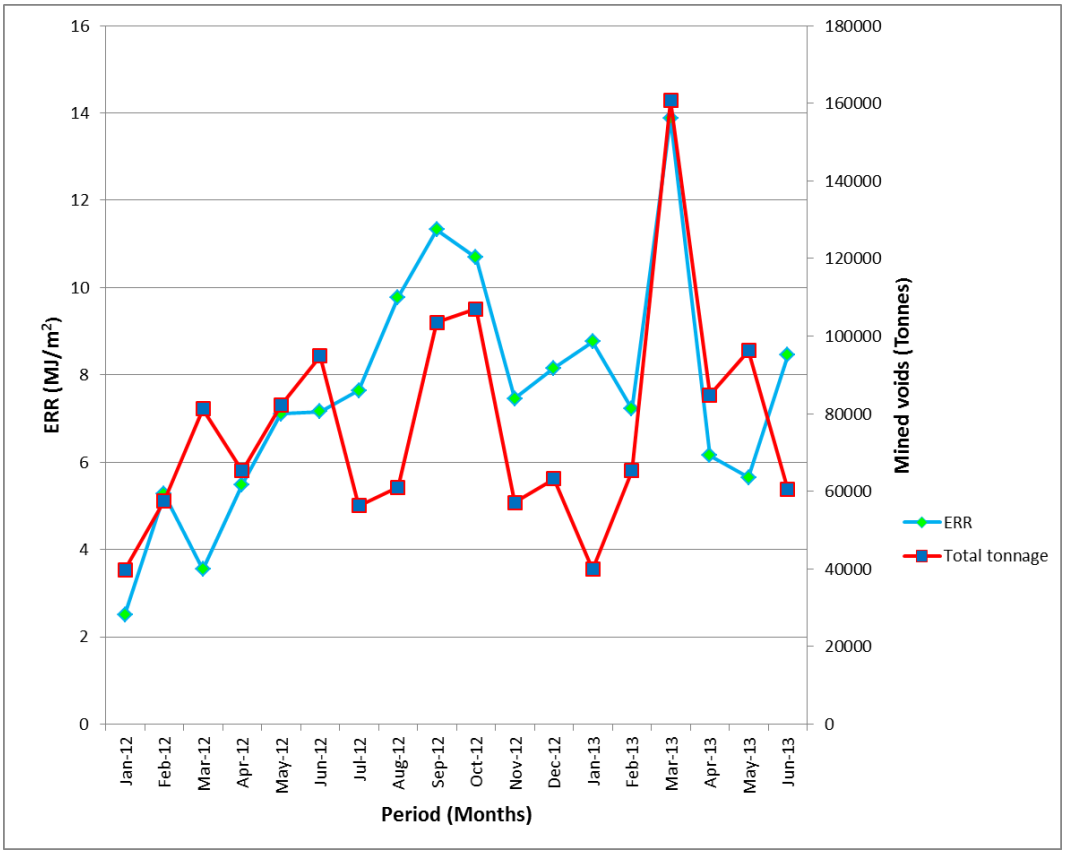


Figure 6: 2: 8 Association between energy release rate (ERR) and mined tonnages

6.2.2 Phase 2

Phase2 is a two-dimensional elasto-plastic finite element program for computing stresses and displacements around underground openings. It is a numerical method for solving differential or integral equations. The method assumes the continuous function for the solution and obtains the parameters of the functions in an approach that reduces the error in the solution (Dixit, 2008)

6.2.2.1 Elastic

The elastic model in Phase 2 was done first for simplicity. The rule of numerical modelling (Stacey, 2013) states that when creating a complex model, you start with a simple one in order to understand the situation and then add complexities gradually to minimise numerical errors.

The model acts as a control experiment to check for any numerical errors that might be encountered in the inelastic model. The field stresses and the rockmass elastic properties of the mine are represented in Table 6: 3 and Table 6: 4 respectively.

Table 6: 3 Field stresses

Field stress type	σ_1 (MPa)	σ_3 (MPa)	σ_z (MPa)
Constant	68	41.48	61.88

Table 6: 4 Elastic properties

Young's Modulus (GPa)	Poisson's Ratio	Peak Tensile Strength (MPa)	Peak Friction Angle (degrees)	Peak Cohesion (MPa)
49	0.28	1.5	30	18

Figure 6: 2: 9 illustrates the principal stresses re-distribution as the de-stress cut is being mined out. High stresses are highlighted at the excavations' faces and decrease as you approach the pillar centre. At the corners of the de-stress cut faces, there is exceptionally high stress contours indicating potential dog-earing of the excavation at those areas. These stresses, however, reduce until they reach virgin state (68 MPa) as distance from the excavation increases.

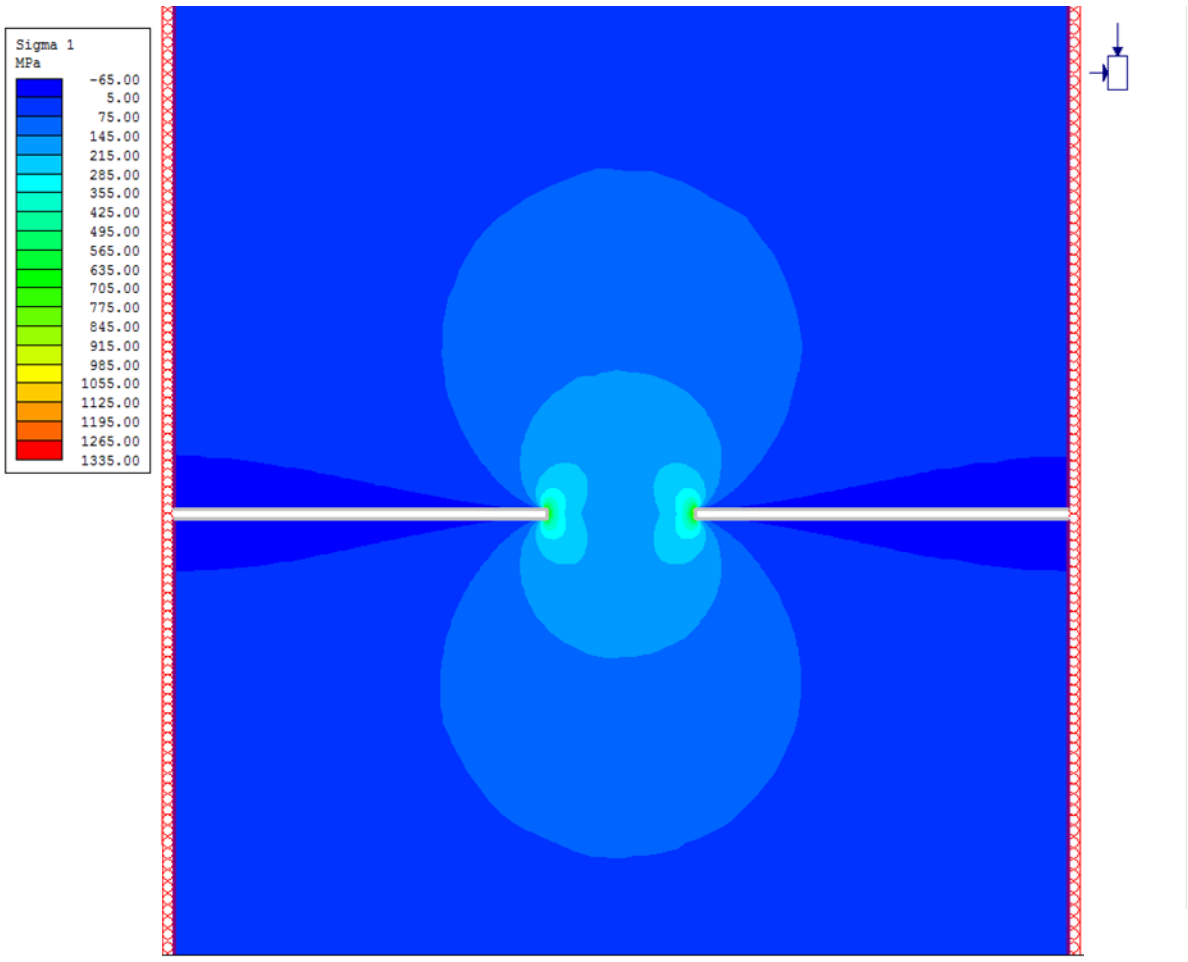


Figure 6: 2: 9 Major Principal Stresses across the pillar

Map 3D (Figure 6: 2: 6) and Phase 2 (Figure 6: 2: 9) elastic results are consistent showing generally high pillar skin stresses hence no theoretical contradictions. The skin stresses of the Map 3D model are around 650 MPa (Figure 6: 2: 6) while Phase 2 model records skin stresses of around 750 MPa (Figure 6: 2: 9). These stresses reach their lowest at the pillar centre.

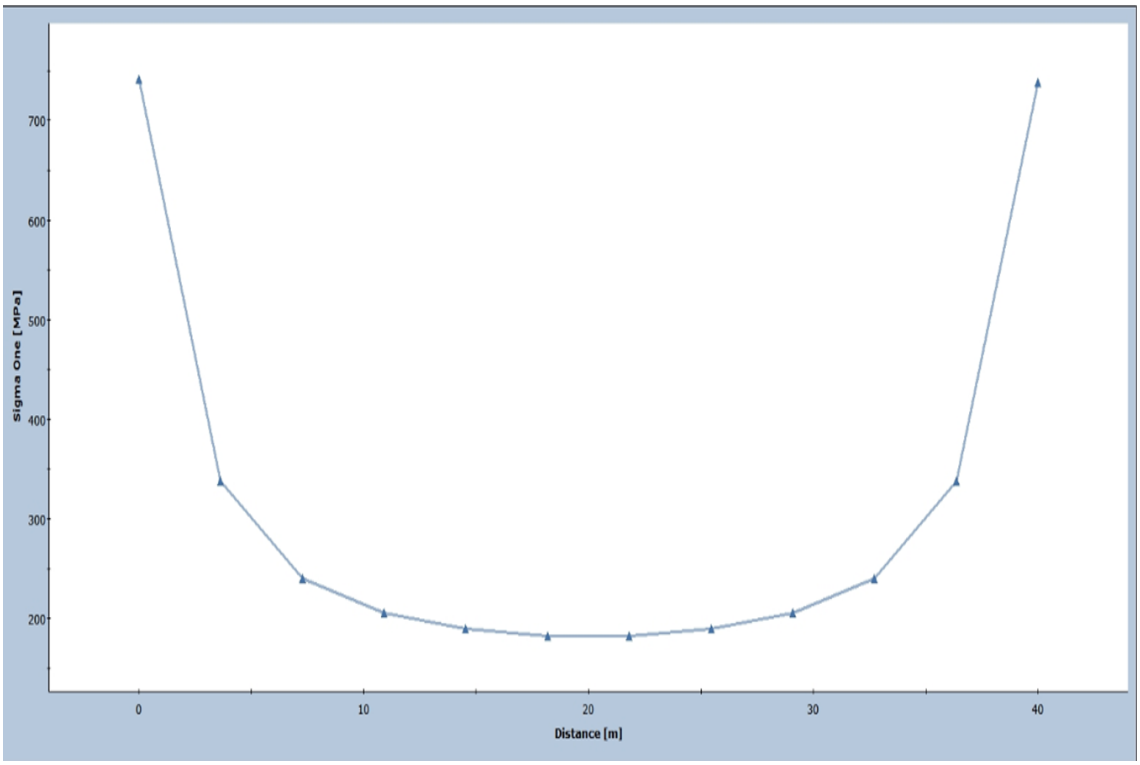


Figure 6: 2: 10 Major Principal Stress across the pillar in an elastic model

6.2.2.2 In-elastic

Information on the inelastic properties of the rockmass used in the modelling as well as the joint properties assigned on the fault was provided by the mine and is illustrated in Table 6: 5 and Table 6: 6.

Table 6: 5 Inelastic properties

Residual Friction Angle (degrees)	Residual Cohesion (MPa)
30	18

Table 6: 6 Joint properties

Normal stiffness (GPa/m)	Shear stiffness (GPa/m)	Friction Angle (degrees)
109	42.8	30

Strength reduction is a way of assessing the stability of a material up to a point where failure is induced. The strength reduction factor is represented by a value assigned to show the rate at which the material is degraded (reduce strength) for failure to occur.

For slip to occur along the fault, shear stress should be greater than the clamping stresses. Phase 2 modelling was used to investigate the possible shear along the faults. Phase 2 modelling was carried out to model the inelastic property of the rock mass, taking into account two faults, namely Fault 7 and Fault 9 (whose actual names have been described in Map 3D), that cut across the pillar. Figure 6: 2: 11 shows the strength reduction factor through the cross sectional view of the pillar highlighting parts of the faults that will fail in shear. These are areas where there events are likely to occur in future.

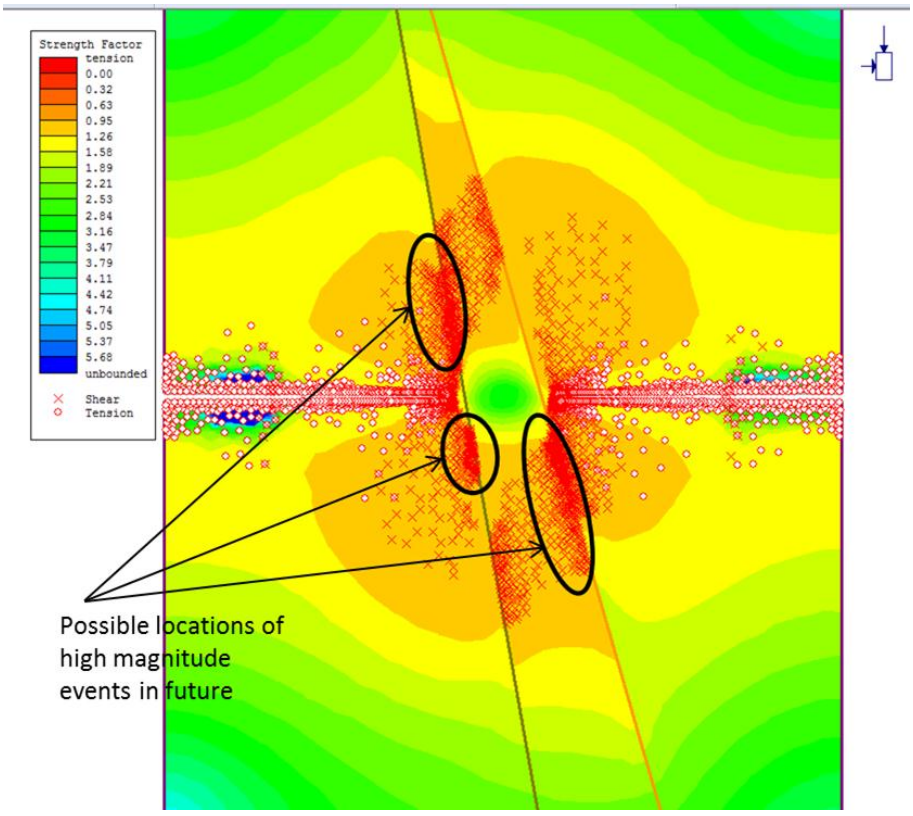


Figure 6: 2: 11 Strength factor across the pillar from Phase 2 model

Figure 6: 2: 12 illustrates the maximum principal stress contours from the 2D model done using Phase 2. However, the average pillar stress from the elastic Map 3D in June was around 314 MPa while inelastic Phase 2 modelled a lower value of 234 MPa. The numerical average pillar stress for Phase 2 was calculated from the values taken at 1.9 m intervals across the pillar. This might be due to the over-estimation of the strength of the rockmass assumed in Map 3D caused by its inadequate consideration of the rock properties affecting stability. At the pillar edges Map 3D records the highest pillar stresses (since it does not simulate failure) contributing to the high average pillar stresses. Phase 2 model, on the other hand, is showing failure at pillar edges, recording lower average pillar stresses than Map 3D.

The other factor is that Map 3D calculates the real average pillar stress while Phase 2 assumes that the pillar is infinitely long with constant width of 40 m (plane strain conditions). In reality, the pillar is approximately 160 m long with varying widths across the whole length.

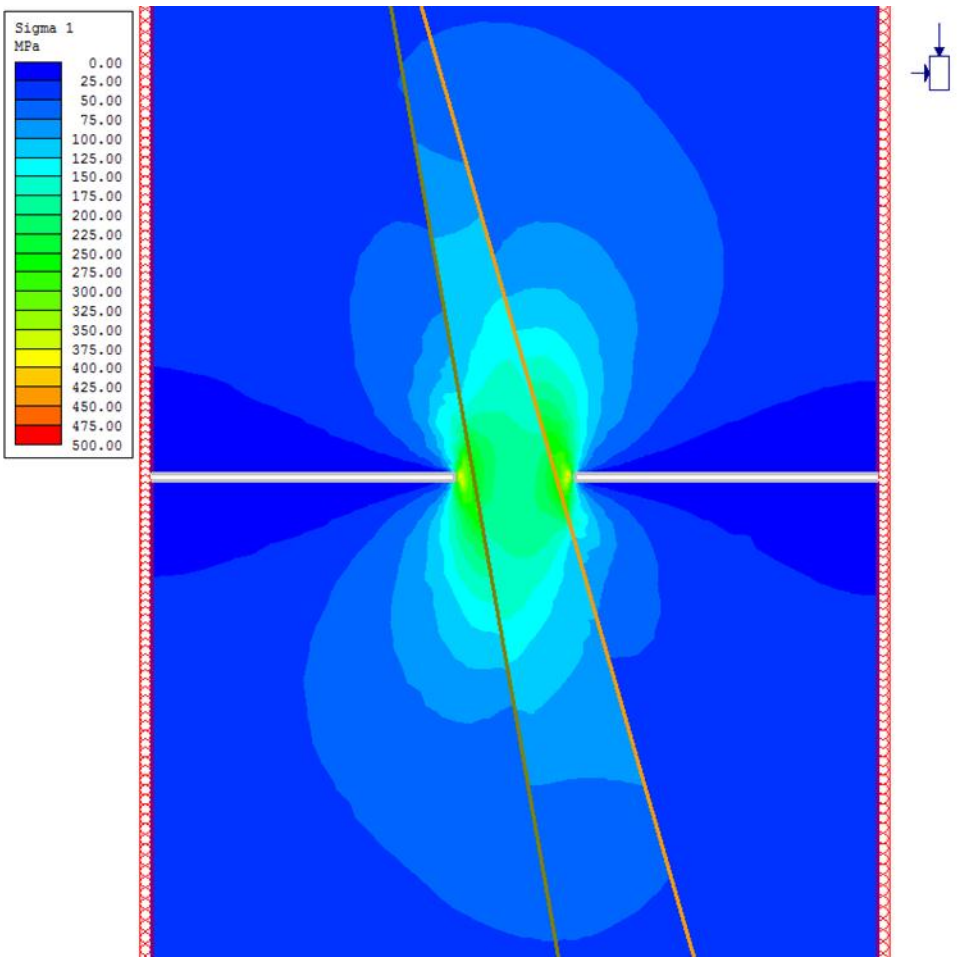


Figure 6: 2: 12 Major principal stress across the pillar from Phase 2 model

Figure 6: 2: 13 shows the distribution of principal stresses across the pillar from left to right. At the edges, the stresses are low (195 MPa) and they increase up to a point they reach the maximum (330 MPa) at about 3 m into the pillar. After that they follow the same profile as that of an elastic model which is a curve shape. The profile of the 3 m edges of the pillar is signifying pillar scaling (failing). However, the stresses of the scaled portion on the left side are higher (195 MPa) than on the right side (95 MPa) due to the orientation of the geological structures included in the model providing a de-stress shadow on the left.

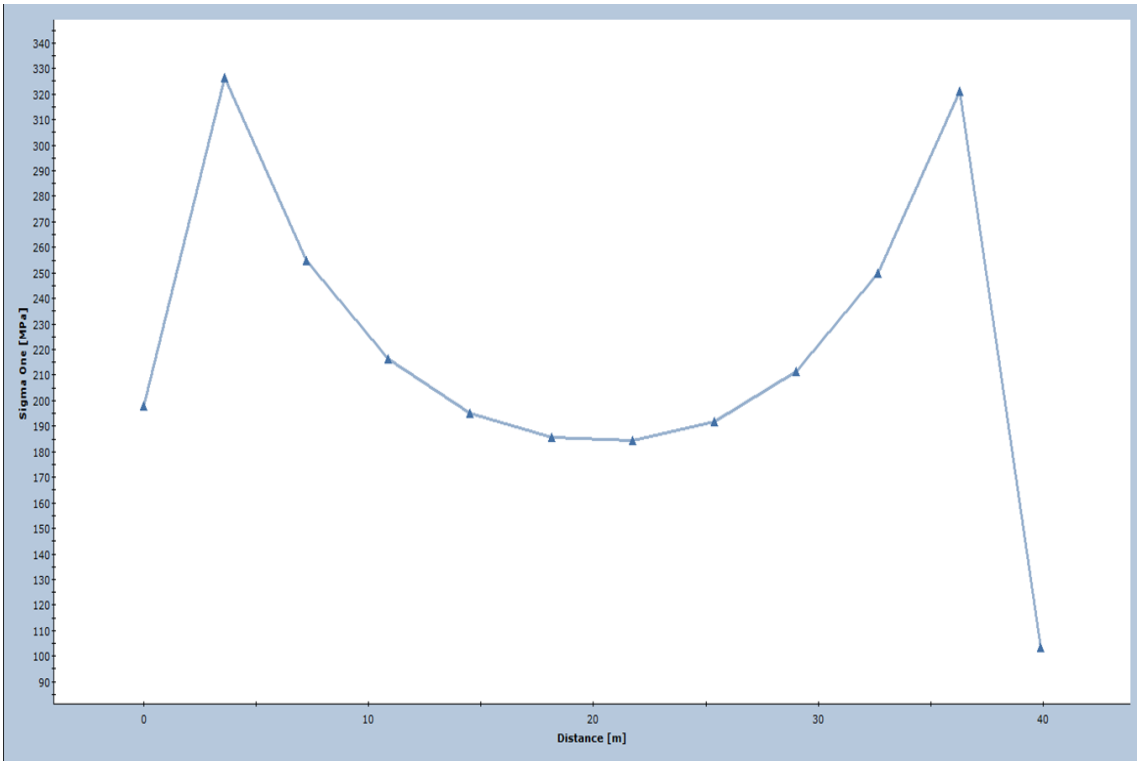


Figure 6: 2: 13 Distribution of major principal stress across the pillar

6.3 Measured strain and seismic analysis

A line grid which represents the strain-meter borehole in Map 3D modelling is positioned along the borehole axis. The modelled strain at the position of the strain meter is compared with the measured for each mining step since the model was constructed on monthly step basis. ε_{1i} and ε_{3i} represents the diametrical strains recorded inside the borehole. It should be noted that since the model is elastic, strain changes associated with seismic events will not be captured.

Figure 5: 6 of Chapter 5 shows the strain readings recorded during the period of August 2012 and June 2013. The jump in values of strain readings from end of September 2012 to early October 2012 which occurred when recording commenced are as a result of the malfunctioning

of the strain-meter. The second significant jump in measured strain in March 2013 coincides with increases in mined tonnages Figure 6: 1: 1.

The strain data recorded was used to calculate the three dimensional stress changes on the strain meter resulting from mining. The major principal stress (σ_1) and minor principal stress (σ_3) changes as well as the maximum shear stress (τ_{max}) were calculated on a monthly basis using the strain rosette back stress calculations. The strain reading at the beginning of the month is subtracted from that recorded at the end of the month. This was done to correlate the measured stress changes with the modelled changes hence the monthly deviations because the mining voids were updated on the same time interval. Initially the strains (ε_x, ε_y and γ_{xy}) are calculated from the induced directional strain readings with the vertically oriented strain-meter being in the reference direction ($\varepsilon_y = \varepsilon_0 = \varepsilon_{vertical}$). The major and minor principal stresses as well as their orientations from the vertical strain meter are then calculated. From the rosette equations used for the calculations, the maximum shear stresses are also determined.

6.3.1 Principal stresses calculations from measured strain

Given $\varepsilon_{\theta 1} = a$,

$\varepsilon_{\theta 2} = b$ and

$\varepsilon_{\theta 3} = c$

Where θ_1, θ_2 and θ_3 are the orientations of the strain-gauge inside the borehole and a, b and c are the strain readings on the strain-gauges θ_1, θ_2 and θ_3 assuming $\varepsilon_{\theta 1}$ is in the reference direction θ_1 which is the zero direction, $\varepsilon_{\theta 2}$ is 120^0 from θ_1 and $\varepsilon_{\theta 3}$ is 240^0 from θ_1 then;

$$\varepsilon_{\theta 2} = a\cos \quad + \gamma_{xy} \sin\theta_2 \cos\theta_2 + \varepsilon_y \sin^2\theta_2 = b \qquad \text{Equation 1}$$

$$\varepsilon_{\theta 3} = a\cos^2\theta_3 \quad + \gamma_{xy} \sin\theta_3 \cos\theta_3 + \varepsilon_y \sin^2\theta_3 = c \qquad \text{Equation 2}$$

From solving the simultaneous equations we get the values of ε_x, ε_y and γ_{xy}.

Given the Young's modulus (E) and Poisson's ratio (v), the values of σ_x, σ_y and τ_{xy} are calculated using the following formulas (Hooke's Law in 2D);

$$\sigma_x = \{E/(1-v^2)\}(\varepsilon_x + v\varepsilon_y) \quad \text{Equation 3}$$

$$\sigma_y = \{E/(1-v^2)\}(\varepsilon_y + v\varepsilon_x) \quad \text{Equation 4}$$

$$\tau_{xy} = \{E/(2(1+v))\}\gamma_{xy} \quad \text{Equation 5}$$

Finally principal stresses are calculated as follows;

$$\sigma_1 = 0.5(\sigma_x + \sigma_y) + 0.5\left\{\left((\sigma_x - \sigma_y)^2 + \left(4(\tau_{xy})^2\right)\right)^{0.5}\right\} \quad \text{Equation 6}$$

$$\sigma_2 = 0.5(\sigma_x + \sigma_y) - 0.5\left\{\left((\sigma_x - \sigma_y)^2 + \left(4(\tau_{xy})^2\right)\right)^{0.5}\right\} \quad \text{Equation 7}$$

$$\tau_{max} = 0.5\left\{\left((\sigma_x - \sigma_y)^2 + \left(4(\tau_{xy})^2\right)\right)^{0.5}\right\} \quad \text{Equation 8}$$

(Watson, 2012), confirmed that $E = 49GPa$, $v = 0.28$ and vertical is the reference direction, therefore, induced strain is calculated from subtracting the strain value at the beginning of the month from the month-end strain value. The results of the calculations are summarised in Figure 6: 3: 1. Where there is little difference between the major and minor principal stress, the maximum shear stress is close to zero as expected. The increase and decrease in these principal stresses results in the same trend observed in the shear stresses.

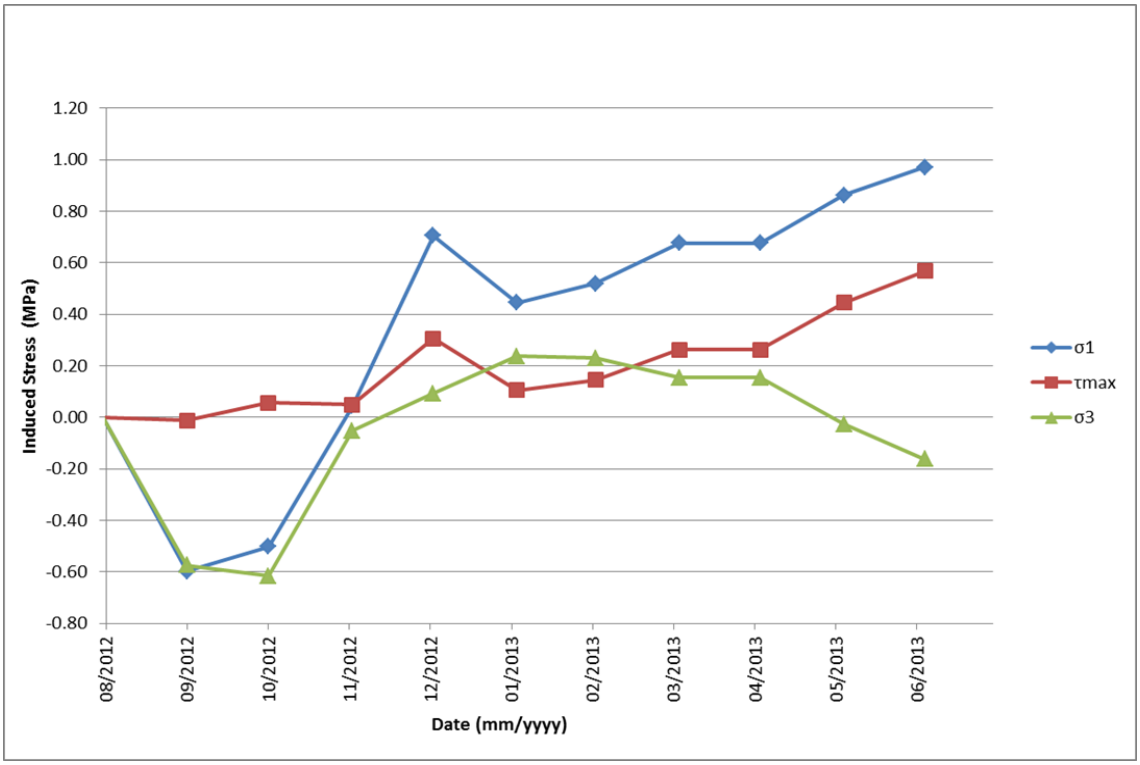


Figure 6: 3: 1 Induced principal stress changes from strain readings

The calculated stress (from strain readings) changes are influenced by geological structures so there is bound to be greater variations from the modelled strain changes as indicated in Figure 6: 3: 2. Since the Map 3D model assumes a perfectly elastic environment, hence only simulates elastic deformation, the difference between the modelled and calculated stress changes signifies the inelastic (plastic) deformation of the rock-mass.

Both modelled and measured stress change graphs show no changes in stresses in March 2013, (Figure 6: 3: 2). This period coincides with the time where maximum tonnages were mined (Figure 6: 1: 1) and also where high magnitude events were recorded (Figure 5: 7) from Chapter 5. This might be due to stress relaxation after the occurrence of high magnitude events earlier that same month. Previous mining caused stress build up and these stresses became sufficient to incite slip along geological structures manifesting as seismic events thereafter

resulted in stress relaxation hence no recorded stress changes by both the strain-meter and the model.

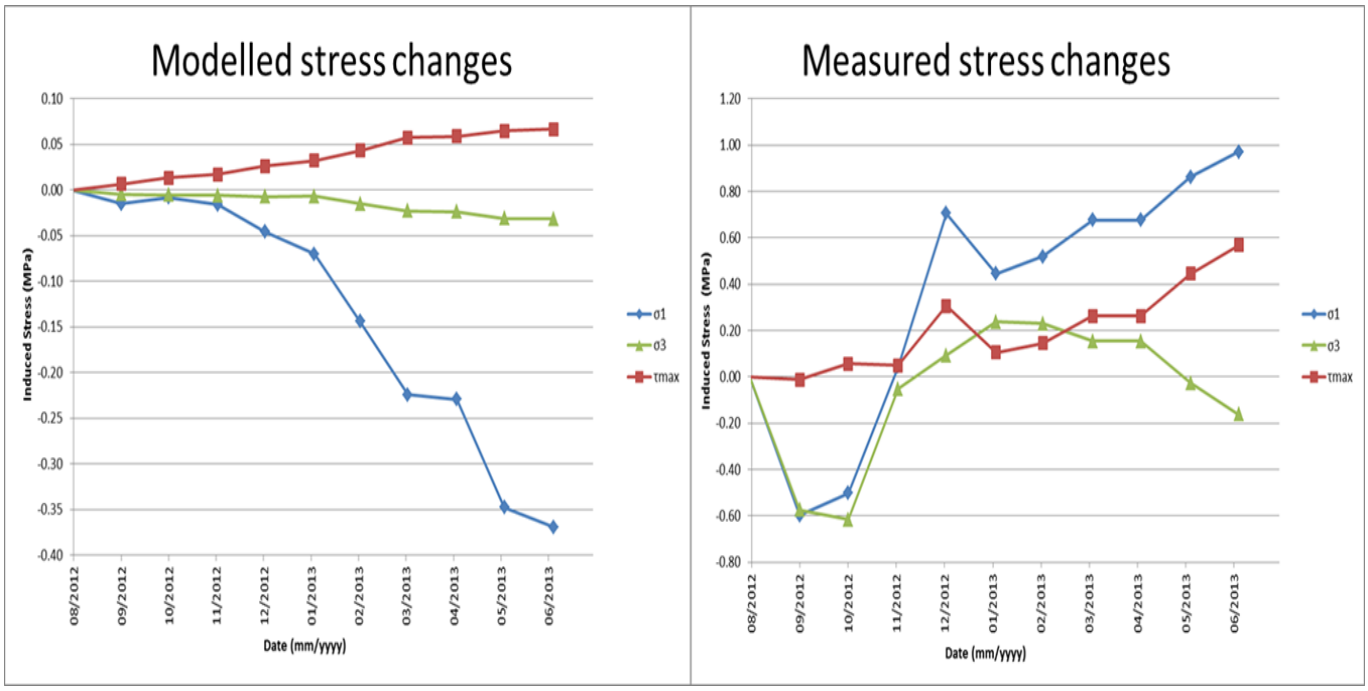


Figure 6: 3: 2 Comparison between modelled and calculated stress changes

Figure 6: 3: 3 below displays the seismic events recorded in close proximity to the pillar. These events were demarcated using a polygon, a tool available in JDi seismic software for defining the boundary extent of the regional pillar. The size of the balls indicate the magnitude of the events, i.e, the greater the ball, the higher the magnitude.



Figure 6: 3: 3 Seismic events defined by a polygon extrapolated from JDi

Figure 5: 7 (Chapter 5) shows the updated magnitude of events recorded during the period of August 2012 to June 2013. There is a decrease in the number of events with magnitude zero or more from March (9 events) to April (3 events).

Between August and September 2012 there is no change recorded in the strain data (Figure 5: 6 of Chapter 5) because the strain meter was mal-functioning. An increase in measured stress change in December 2012 correlates with the slight increase in production as shown earlier in Figure 6: 1: 1.

A comparison between strain readings and seismic data is presented in Figure 6: 3: 4. The graphs recorded jumps in strain readings (December 2012, March 2013 and May 2013) as a result of a high concentration of low magnitude (between 0 and 1) events in December 2012 as well as high magnitude events recorded in March 2013 and May 2013. Generally high

magnitude events cause inelastic deformation of the rock-mass indicated by jumps in the strain readings as shown in Figure 6: 3: 4. The March 2013 increase corresponds with high production tonnages mined in the same month indicated earlier by Figure 6: 1: 1.

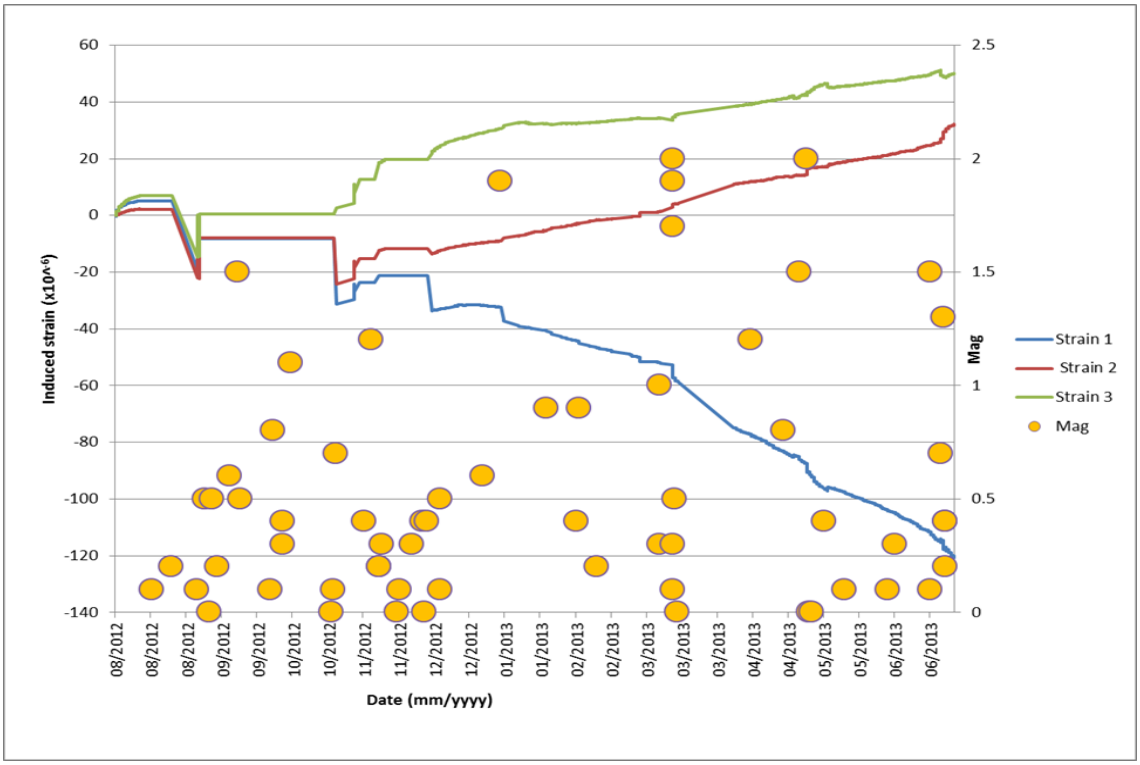


Figure 6: 3: 4 Correlation between seismic events (M>=0) and strain data from Aug 2012 to June 2013

Figure 6: 3: 5 shows the influence of production mining on the occurrence of seismicity. The graph indicates that high volumes of ore and waste mined results in an increase in high magnitude events (March 2013). Increased production creates large mined spans leading to rapid build-up of induced stresses. This increases stress concentrations ahead of the mining faces and hence trigger slip along geological structures. The slip will manifest in the form of seismic events which will in turn cause permanent (inelastic) deformation in the rock mass perceived as jumps in the strain-meters readings (Figure 6: 3: 4).

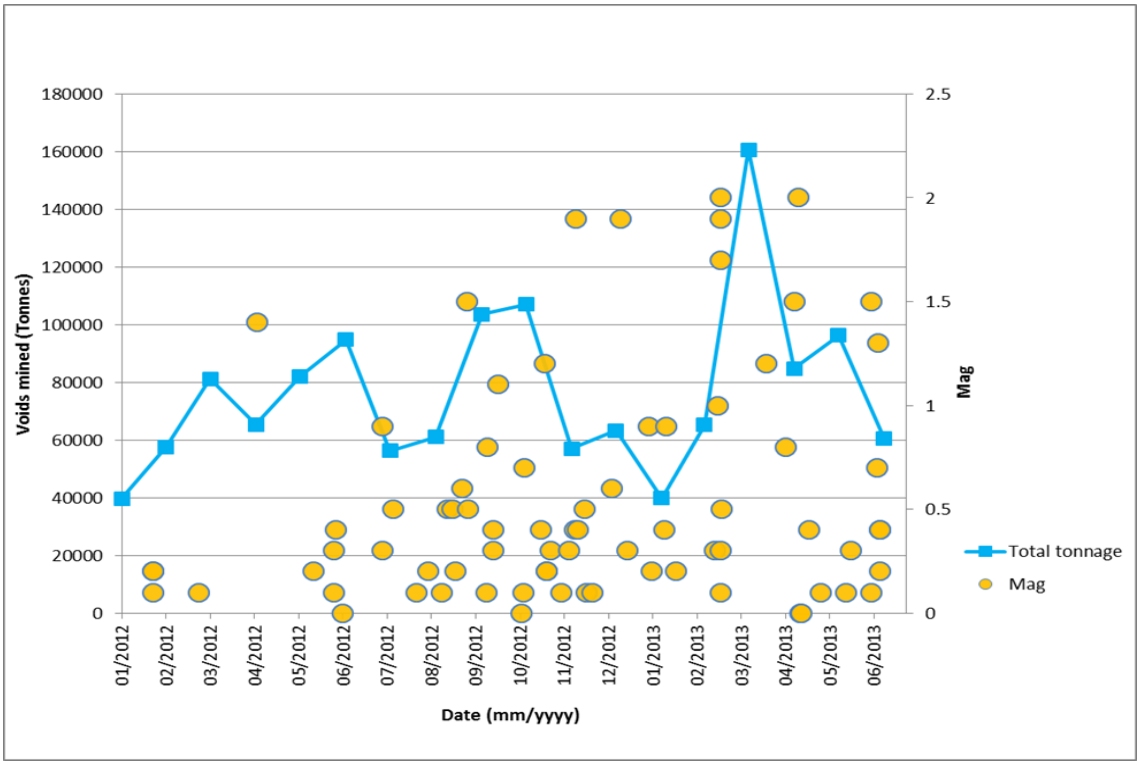


Figure 6: 3: 5 Correlation between seismic events (M>=0) and mined tonnages from Aug 2012 to June 2013

Figure 6: 3: 6 shows the correlation between the rate of mining and the cumulative potency. An increase in mining rate may have activated many previously inactive geological structures causing slip along those faults resulting in high magnitude events. The events would in turn cause significant permanent inelastic deformation of the rockmass which were observed as jumps in potency especially noticeable during March 2013, hence steep gradients on the cumulative potency graph during same period.

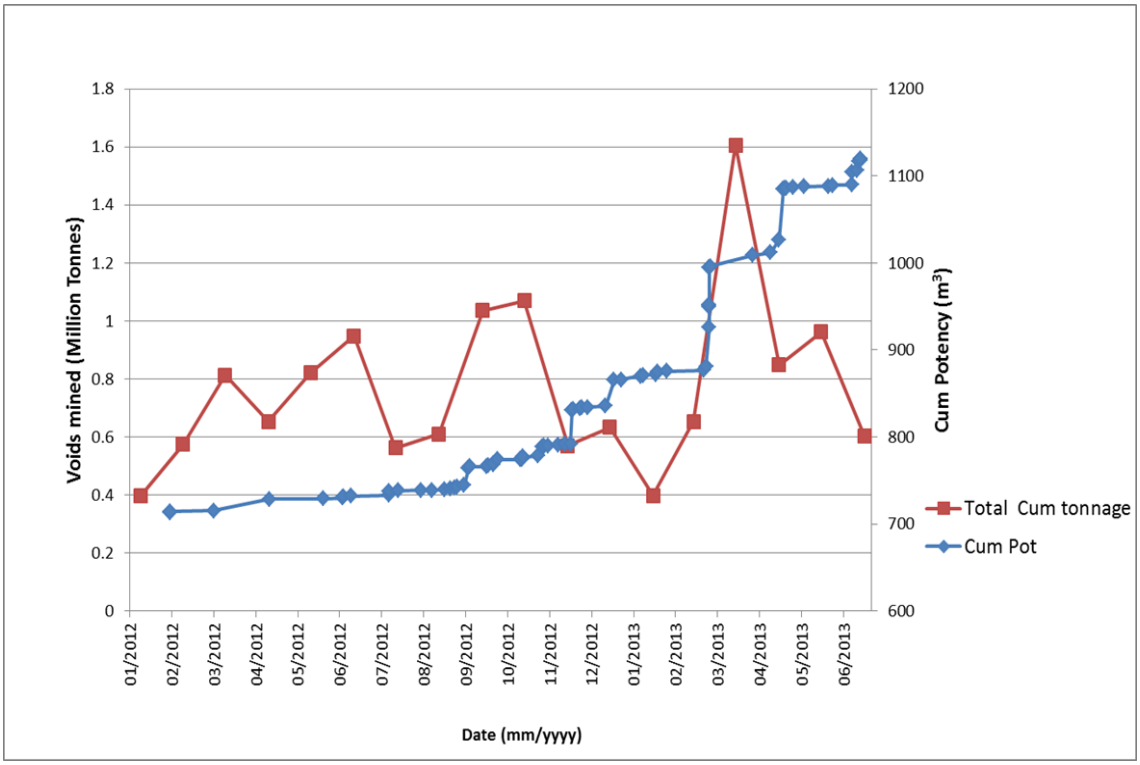


Figure 6: 3: 6 Correlation between cumulative potency and mining tonnages from Aug 2012 to June 2013

The nearer the event the larger and it is to the strain meter, the larger the strain change becomes. According to Hiroshi (2013), taking into account theory, the elastic strain change induced by rock mass movement is expected to be proportional to seismic moment and inversely proportional to cube of the distance from the event to the strain-meter. To find the seismic events with the largest impact on the strain recording, a plot of $\frac{M_o}{D^3}$, is presented as shown in Figure 6: 3: 7 where;

Mo: seismic moment and

D: distance of seismic event from strain-meter.

The onset of pillar instability is observed as the change in the general trend of the $\frac{M_o}{D^3}$ graph from linear to exponential. At the present moment the pillar is considered stable since the linear correlation coefficient (R^2) of the $\frac{M_o}{D^3}$ graph is still close to 1.

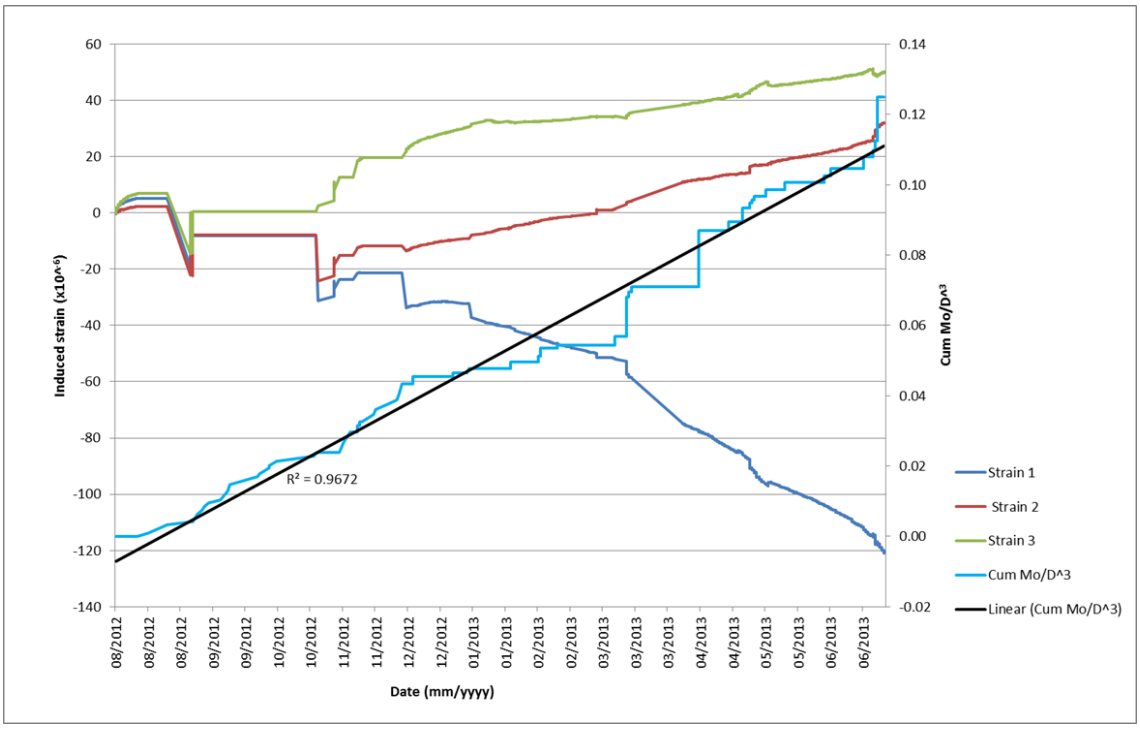


Figure 6: 3: 7 Correlating strain with $\frac{M_o}{D^3}$

The strain data is correlated with the co-seismic cumulative displacement (seismic deformation) from the assumption that the strain-meter, even though it is placed in the elastic zone of the rockmass, also measures the inelastic (plastic) deformation as a result of the seismic events. A jump in the deformation graph indicates unstable rock mass deformation as a result of high magnitude events as presented in Figure 6: 3: 8 and this means a higher likelihood of seismic damage in the future.

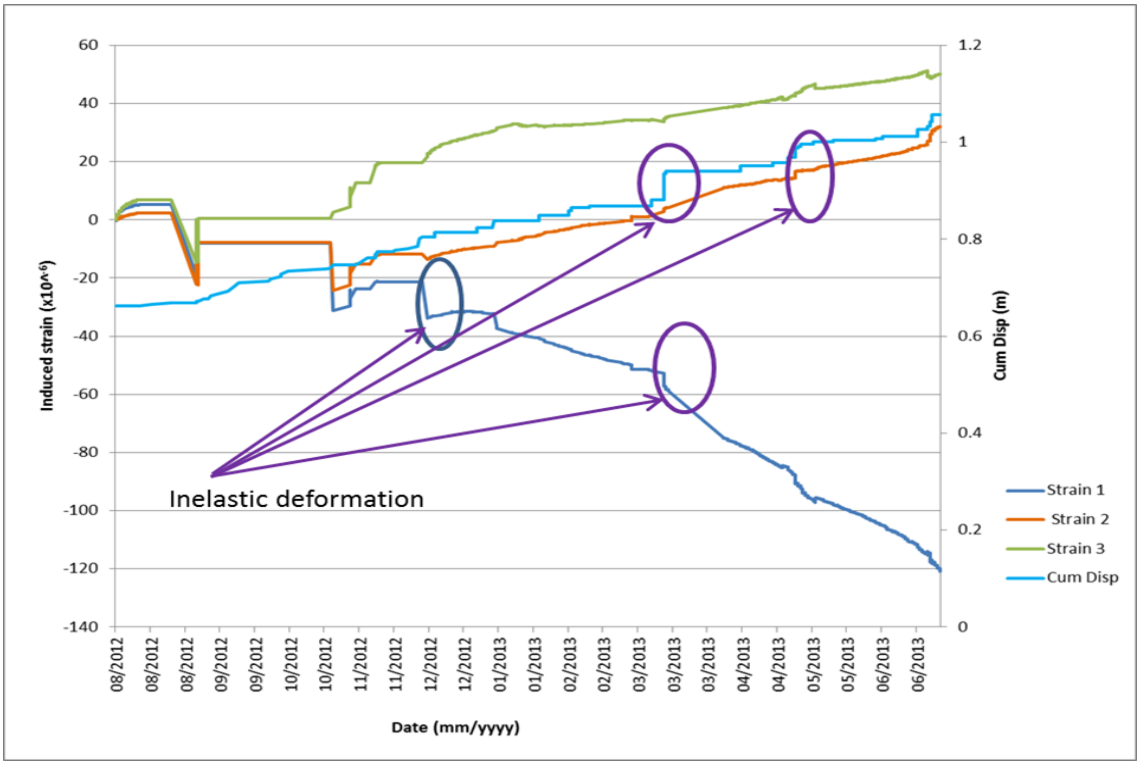


Figure 6: 3: 8 Co-seismic cumulative displacement and strain analysis from August 2012 to June 2013

Seismic potency is defined as the measure of strain change at the source volume. Figure 6: 3: 9 shows the correlation between cumulative potency and strain data. The graph shows that strain changes (plastic deformation) at the seismic sources were recorded by the strain meter together with the elastic strain change in the rockmass. The inelastic deformation in the rock mass recorded by the strain-meter was also recorded in the JDi seismic analysis, hence coinciding jumps in the cumulative data indicating a good correlation.

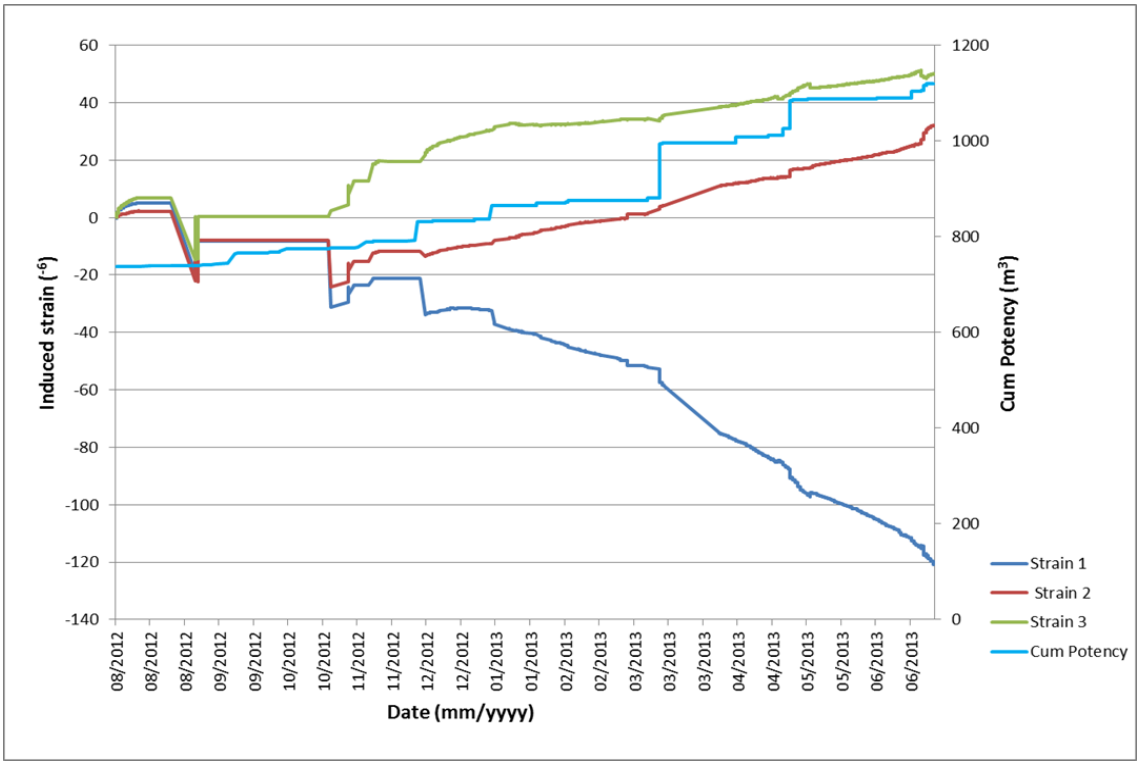


Figure 6: 3: 9 Co-seismic cumulative potency and strain analysis from August 2012 to June 2013

Figure 6: 3: 10 displays the energy index which is the comparison of energy of a specific event to the average energy released by a large number of events of the same moment. It is the ratio of radiated energy by a given event to that event's inelastic deformation at that source. The average energy release as a function of moment is determined through linear regression. The graph shows a good correlation in the data because the data is concentrated on the line of best fit.

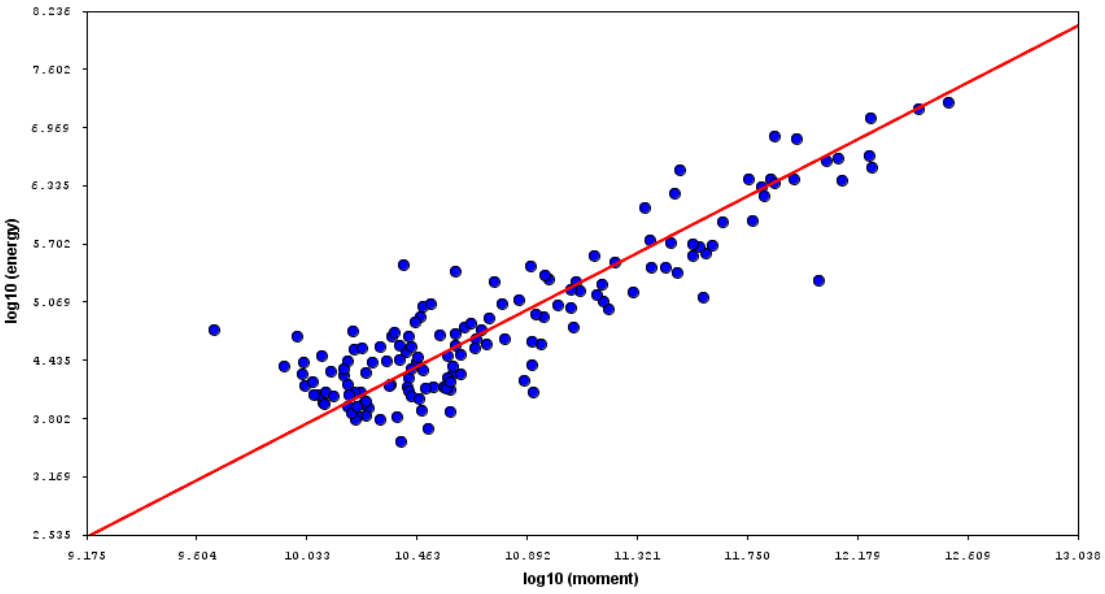


Figure 6: 3: 10 Log Energy vs Log Moment for 90 3W Remnant

After an event has occurred, there is reduction in stresses which represents strain softening indicated by the drop in the viscosity in Figure 6: 3: 11. Viscosity characterises the flow of the inelastic deformation process and is calculated as;

$$S = \frac{\sigma_s}{\varepsilon_s}$$ (after Mendecki and van Aswegen, 1999)

Where;

S seismic viscosity,

σ_s seismic stress and

ε_s seismic strain.

Lower seismic viscosity suggests easier flow of inelastic deformation or larger stress transfer due to seismicity (Jager and Ryder, 1999). The figure shows that a rapid drop in viscosity is preceded by large number of events per given time (activity rate) as illustrated in July 2011 and March 2013. This results in an increase in the overall strain rate and decreases strength of the

rockmass after failure thereby disturbing stability of excavations to be made in such an environment.

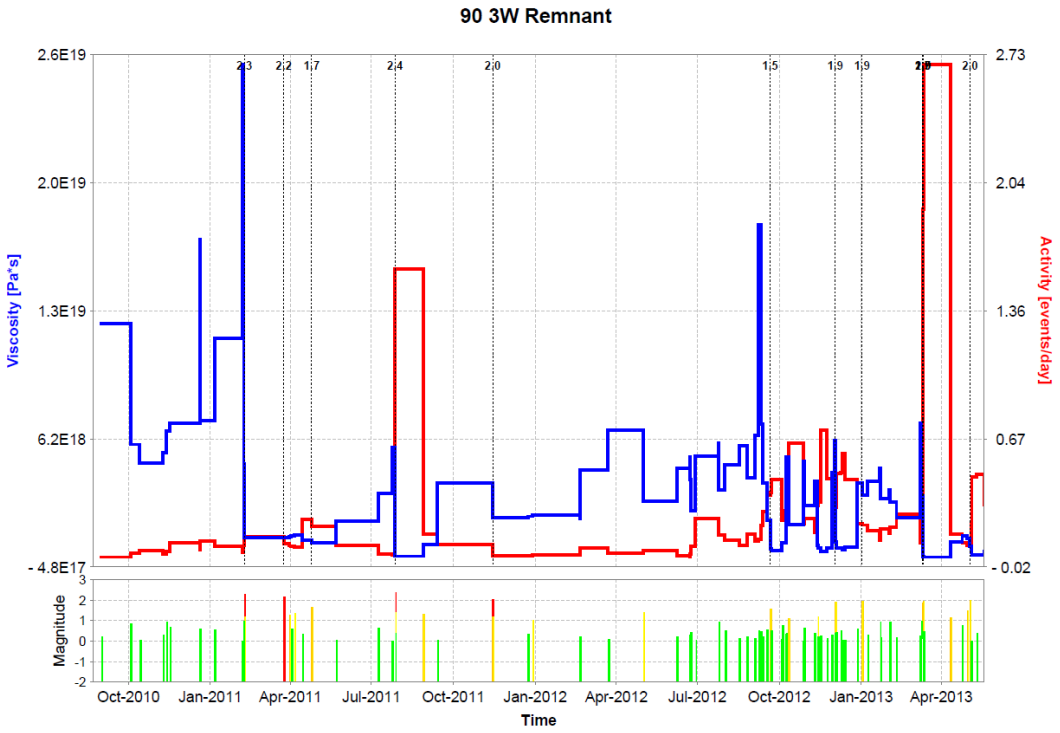


Figure 6: 3: 11 Viscosity and Activity against time graph from JDi software

A drop in stress, indicated by a drop in Energy Index (March 2013 and May 2013), in seismic analysis follows a large seismic event resulting in an increase in apparent volume and this signifies rock mass instability (Ogasawara, 2013). This relationship between cumulative apparent volume, large seismic event occurrence and energy index is illustrated in Figure 6: 3: 12.

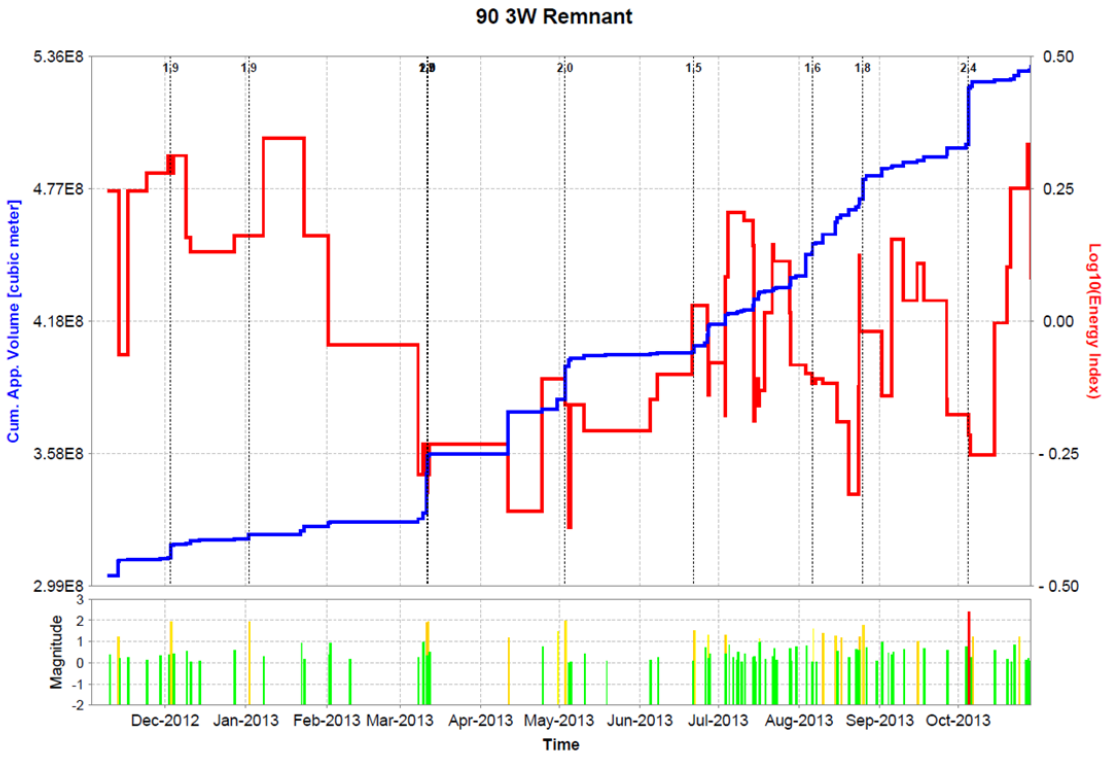


Figure 6: 3: 12 Cum apparent volume against Energy Index

Table 6: 7 shows the probability of occurrence of an event of a certain magnitude in a given volume during a specific time period. The probability determination is part of the in-built calculations carried out in JDi seismic analysis software. For example, the probability of a 1.2 magnitude event occurring in a month is 0.41 and the mean recurrence days for that size event is 48 days. This indicates that a 1.2 magnitude event is expected once in every one and half months.

Table 6: 7 Magnitude probability table

Magnitude	**1.2**	**1.3**	**1.4**	**1.5**	**1.6**	**1.7**	**1.8**	**1.9**	**2**	**2.1**	**2.2**	**2.3**	**2.4**	**2.5**	**2.6**	**2.7**	**2.8**	**2.9**
mean recurrence days	48	61	77	97	123	155	195	247	312	394	497	628	793	1002	1265	1598	2018	2548
1month	0.41	0.35	0.29	0.23	0.19	0.15	0.12	0.10	0.08	0.06	0.05	0.04	0.03	0.03	0.02	0.02	0.01	0.01
2months	0.65	0.57	0.49	0.41	0.34	0.28	0.23	0.19	0.15	0.12	0.10	0.08	0.06	0.05	0.04	0.03	0.03	0.02
3months	0.79	0.71	0.63	0.55	0.47	0.39	0.33	0.27	0.22	0.18	0.14	0.12	0.09	0.07	0.06	0.05	0.04	0.03
6months	0.96	0.92	0.86	0.80	0.72	0.63	0.55	0.47	0.40	0.33	0.27	0.22	0.18	0.15	0.12	0.09	0.08	0.06
1year	1.00	0.99	0.98	0.96	0.92	0.86	0.79	0.71	0.63	0.55	0.47	0.39	0.33	0.27	0.22	0.18	0.14	0.12

CHAPTER 7

7 Conclusions

The analysis carried out on data gathered during the course of the project indicates that the average pillar stress is gradually increasing as the pillar is being cut during de-stress mining and also because of concurrent massive mining nearby. Plastic (inelastic) numerical modelling (Phase 2) was done to complement the elastic model for the regional pillar assessment. Inelastic modelling tools help in identifying the stages of failure in the pillar, if any, so that management can make an informed decision whether to stop cutting the pillar or to continue mining it with adjusted mining sequence.

7.1 Numerical modelling

The monitoring of the regional pillar at South Deep gold mine using numerical modelling in correlation with production rate, seismic and strain data following the proposed mining sequence predicts that seismic events are likely to increase in future. This requires additional measures to manage the risk. The monitoring system was used in an attempt to identify hazardous areas in the mine and the prediction of rock-bursts. A reasonable prediction of the location of events and their corresponding magnitudes in future will be based on the analysis of seismic history and of stress changes. However, the time of occurrence is impossible to predict. South Deep mine is anticipating a higher daily rate of seismicity and larger events as mining progresses to greater depths and as mining takes place closer to the geological structures. Increases in mined out voids escalate the ERR and also accelerate slip along faults and consequently large seismic events (Figure 5: 8 in Chapter 5) occurrences. Higher stress changes in the model are an indication of the likelihood of seismic events later on.

Since South Deep gold mine is practicing the cut-and-fill mining method, generally, seismic events increase as large unsupported spans increase and hence monitoring needs to be done on an ongoing basis. Rock strength at the mine is variable, therefore it is necessary to monitor such critical areas so that measures can be taken before risk occurs.

Many engineers strongly support the use of numerical techniques for the analysis of the mining layouts. In the South African hard rock mines, back analysis using numerical modelling is used to evaluate the mining sequence or stope layout by assessing the seismicity caused by mining following that sequence. Numerical analysis approaches do have some limitations, predominantly in relation to the fact that results depend on variability in the material properties, hence care needs to be exercised when using such an approach. In order to identify faults where slip can occur, seismic records and knowledge of the location of active faults, as well as the location of faults that can be activated is necessary. This can only be achieved through the use of inelastic modelling software.

A number of conclusions can be drawn regarding the regional pillar performance in response to the mining sequence.

7.1.1 Seismic monitoring

- The research confirmed the expectation of increased frequency of high magnitude events from high production rate. These seismic events in turn result in both elastic and inelastic deformations in the rock mass causing abrupt increases in measured strain as shown by underground measurements. However inelastic deformation cannot be accurately modeled using Map 3D due to the limitations of the software hence the introduction of Phase 2 modelling.

- A correct prediction of location and size of an event would increase safety and decrease production losses by avoiding production stoppages as a result of stopes and drifts losses.
- Fault slip events may result in severe damage, such as rock-bursts and large falls of ground due to shake down. The severity of these events may cause damage to the mine workings, personnel, especially those working at the faces.
- The analyses show that the modeled events are very high with magnitudes that are above 3.5 using the method that estimates moment from the maximum excess shear stress. However, the magnitudes drop significantly (closely representing reality) when ESS is averaged or capped at 15 MPa as suggested by Ryder (1988). The method which caps the ESS value at 15MPa is recommended since Ryder explained that if ESS is greater that value, the event would have already occurred.
- Fault 7 exhibited comparable modelled results with measured seismic data when using Map 3D model. In Phase 2 inelastic modelling, there is also evidence of shearing along parts the same fault therefore both analysis techniques are analogous.
- The onset of pillar stability is observed as the change in the general trend of the $\frac{M_o}{D^3}$ graph from linear to exponential (Ogasawara, 2013). Continuous monitoring of the above mentioned graphs will alert of any instability if their correlation coefficients become nearer to 1 in the exponential trend as compared to the present linear one.
- Altering the mining sequence accordingly will reduce high magnitude seismic occurrences which can potentially hinder the mine operations significantly.

7.1.2 Pillar strength and stress

- At South Deep gold mine the planned final pillar layout has a width to height ratio of 30:1, and such a pillar generally fail by foundation failure on the footwall or hangingwall. The failure depends on the rock strength making up the footwall or the hangingwall. The strength of the rock making up the pillar is about 200 MPa while the footwall is from 60 MPa to 160 MPa and the hangingwall ranges from 60MPa to 90MPa.
- The average pillar stress (from Map 3D modelling) by June 2013 was around 314 MPa. Likewise, the average pillar stress from Phase 2 during the same month was around 234 MPa, which is less than 2.5 times the UCS of the footwall but greater than that of the hangingwall material for both models. Foundation failure is likely to occur on the hangingwall.
- Moreover, Map 3D (Figure 6: 2: 6) and Phase 2 (Figure 6: 2: 13) results are generally analogous showing high pillar skin stresses.
- Inelastic modelling carried out using Phase 2 indicated shear along the faults cutting across the pillar where slip failure is likely to occur, which Map 3D software could not model. These areas are potential locations for seismic events in future.

7.1.3 Energy Release Rate (ERR) and Rockbusrts

- ERR values from the modelling are all less than 40 MJ/m^2.This could be due to the limited closure rate as a result of mining span.
- A sharp increase is noted in March 2013 which corresponds to the increase in production in that month. Generally, increasing the production mining resulted in

wider ranging spans underground which facilitated high convergence rate of the stopes. This resulted in high energy being released at the excavation boundaries posing a danger to the workers and equipment exposed.

- The obtained values of ERR and ESS were used to assess the seismic hazard but the modeled expected seismic magnitude values were generally higher than the recorded, therefore other modelling softwares such as FLAC 3D into which previous seismic data can be input into the model together with the current mining sequence for correct analysis have to be employed. FLAC 3D also enables incorporation of the inelastic properties of the rockmass as well as geological structures.
- Well-known faults crossing the active mining area have so far resulted in the modification of the mining sequence (Watson, 2012).
- There are still more known faults passing through the mining area, but do not cross any openings underground, making it difficult to determine the presence of any movement along these faults.
- The damage caused by an event was found to be correlated to the estimated ERR for each mining period (step).

CHAPTER 8

Recommendations

Conclusions made from the analysis carried out on the remnant pillar suggest the need for continuous assessment of the mine geotechnical model on the proposed mining sequence and that model needs to be further updated to correlate geology with seismic events. Monitoring needs to be continued on this pillar, so that in future, optimum and efficient pillars are left for regional support. Some of the recommendations are highlighted as follows;

- A database of parameters obtained from a seismic monitoring system, the strain data as well as the numerical modelling needs to be archived for future references. This data will provide valuable information about the state of the rock mass, which can in turn assist in the determination of seismically active areas. Since analysis of the seismic source parameters has proven be very valuable, though it requires a considerable effort and time, these parameters need to be continuously monitored. The database capture and analysis on a regular basis are essential so that values departing from the average can be noted.
- History of previous high magnitude events need to be archived to investigate if they are weakening the cohesive strength properties of the existing neighbouring structures.
- The seismic database needs to incorporate failure mapping in the field to provide information on the type of damage and failure mechanism associated with a rock failure of a certain event magnitude.
- Following a case study by Lenhardt and Hagan (1990), there is noteworthy closure in a step-wise fashion that follows any major pillar event and this makes prediction of pillar foundation failure possible. Therefore there is need for further study to assess this closure pattern.

- The geomechanical model should include stiffness and strength of different rock types and their location in the mine, rock mass classification results, locations of previously recorded seismic events, type and descriptions of damage, failure observations and descriptions and present production rate. This would result in a better appreciation of the rock mass response to mining as well as identification of seismically hazardous areas.
- Although a number of pillar design methods are available in tabular mining layouts, pillar failure inevitably occur so additional work is required to obtain a better understanding of pillar strengths. Additional research into the regional pillar strength and behaviour still need to be emphasized strongly as this predicament has not been clearly resolved. It is recommended that non-linear models be investigated to get a better understanding of the behaviour of the rock mass.
- It is recommended to optimize regional pillars in order to maximize resource extraction. This could be done through highlighting the consequences of improper mining of the regional pillars. Leaving too large pillars results in resource losses due to locked up reserves and very small pillars are likely to fail causing stope closures hence losses of the ore resource.
- Mining sequence should be planned so that seismicity is kept to a minimum, avoiding highly stressed pillars between mining voids.
- When mining where there are predominant geological structures, it is desirable to design the mining sequence to ensure optimum angle of approach in order to reduce the sizes of ESS lobes on the concerned structures.
- Furthermore, unmined ground rock (known as bracket pillars) must be left on either side of these faults and dykes to reduce the occurrence of high magnitude events.

- Increase the number of instruments in the footwall of the pillar will benefit the seismic network with improved location accuracy of events.
- Regional pillars, which cannot be avoided during massive mining, are likely to become highly stressed as mining progresses resulting in seismic events in the future. If events occur when mining has moved away and the effects do not affect other active areas, then there is no problem because the damage is negligible.

References

Aki, K., & Richards, P. G. (1980). *Quantitative seismology.* New York: Freeman and Co.

Amadei, B., & Stephansson, O. (1997). *Rock stress and it's measurement.* UK: Chapman & Hall.

Annon. (1915). *Report of the Witwatersrand Rockburst Committee.1915.* Pretoria: The Government Printing and Stationery Office, Union of South Africa.

Annon. (1924). *Report of the Witwatersrand earth tremours. 1924.* Cape Town: The Government Printer, Union of South Africa.

Ashanti, A. (2004). *04- Report to Society-Control of mining-induced seismicity in the South Africa region.* Retrieved 2004, from http://www.anglogold.co.za

Bester, W., Joughin, W., & Du Plooy, M. (2011). *Mining methods and backfill at South Deep gold mine- Presentation to the mine managers.* Johannesburg: Not published.

Cairncross, B., & Dixon, R. (1995). *Minerals of South Africa.* Singapore: Johannesburg geological survey.

Chamber of mines. (2003). *Geology of the Wits Basin- Wits gold report (from American scientist- the origin of gold in South Africa).* Johannesburg: Wits gold publication.

Cook, A. P. (1998). *The occurrence, emission and ignition of combustible strata gases in Witwatersrand gold mines and Bushveld platinum mines, and means of ameliorating related ignition and explosion hazards- Part 1.* South Africa: SIMRAC.

Cook, N. (1976). *Seismicity associated with mining.* Johannesburg: Chamber of Mines, Johannesburg, South Africa & Department of Civil and Mineral Engineering Minneapolis, USA.

Cook, N. G., Hoek, E., Pretorious, J. P., Ortlepp, W. D., & Salamon, M. D. (1966). Rock mechanics applied to the study of rockbursts. *Journal of South African Institute of Mining and Metallurgy, 66*(10), 435-528.

De Beer, W. (2000). *Seismology for rockbusrst prediction.* Johannesburg: Safety in Mines Research Advisory Committee.

Dixit, U. (2008). *Finite Element Method: An introduction.* Guwahati, India: India Institute of Technology.

Dunnilciff, J., & Green, G. E. (1988). *Geotechnical instrumentation for monitoring field performance.* New York: John Wiley & Sons Inc.

Durrheim, R. J. (2010). *A research on mitigating the risk of rockbursts in the deep hard rock mines of South Africa: 100 years of research.* Phoenix, Arizona: Society of Mining, Metallurgy and Exploration Inc.

Durrheim, R. J., Milev, A., Spottiswoode, S. M., & Vakalisa, B. (1998). *Improvement of worker safety through investigation of the site response to rockburst-SIMRAC Final Project report.* Pretoria: Department of Minerals and Energy.

Ebrahim-Trollope, R., & Jooste, Y. (2005). *Seismic hazard quantification- Proceedings of the sixth symposium on Rockbursts and Seismicity in mines.* Perth, Western Australia: Australian Centre for Geomechanics.

Gold Fields. (2011, December 31). *South Deep gold mine-Technical short form report.* Retrieved 2011, from www.goldfields.co.za/reports/ar_dec_2011

Goldswain, G. (2013, April 23). Insturmentation types and specifications-Institute of Mine Seismology (IMS).

Grandin, R., Jacques, E., Nercessian, A., Ayele, A., Doubre, C., Socquet, A., et al. (2011). *Seismicity during lateral dike propagation: Insights from new data in the recent Manda Hararo- Dabahu rifting episode (Afar, Ethiopia).* USA: Geochem Geophys Geosyst.

Hoek , E., & Brown, E. T. (1982). *Underground excavations in rocks* (Second ed.). England: Publication of the Institute of Mining and Metallurgy.

Ishii, H., Yamachii, T., Matsumoto, S., Hirata, Y., & Nakao, S. (2002). *Development of multi-component borehole instrument for earthquake prediction study; Some observed examples of precursory and co-seismic pheonomena relating to earthquake swarms and application of the instrument for rock mechanics.* Rotterdam: Balkema.

Jager, A. J., & Ryder, J. A. (1999). *A handbook on rock engineerign practice for tabular hard rock mines.* Johannesburg: SIMRAC.

Jager, J. A. (1988). Excess Shear Stress in the assessment of geological hazardous situations. *Journal of the South African Institute of Mining and Metallurgy, 88*(1), 27-39.

Joughin, W. C. (2010, February 11). Course on Mine Seismology- Course for Newcrest mining (Ltd)- Cadia Valley Operations. Johannesburg, South Orange, NSW2800: Not published.

Joughin, W. C., Bester, W. M., & Du Ploy, M. (2011). *Mining methods and backfill at South Deep gold mine.* Johannesburg: SAIMM.

Joughin, W. C., Petho, S. Z., & Thompson, J. J. (2007). *South Deep Regional pillar modelling Part 1- Design of regional pillars at South Deep gold mine.* Perth: Australian Centre for Geomechanics.

Larsson, K. (2004a). *Mining Induced seismicity in Sweden.* Sweden: Lulea University of Technology.

Larsson, K. (2004b). *Seismicity in mines-A Review.* Sweden: Lulea University of Technology.

Lee, W. K. (2002). *International handbook of earthquake and engineering seismology.* Amsterdam: Academic Press.

Lenhardt, W. A., & Hagan, T. O. (1990). *Observations and Possible Mechanisms of Pillar-associated Seismicty at great depth- Technical challenges in deep level mining.* Johannesburg: SAIMM.

Maccelari, M. C., & Cichowicz, A. (1999). *Strike stabilizing pillars as regional support strategy for ultra-deep level mines.* Auckland Park- South Africa: Kluwer Academic Publishers.

Martin , C. D., & Maybee, W. G. (2000). *Strength of hard rock pillars- International Journal of Rock Mechanics and Mining Services 37.* Sudbury, Canada: Eisevier Science Ltd.

Maybee, C. M. (2000). *A text book on the strength of hard rock pillars.* Sudbury, Canada: University of Alberta.

Mc Garr, A. (1991). *Observations constraining near-source ground motion estimated from locally recorded seismograms.* USA: US Gelogical Survey- Journal of Geophysical Research.

Mc Garr, A., Spottiswoode, S. M., & Gay. (1991). *Relationship of mine tremours to induced stresses and to rock properties in the focal region.* USA: US Geophysical Survey.

McCully, P. (1996). *The Ecology and Polotics of Large Dams.* London: Zed Books.

McGarr, A. (1976). *Physical properties of Rocks.* USA: US Geological Survey.

Mendecki, A. J., & Van Aswegen , G. (1999). *Seismic monitoring in mies: Selected terms and definitions- Prepared for the Handbook on Rock Engineering Practise for Tabular Hard Rock Mines by Jager and Ryder.* Johannesburg: The Safety in Mines Research Advisory Committee (SIMRAC).

Mendecki, A. J., Ilchev, A., Napier, J. A., & Sellers, E. J. (2001). *Fundamental sapects of the intergartion of seismic monitoinr with numerical modelling-CSIR, miningtek.* JOhannesburg: SIMRAC.

Mendecki, A. J., Mountfort, P., Dzhafarov, H. A., Sciocatti, M., Van Aswegen, G., & Maxwell, S. C. (1996). *Seismology for rockburst prevention, control and prediction.* South Africa: SIMRAC.

Mongillo, C. B. (2008). *Geothermal energy from fractured reserviors- Dealing with Induced seismicity.* United States: International Energy Agency OPEN Technology Bulletin.

'O' Hearne, B. (2009). *Mine backfill.* Canada: Lafarge.

Obermeyer, P. (2009). *Role of geologist in Goldfields- Presentation at Nelson Mandela Metropolitan University.* Port Elizabeth: Not published.

Ogasawara, H. (2011). Monitoring of stress build-up and instability on faults-Observational studies to mitigate seismic risks in mines. Arbella Estate, South Africa: Ritsumeikan University.

Ogasawara, H. (2013, July 03). Specifications of strain meter installed at South Deep gold mine, South Africa.

Ogasawara, H., Ishii, H., Nakao, S., Kawakata, H., & Ohkura, T. (2005). High-resolution strain monitoring during M>2 events in a South african deep gold mines in close proximity to hypocentres. Perth: International Symposium on Rockbursts and Seismicity in mines (6th proceeding).

Ortlepp, D. W. (1997). *Rock fractures and rockbursts: An illustrative study.* Johannesburg, South Africa: SAIMM.

Ortlepp, W. D., & Stacey, T. R. (2004). *Assessment fo the risk of plug or water barrier failure due to seismicity at South Deep gold mine- colloqium water barries in underground mines.* Johannesburg, South Africa: SAIMM.

Petho, S. Z., & Joughin, W. C. (2007). *Design of Regional Pillars at South Deep Gold mine- South Deep Regional Pillar Modelling Part 1.* Perth: Australian Centre for Geomechanics.

Prestorius, W. M. (2012). *South Deep support starndard and proceedure for mining, support and backfill sequence for the horizontal de-stress mechanised mining method.* Johannesburg: Not published.

Robb, L. J., & Meyer, M. F. (1995). *The Witwatersrand Basin, South Africa: Geological framework and mineralization process.* Gauteng: Elsevier Science B V.

Ryder, J. A., & Jager, J. A. (2002). *A textbook on rock mechanics for tabular hard rock mines.* Johannesburg: SIMRAC.

Salamon, P., Berry, R. S., Ondrechen, M. J., & Andderssen, B. (1984). *Thermodynamics for process in finite time.* USA: American Chemical Society.

Sears, M. M. (2009). *Implementing Energy Release Rate Calculations into the LaModel program.* Morgantown, West Virginia: University of West Virginia.

Spearing, A. J. (1995). *Handbook on Hard-rock Strata Control-SAIMM.* Johannesburg: HL & H Mining Tmiber.

Stacey, T. R. (2012). *Numerical modelling techniques in Rock Engineering- Course notes.* Johannseburg: Witwatersrand University.

Toper, A. Z., Kabongo, K. K., Stewart, R. D., & Daehnke, A. (2000). *The mechanism, optimisation and effects of pre-conditioning.* South Africa: SAIMM.

Trifu, C. (2010). *Use of microseismic monitoring for rockbursts management at Vale inco mines.* New York: Rinton Press.

Trifu, T. U. (2000). *Recent advances in seismic monitoring technology at Canada mines-Journal of appiled geophysics* . Canada: Elsevier.

Vieira, F. M., Dierring, D. H., & Durrheim , R. J. (2001). *Methods to mine ultra deep tabular gold bearing reefs of the Witwatersrand basin, South Africa, Underground Mining methods: Engineering Fundamentals and International Case Studies.* South Africa: Society for Mining, Metallurgy and Exploration Inc.

Watson, B. (2012). *Philosophy of mining at great depth-Presentation to the association of mine managers-South Deep gold mine.* Johannesburg: Not published.

Watson, B. (2012, December 7). South Deep gold mine seismic instrumentation.